ELECTROCHEMICAL EVALUATIONS OF TiO_2 NANO FILMS FOR ADVANCED ENGINEERING APPLICATIONS

A Thesis

by

Rawana Yagan

Submitted to the

Graduate School of Sciencesand Engineering
In Partial Fulfillment of the Requirements for
the Degree of

Master of Science

in the
Department of Electrical and Electronics Engineering

Özyeğin University
May2018

Copyright © 2018 by Rawana Yagan

ELECTROCHEMICAL EVALUATIONS OF TiO_2 NANO FILMS FOR ADVANCED ENGINEERING APPLICATIONS

Approved by:

Associate Prof. Dr. Bahar Basim,
Thesis Advisor,
Department of Mechanical Engineering
Özyeğin University

Assistant Prof. Dr. Özkan Bebek,
Department of Mechanical Engineering
Özyeğin University

Assist. Prof. Dr. Sedat Nizamoglu
Department of Electrical and Electronics Engineering
Koç University

Date Approved: 16/5/2018

To…

My teachers, family and friends

ABSTRACT

This study evaluates the performance TiO_2 nano-film for engineering applications, both in biomedicine and microelectronics, were Chemical Mechanical Planarization (CMP) is a main process used for planarizing the metal surface by producing such oxide nano-film that is known to be an intact and protective film.

Titanium oxide nano-film evaluation in biomedical applications is investigated. Electrochemical experiments are done on biomedical grade Titanium plates such as Potentiostatic sweeps and potentiodynamic polarizations of Ti as a function of oxidizer concentration. In surface characterizations on TiO_2 films two main methods are addressed; which are contact angle and wettability measurements and surface roughness measurements. CMP application on Ti surface is performed by controlling slurry oxidizer concentration. Which leads to material removal rate evaluations and surface characterization of chemical mechanical polished Ti surfaces.

CMP is also a widely used process for the manufacturing of the microelectronic circuits. It is common to planarize the metallic layers such as tungsten in the transistor via and copper in the metallization lines. The integration of the metallization also involves the deposition of the barrier layers, which are necessary to stop the diffusion of metal to the transistor as well as to improve the adhesion of the metal to the underlying layers. In this study, titanium barrier CMP was thoroughly studied by electrochemical analyses with respect to the tungsten metal itself. Ti has the unique ability to form a protective oxide layer, which was characterized and analyzed under different oxidizer concentrations. Potentiodynamic and potentiostatic scans were performed in $H_2O_2$to provide more information on the passivation and corrosion behavior under the selected conditions. Moreover, the effect of slurry solid loading in relation with oxidizer

concentrations on the film formation and removal during the CMP was investigated for both materials. The application of corrosion behavior of Ti as barrier materials for W based interconnects was further studied by evaluating the surface wettability, roughness and topography analyses.

ÖZET

Bu çalışma, hem biyomedikal hem de mikro elektronikteki mühendislik uygulamaları için TiO2 nano filmin performansını değerlendirmektedir. KimyasalMekanikPlanarizasyon (CMP), sağlamvekoruyucuolduğubilinenbuoksit nano filminüretilmesiiçin metal yüzeyinplanlanmasındakullanılananaişlemdir Biyomedikaluygulamalardatitanyumoksit nano film uygulamalarideğerlendirilmiştir.Elektrokimyasaldeneyler, PotansiyostatiktaramalarveTi'ninpotansiyodinamikpolarizasyonlarıgibibiyomedikalkalit edeTitanyum plakalar üzerinde, oksitleyici konsantrasyonunun bir fonksiyonu olarak yapılır. TiO_2filmlerindeyüzeykarakterizasyonlarındaikianayöntemelealınmıştır; temasaçısıveıslanabilirlikölçümleriveyüzeypürüzlülüğü ölçümleridir. Ti yüzeyinde CMP uygulaması, bulamaç oksitleyici konsantrasyonunun kontrol edilmesiyle gerçekleştirilir. Bu, kimyasal mekanik cilalıTiyüzeylerinmalzemekaldırmaoranıdeğerlendirmelerineveyüzeykarakterizasyonun ayolaçar.

CMP ayrıcamikroelektronikdevrelerinüretimiiçinyaygınolarakkullanılan bir işlemdir. Transistördeki tungsten gibimetaliktabakalarınvemetalizasyonhatlarındakibakırın planarize edilmesiyaygındır. Metalizasyonunentegrasyonuayrıcametalintransistöredifüzyonunudurdurmanınyanı sıra metalin alttaki tabakalara yapışmasını iyileştirmek için gerekli olan bariyer tabakalarının birikmesini de içerir. Bu çalışmada titanyum bariyer CMP, tungsten metalin kendisiyle ilgili olarak elektrokimyasal analizler ile incelenmiştir. Ti, farklı oksitleyici konsantrasyonları altında karakterize edilen ve analiz edilen koruyucu bir oksit tabakası oluşturma özelliğine sahiptir.

Seçilenkoşullaraltındapasivasyonvekorozyondavranışıhakkındadahafazlabilgisağlamaki çin H_2O_2'de potansiyodinamikvepotansiyostatiktaramalaryapıldı. Üstelik, her iki malzeme için film oluşumu ve çıkarılması üzerine, oksitleyici konsantrasyonları ile ilgili olarak bulamaç katı yükünün CMP sırasında etkisi araştırılmıştır. Ti'ninkorozyondavranışının W bazlıarabağlantılariçinbariyermalzemesiolarakuygulanması, yüzeyıslatılabilirliği, pürüzlülükvetopografyaanalizlerideğerlendirilerek daha fazla incelenmiştir.

ACKNOWLEDGMENTS

I would first like to thank my thesis advisor Dr. G. BaharBaşım, Associate Professor in the department of mechanical engineering at Özyeğin University, Istanbul, Turkey. She provided me with all the help and knowledge that assisted me greatly throughout my research study and opened my eyes to such great potentials that the work can reach to.

Further, I would like to thank ZeynepOzdemir, PhD for providing me with great help and instruction at the beginning of my research with Ti bulk based implants. Along with other technicians and our group members whom their help I appreciate too.

Finally, I must express my very deep gratitude to my family and friends fortheir never ending support and encouragement especially throughout the period of this study.

This work would nothave been accomplished without you, all.

Author,

Rawana Yagan

TABLE OF CONTENTS

ABSTRACT IV

ÖZET VI

ACKNOWLEDGMENTS VIII

TABLE OF CONTENTS IX

LIST OF TABLES XI

LIST OF FIGURES XII

INTRODUCTION 1

1.1 LITERATURE REVIEW 1
1.1.1 Application of titanium in advanced processing of materials 1
1.1.2 Self-protective properties of titanium through surface oxide (TiO_2) formation 15
1.1.3 Electrochemical methods for surface passivation evaluation 19
1.1.4 Impact of self-protective surface film for application of titanium in biomedicine 25
1.1.5 Use of titanium and its films in microelectronics applications 33
1.1.5.1 Tungsten in interconnects and vias 33
1.1.5.2 Introduction of metal barrier (Ti/TiN) 35
1.1.5.3 Tungsten and barrier (Ti/TiN) CMP: 35

CHAPTER II 38

TITANIUM OXIDE NANO-FILM EVALUATION IN BIOMEDICAL APPLICATIONS 38

2.1 INTRODUCTION 38
2.2 EXPERIMENTAL APPROACH 39
2.2.1 Electrochemical analyses on biomedical grade Titanium plates 39
2.2.1.1 Electrochemical measurements on pure Ti plates 39
2.2.2 Application of Chemical Mechanical Polishing on Ti plates 42
2.2.2.1 CMP application on Ti surface by controlling slurry oxidizer concentration 42
2.3 RESULTS AND DISCUSSIONS 44
2.3.1 Corrosion studies on titanium and TiO_2 film 44
2.3.1.1 Electrochemical analyses on pure Ti 44
2.3.2 Application of Chemical Mechanical Polishing on biomedical Ti surface 50
2.3.3 Effect of slurry solids loading on bulk titanium plate CMP performance 54
2.4 SUMMARY AND CONCLUSIONS 54

CHAPTER III 56

MICROELECTRONICS APPLICATIONS OF TITANIUM/TITANIUM NITRIDE FILMS AS A BARRIER FOR TUNGSTEN BASED INTERCONNECTS IN CMP APPLICATIONS 56

3.1 INTRODUCTION 56
3.2 EXPERIMENTAL APPROACH 57
3.2.1 Corrosion evaluation of tungsten, titanium and TiN through electrochemical measurements 57
3.2.2 CMP application on W and Ti/TiN barrier films and surface characterization 58
3.3 RESULTS AND DISCUSSIONS 59
3.3.1 Corrosion evaluation of tungsten through electrochemical measurements 59
3.3.2 Ti/TiN electrochemical corrosion evaluations as a barrier for tungsten 65
3.3.3 CMP application and performance evaluations on W and Ti/TiN barrier films as a function of slurry oxidizer concentration 74
3.4 SUMMARY AND CONCLUSIONS 80

CHAPTER IV 84

OPTIMIZATION OF TIO_2 NANO-FILM FORMATION AND PERFORMANCE IN TUNGSTEN BARRIER CMP APPLICATIONS 84

4.1 INTRODUCTION 84
4.2 EXPERIMENTAL APPROACH 85
4.2.1 CMP Experiments on titanium/titanium nitride and tungsten Chemical Vapor Deposited (CVD) films 85
4.3 RESULTS AND DISCUSSIONS 87
4.3.1 CMP selectivity evaluations based on electrochemical measurements on Ti/TiN/W films 87
4.3.2 Material removal rate selectivity calculations of Ti/TiN/W films 91
4.3.3 CMP slurry solids loadings effect against fixed oxidizer concentration. 92
4.4 SUMMARY AND CONCLUSIONS 95

CHAPTER V 97

CONCLUSIONS AND SUGGESTIONS FOR FUTURE WORK 97

5.1 GENERAL CONCLUSION 97
5.2 SUGGESTIONS FOR FUTURE WORK 102

BIBLIOGRAPHY 104

LIST OF TABLES

Table 1.1: Types of titanium dental implants 5

Table 1.2: Various properties of titanium and TiO_2.. 18

Table 2.1: Calculated slopes of titanium curves in H_2O_2 solutions................................ 46

Table2.2: Tafel extrapolation data of titanium potentiodynamic curves......................... 48

Table 3.1: Tafel data and calculated corrosion rates of tungsten at five concentrations.

.... 61

Table 3.2: Calculated slopes of W curves in H_2O_2 solutions.. 63

Table 3.3: Tafel data of deposited titanium potentiodynamic scans. 67

Table 3.4: Tafel data of deposited tin potentiodynamic scans. 68

Table 3.5: Calculated slopes of Ti and Tin curves in H_2O_2 solutions. 70

Table 3.6: Calculated removal rates of Ti, Tin and W under the effect of varying slurry oxidizer concentrations... 74

LIST OF FIGURES

Figure 1.1: Schematic diagram of artificial hip joint. 4

Figure 1.2: Examples of commercial dental implant designs. 5

Figure 1.3: Artificial heart value. 7

Figure 1.4: Ti/TiN barrier layer with the W contact integration. 8

Figure 1.5: Left: Principle setup for measurements of neuronal activity by capacitive stimulation; Right: TEM cross sectional micrograph of thin film stack with TiO_2 as dielectric layers 10

Figure 1.6: Front fans of commercial Rolls-Royce engines made of Ti-6Al-4V 13

Figure 1.7: Pressure tanks manufactured from titanium. 14

Figure 1.8: Unit lattice crystalline structure. 16

Figure 1.9: Schematic view of the oxide film on pure titanium. 17

Figure 1.10: Setup of electrochemical measurement. 20

Figure 1.11: Potentiostatic current–time transient 22

Figure 1.12: Corrosion process showing anodic and cathodic components of current. 23

Figure 1.13: Metallization scheme used in IC technology, showing evolved multilayer structures 34

Figure 1.14: Schematic of metal CMP mechanisms 36

Figure 2.1: Electrochemical cell setting 40

Figure 2.2: Potentiostatic (current vs time) curves of titanium in different H_2O_2 molar concentrations mediums. 45

Figure 2.3: Potentiodynamic curves of bulk titanium at seven H_2O_2 concentrations. ... 47

Figure 2.4: Contact angle data of titanium post potentiostatic scans at different H_2O_2 solutions concentrations. 49

Figure 2.5: RMS roughness series of Ti post potentiostatic measurements. *50*

Figure 2.6: AFM images of titanium surface at potentiostatic tested molar concentrations. *50*

Figure 2.7: Removal rates of Ti CMP at 5 different concentrations. *51*

Figure 2.8: Ti bulk contact angle data post CMP at 5 H_2O_2 concentrations. *52*

Figure 2.9:Post CMP roughness RMS data of Ti with different slurry oxidizer concentrations. *53*

Figure 2.10: AFM images of titanium surface under CMP at different concentrations. *53*

Figure 2.11: Removal Rates of bulk Ti at different solids loading percentages. *54*

Figure 3.1: Potentiodynamic polarization curves of tungsten in hydrogen peroxide mediums. *60*

Figure 3.2: Corroded W surface post potentiodynamic treatment at 1 M. *61*

Figure 3.3: Potentiostatic responses of tungsten at different H_2O_2 concentrations. *62*

Figure 3.4: Roughness RMS value of W surface post potentiostatic transients in H_2O_2 mediums. *64*

Figure 3.5: AFM images of tungsten post potentiostatic scan. *64*

Figure 3.6: Contact angle data of W surface post potentiostatic transients in H_2O_2 mediums. *65*

Figure 3.7: Potentiodynamic curve of deposited Ti in five H_2O_2 concentrations. *66*

Figure 3.8: Potentiodynamic curve of deposited TiN in five H_2O_2 concentrations. *66*

Figure 3.9: Potentiostatic (current-time) sweep of titanium in hydrogen peroxide solutions. *69*

Figure 3.10: Potentiostatic (current-time) sweep of TiN in hydrogen peroxide solutions. *69*

Figure 3.11: RMS roughness of deposited titanium post potentiostatic. *71*

Figure 3.12: AFM topographic images of titanium post potentiostatic. *71*

Figure 3.13: RMS roughness of deposited TiN post potentiostatic. *72*

Figure 3.14: AFM topographic images of TiN post potentiostatic............................... *72*

Figure 3.15: Contact angle data of deposited titanium post potentiostatic. *73*

Figure 3.16: Contact angle data of deposited TiN post potentiostatic........................... *73*

Figure 3.17: Titanium (deposited) RMS roughness data post CMP at five concentrations. *75*

Figure 3.18: Titanium (deposited) AFM images post CMP at five concentrations. *76*

Figure 3.19: TiN (deposited) RMS roughness data post CMP at five concentrations. .. *77*

Figure 3.20: TiN (deposited) AFM images post CMP at five concentrations. *77*

Figure 3.21: Tungsten (deposited) RMS roughness data post CMP at five concentrations. *78*

Figure 3.22: Tungsten (deposited) AFM images post CMP at five concentrations. *78*

Figure 3.23: Titanium (deposited) contact angle data post CMP at five concentrations. *79*

Figure 3.24: TiN (deposited) contact angle data post CMP at five concentrations........ *80*

Figure 3.25: Tungsten (deposited) contact angle data post CMP at five concentrations. *80*

Figure 4.1: Potentiostatic passivation slopes in A/s for Ti/TiN and W in H2O2 mediums. *88*

Figure 4.2: RMS roughness series of deposited Ti, TiN and W post potentiostatic scan at different H_2O_2 concentrated mediums. *89*

Figure 4.3: Contact angle series of deposited Ti, TiN and W post potentiostatic scan at different H_2O_2 concentrated mediums. *89*

Figure 4.4: Corrosion rates series of Ti, TiN and W extrapolated from Tafel data of potentiodynamic in oxidizing mediums. *90*

Figure 4.5: Post CMP calculated removal rates for Ti/TiN and W in H_2O_2 mediums.. *91*

Figure 4.6: Overlaid RMS roughness series for Ti, TiN and W post CMP application. *92*

Figure 4.7: Removal rates as a function of silica solids loadings on CMP of Ti, TiN and W at a fixed oxidizer concentration. *93*

Figure 4.8: RMS roughness data as a function of silica solids loadings on CMP of Ti, TiN and W at a fixed oxidizer concentration. *94*

Figure 4.9: AFM surface images of Ti, TiN and W post CMP in different silica solids loadings percentages. *94*

CHAPTER I

INTRODUCTION

This chapter introduces the various applications of titanium as this metal produces valuable traits and properties. Such applications are in biomedicine and titanium biocompatibility and microelectronics which are investigated according to the surfaces qualities that titanium exhibits. In addition, self-protective properties of titanium are discussed in regards to surface oxide (TiO_2) formation and the properties it adds to titanium performance. Finally, several surface evaluation and modification methods are used on titanium surface which are also further explained in this chapter.

1.1 Literature Review

1.1.1 Application of titanium in advanced processing of materials

Titanium is considered as a very valuable material in many engineering applications due to its specific mechanical and chemical characteristics. A review of two engineering applications of titanium are detailed in this section which are the focus of this thesis namely the applications in biomedicine and microelectronics. In addition, other engineering applications are discussed where titanium has a great history of enabling effective engineering solutions and durable performance.

1.1.1.1 Biomedical applications of titanium

Metals and their alloys used for biomedical applications cover a wide spectrum and must demonstrate specific properties such as biocompatibility, corrosion resistance and durability for a long period of time in-vivo. Typical metallic materials used in

biomedical applications are stainless steels, cobalt alloy, titanium and titanium alloys. Titanium is the newest metallic biomaterial that has been introduced in both medical and dental fields, and has demonstrated success due to its lower modulus (enabling a high strength to density ratio), low level of electronic conductivity, thermodynamic state of stability at physiological pH values in addition to low ion-formation tendency in aqueous environments, and an isoelectric point of the titanium oxide being at pH 5 to 6 leading to superior biocompatibility and better corrosion resistance. These attractive properties were the driving force for the early introduction of (cpTi) and (Ti–6Al–4V) alloys as well as the more recent development of modern Ti-based alloys and orthopedic metastable titanium alloys. Commercially pure titanium (cpTi) is considered to be the best biocompatible metallic material because its surface properties result in the spontaneous build-up of a stable and inert oxide layer that tends to be self-protective. [LIU2004] The applications of titanium and its alloys can be classified according to their biomedical functionalities which are introduced next.

1.1.1.2 Bone and other hard tissue replacements:

The hard tissue replacements are one of the predominant applications of titanium and its alloys as in-vivo implantations. This type of joints consists of a femoral head and cap, so called an articulating bearing and stem as demonstrated in Figure 1.1 [Bo1980]. The positioning of the articulating bearing should be maintained in a way that it reproduces the natural movement inside the hip with the assistance of the stem, which in regards to the joint it works to secure the positioning of the femoral head in relation to its other components. Titanium and titanium alloys are also often used in knee joint replacements, which consist of (i) femoral component, (ii) tibial component and (iii) patella. For such types of artificial joints, two types of bone fixation methods are

currently being used. The first is bone cement fixation and the second is the cement-less fixation. The method of fixation depends directly on the type of anchoring in the human body. For the cement type, a continuous cement mantle is applied which is well anchored in the bone and lies closely against the implant. Failure in such type of prostheses happens when the interface accompanied by the micro-movements between the metal and the cement starts loosening, consequently initiating the formation of metal particles and release of metal ions. Anchoring of the prosthesis directly to the living bone as in the case of cement-less method (which is done through osseointegration) is a more recent technique. Cementless prostheses implantation with an optimized surface structure and composition can create durable mechanical interlocking between the implant and the bone tissue through enabling osseointergration. Hence, surface structuring becomes critical and commonly practiced such as rough surfaces, porous coatings and surfaces with osteoconductivity and osteoinductivity in the body fluids. [Bo1980]

Undesirable tissue reactions can arise from hard tissue replacements when the biocompatibility of the material is poor. Therefore, bio-inert materials are utilized to minimize the risk. Titanium, with its native surface oxide that forms spontaneously when in contact with oxygen is known to be bio inert, but it is difficult to achieve good chemical bonding with bones and form new bones on its surface at the early stages after implantation. Hence, titanium and titanium alloys are subjected to surface modification techniques as to produce properties such as less wear, fatigue strength, and long-term biocompatibility and meet the corresponding requirements to be able to meet the longer human life expectancy and the durability for younger patients requiring implants.

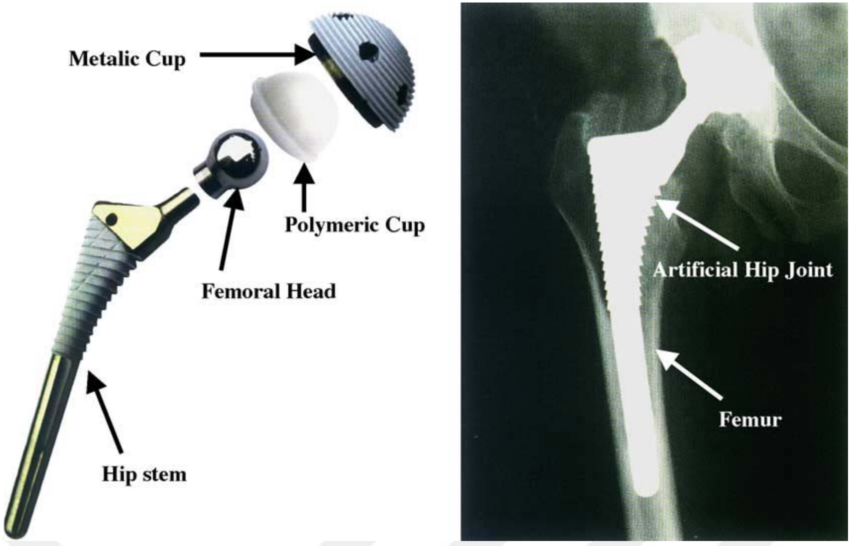

Figure 1.1: Schematic diagram of artificial hip joint. [Bo1980]

1.1.1.3 Dental implants:

Titanium and its alloys are widely used in dental implants and are classified into subperiosteal, transosteal, and endosseous; which are described in table 1.1. The last two are the most commonly used type of implants where endosseous implants can be placed in both the upper and lower jaws via a mucoperiosteal incision while transosteal implants can only be placed in the frontal lower jaw. Figure 1.2, shows a type of endosseous implants which are screw-shaped devices and cylinders. Surface modification technologies, such as grist blast, chemical etching, and plasma spraying are mainly used to improve the osseointegration ability of the titanium based dental implants.

Table 1.1: Types of titanium dental implants [Ta2018]

Implant Type	Description	Illustration
Endosseous	These implants are usually shaped like a screw or cylinder and are made either of metal, metal covered with ceramic, or ceramic material. They are placed within the jawbone. There are also blade-shaped endosseous implants.	
Subperiosteal	These implants consist of a metal framework that attaches on top of the jawbone but underneath the gum tissue.	
Transosteal	These implants are either a metal pin or a U-shaped frame that passes through the jawbone and the gum tissue, into the mouth.	

Figure 1.2: Examples of commercial dental implant designs. [Con, Brazil]

1.1.1.4 Cardiac and cardiovascular applications:

Another common application of titanium in the field of biomedicine is in cardiovascular implants. Titanium outstands due to its advantageous and unique properties as a strong, inert, and non-magnetic material. In artificial heart and circulatory assist devices, titanium and its alloys are used both in the mechanical components of the pump and as a blood-contacting surface. Artificial hearts made entirely out of titanium have in general not been very thriving in clinical applications largely due to problems with blood-clotting taking place on the device surface. [Ri1993]

A Common design of prosthetic heart valve is shown in Figure 1.3. The ring and struts are produced from titanium or titanium alloys while the disk is made of pyrolytic carbon. These metals in such prosthetic heart valves are often coated with a thin carbon film to improve blood compatibility on the implant surface. Nickel–titanium alloy is one of the well-known materials used in vascular stents as a treatment of cardiovascular disease, where they dilate and keep narrowed blood vessels open due to its special shape memory effects.

Figure 1.3: Artificial heart value. [LIU2004]

1.1.1.5 Microelectronics applications of titanium

Integrated circuit device fabrication technology focuses on the techniques and materials to produce smaller and faster devices for higher performance microprocessors to be built. This trend towards miniaturization has led to demand for improved semiconductor integrated circuit (IC) interconnect performance and improved manufacturability, resulting in a shift from conventional Al/SiO_2 interconnect architectures to tungsten-based and copper-based metallization in conjunction with low-K (permittivity) dielectrics. [Pa1998] Recent technologies involving tungsten (W) via connection to transistors require the addition of a barrier between W and the dielectric layer to enhance the adhesion and to limit any diffusion from the metallic layers into the transistors which can stop their activity. Ti/TiN are typical diffusion barriers to tungsten (an example shown in figure 1.4) due to their thermal and chemical stability and their ability to passivate which creates an oxide layer that promotes adhesion.

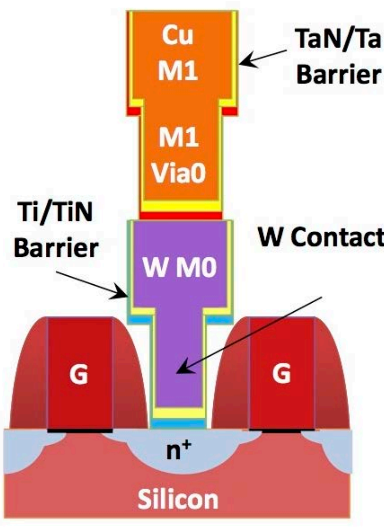

Figure 1.4: Ti/TiN barrier layer with the W contact integration. [Der2017]

The high dielectric constant of titanium dioxide (TiO_2) also leads to multi-faceted prospects for the use of this material in microelectronic devices. The TiO_2 films have been evaluated for various microelectronic applications and presented acceptable properties such as low leakage current density of 1.0×10^{-5} A/cm at 1 V and band gap of 4.6 eV, to be applied in gate oxide in metal oxide semiconductor field effect transistors (MOSFETs). [Ra2011]

1.1.1.6 Challenges presented in MOS devices fabrication:

Metal oxide semiconductor (MOS) transistors are a key element presented as an electrical switch in logic circuits. Developments presented in microelectronics transistor fabrication are focusing mainly on two issues. (i) transistor gate lengths known as the device nodes continuously get smaller and (ii) the number of transistors interconnected on the state-of-the-art chips will be in excess of 10 billion (when, why etc needed). The MOS transistor scaling beyond the present 32 nm design makes it difficult to fabricate

high quality ultra-thin oxides. Even though it is necessary to scale down the gate oxide thickness, there are additional two major limiting factors to overcome;

1. Reliability, as the gate oxide thickness decreases, the breakdown voltage also decreases because of the increased electric field at a given gate bias.
2. Leakage current becomes a problem as the thickness of the dielectric layer (typically SiO_2) reaches its direct tunneling limit below 7 nm. In order to reduce the electric field physical thickness of the gate oxide needs to be increased or the power supply voltage needs to be decreased. Therefore, the challenge is to increase the physical thickness of the gate dielectric or introduce new materials with lower dielectric constant in order to reduce the tunneling current.

So to abide with the trend of scaling down of complementary metal oxide semiconductors (CMOS) transistors, it requires the substitution of conventional SiO_2 layer with higher dielectric constant (K) material for gate dielectrics [Gu2001].

Thin film titanium dioxide capacitors:

In an attempt of finding a material that would yield a dielectric constant higher than silicon monoxide (SiO) and tantalum pentoxide (Ta_2O_5) for microelectronics applications, thin-film titanium dioxide based capacitors were used. TiO_2 in its stable tetragonal rutile structure attains a higher dielectric constant between 90 to 110 as compared to SiO and Ta_2O_5 which possess K values of 4 to 10 and 14 to 28, respectively. Acceptable TiO_x capacitor films are produced by anodic oxidation of base metal films at a temperature of 700°C for one hour. [Se1963] These films show adequate characteristics reported by [Ke1965] such as;

(i) Capacitances ranging from 0.1 pF/cm^2 to 0.6 pF/cm^2 for film thicknesses of 1700 Å to 500 Å.

(ii) Low dissipation factor between 12 to 20 %.

(iii) High insulation or leakage resistance of 5×10^5 Ω.

(iv) Low temperature coefficient as low as +700 ppm/°C and as high as +1500 ppm/°C.

(v) High voltage breakdown ranged from 8 volts to 65 volts.

Figure 1.5 shows an example of a thin film TiO_2 based capacitor compatible with existing thin-film resistors and thin-film conductors which can be produced on inert substrate.

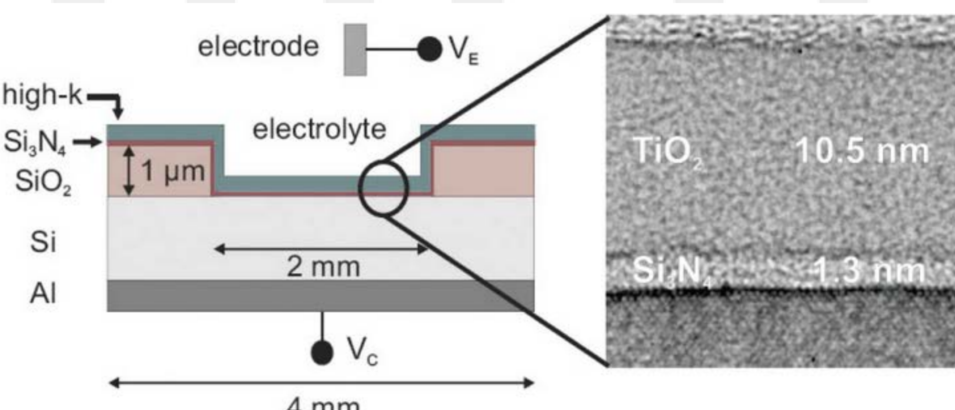

Figure 1.5: Left: Principle setup for measurements of neuronal activity by capacitive stimulation [Fr2003] ; Right: TEM cross sectional micrograph of a "state of the art" thin film stack with TiO_2 ($k \approx 40$) + SiNx ($k \approx 7$) as dielectric layers on conductive Si. [Wa2006]

1.1.1.7 Other engineering applications of titanium

Titanium excels in other engineering application due to its highly corrosion and oxidation resistance, thermal resistivity, relative lower weight than other materials involved in the same application. High durability and chemical compatibility gives it an advantage in several industrial applications which are described and assessed in this section.

Aerospace applications:

The preliminary production of the main titanium alloys that are used in aerospace applications started in 1940s. The main driving properties of titanium and its alloys compared to existing materials used in aerospace applications are:

- Weight reduction (substitutes for steels and Ni-based super alloys.
- Application temperature (substitutes for Al alloys, Ni-based super alloys and steels).
- Corrosion resistance (substitutes for Al alloys and low-alloyed steels).
- Galvanic compatibility with polymer matrix composites (substitutes for Al alloys).
- Space limitation (substitutes for Al alloys and steels).

The percentages of titanium in the structural weight of modern large commercial aircraft and gas turbine engines are 7% compared to Al 65% and Ni 39%, respectively. [Pe1995]

Turbine engines:

One of the main applications of titanium in aerospace industry is in the gas turbine engines. The large front fan blades of modern jet engines are currently often made from titanium alloys; an example is shown in Figure 1.6. The latest generation employed are the wide chord fan blades that improved the engines fuel and aerodynamic efficiencies. General electric was first to use fiber reinforced polymer composites in the fan blades and titanium was used in the design of leading edges of these types of blades to meet erosion resistance necessary. Later, Rolls-Royce and Pratt & Whitney have emerged with a hollow titanium fan blade technology.

Temperature limitations are imposed upon the use of titanium alloys in the hottest part of the engine compressor, i.e. the disks and blades of the last compressor stages. For that, development of alloys which can possess high temperature strengths is needed. Examples of these alloys are IMI 834 (near α-class alloys) with a possible application at almost 600°C, titanium aluminides with an application temperatures of 650°C and 800°C. These alloys are resistant to initiating titanium fire and titanium matrix composites have potential applications in cylindrical components in high-pressure components. [Pet2003]

β types of titanium alloys are extensively used in aircraft component production and the relatively new β alloy, β-21S has an excellent oxidation resistance with good creep properties. It is also resistant to attack by thermally decomposed hydraulic fluid, the only titanium alloy that has been identified to date with this attribute. All the above applications are driven by the need of weight reduction and improved performance. [Bo2005]

Figure 1.6: Front fans of commercial Rolls-Royce engines made of Ti-6Al-4V (Rolls Royce plc., Derby, UK)

Space applications:

Titanium and its alloys are used extensively in space vehicles providing effective density to strength ratios. Fuel and satellite tanks are the main applications of titanium over high-strength steels, due to its lightweight, high strength and long term chemical compatibility as illustrated in Figure 1.7. Ti-3Al-2.5V was developed, among others, for low temperature applications and shows good toughness and ductility as far as cryogenic temperatures. Accordingly, it is used for high-pressure piping in the hydrogen pumping systems of the US Space Shuttle manufacturing. Lastly, β-alloys show very acceptable mechanical properties. Among others, spin forming is used for the production of the half-shells for satellite tanks such as the one used in the Storable Propellant Stage (EPS) tanks for the upper stage of the Ariane 5 (what is this?). This method requires cheaper infrastructure and tooling costs. [Ri2001]

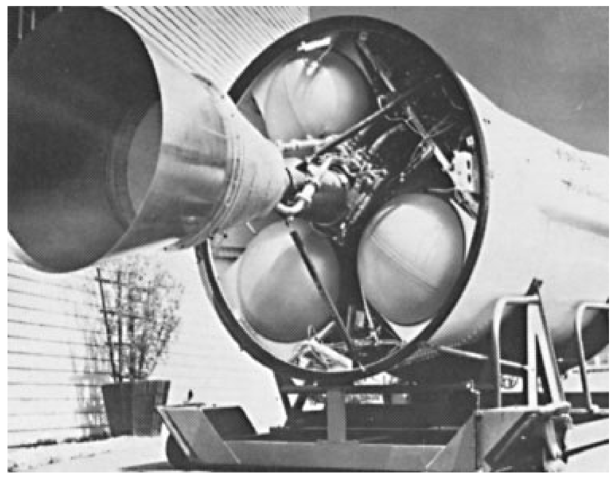

Figure 1.7: Pressure tanks manufactured from titanium. (TIMET, Henderson, NV USA)

Industrial applications:

The investment of titanium in the industry is expanding as it can reduce lifecycle costs across a wide range of tools and processes. Known for its high strength to weight ratio, titanium can perform the same job with half the amount (weight) required for the same strength as compared to an equivalent type of material. The fact that titanium forms an intact surface oxide layer, which is an effective corrosion inhibitor is another important factor for its choice among the other metals.

As an example, in power generating plants, where saline, brackish or polluted waters are used as the cooling medium, titanium thin wall condenser tubings last longer or through the lifetime of the plant, eliminating the need for a corrosion allowance. Likewise, in petroleum exploration and production, titanium pipe's light weight and flexibility makes it an excellent material for deep sea production risers. Also, titanium's resistance to attack by sea water makes it a favored material for topside water management systems. Moreover, since it shows virtually no corrosion in salt water,

titanium is also the material of choice in desalination plants worldwide. In addition, a number of chemical processing operations specify titanium to increase equipment life. It offers lifecycle cost advantages over copper, nickel and stainless steel grades, while providing initial cost advantages over materials such as high nickel alloys, tantalum and zirconium. [AZoM2002]

1.1.2 Self-protective properties of titanium through surface oxide (TiO_2) formation

1.1.2.1 Titanium surface passivation theory (and TiO_2 properties)

As discussed previously in this chapter, the wide use of titanium in applications that require surface stability under mechanical or chemical environment changes is attributed greatly to the oxide film inhibited on the titanium surface under various conditions.

The native oxide film is known to grow spontaneously on titanium surface upon exposure to air, or an oxidizing medium because it is highly reactive with oxygen. The passivity of titanium surfaces is demonstrated in the chemical reaction;

$$Ti + 2H_2O \rightarrow TiO_2 + 4H^+ + 4e \qquad (1.1)$$

The titanium dioxide (TiO_2) is an extraordinary oxide since it does not only meet the passivation requirement but also it has outstanding properties such as non-toxicity and chemical stability in hostile environments. It exists in amorphous form and crystallizes in three distinct crystallographic structures: two tetragonal phases, anatase (a=b= 3.785 Å, c=9.514 Å) and rutile (a=b=4.587 Å, c= 2.953 Å) as shown in Figure

1.8, and a third orthorhombic phase, brookite (a= 5.456 Å,b= 9.182 Å,c= 5.143 Å). [Ma2002]

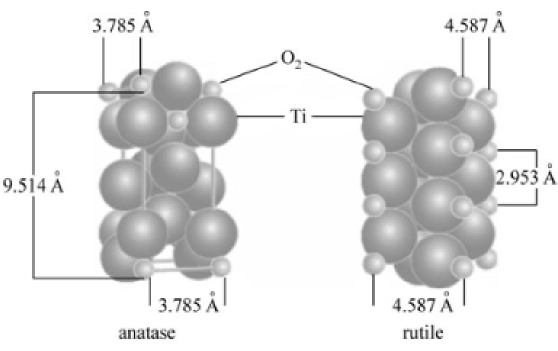

Figure 1.8: Unit lattice crystalline structure.

The amorphous crystal structure of mostly grown oxide layers, their homogenous morphologies and stoichiometric defectivity provide outstanding corrosion resistance. [Liu2015] Titanium dioxide is found in the nature mostly as the minerals rutile, anatase and brookite. In addition, titanium is also known for its re-passivation ability, which is preferable in many polishing treatments tuning its surface biocompatible. All of this is related to titanium oxide’s chemical stability and structure that has a thickness of only few nanometers.

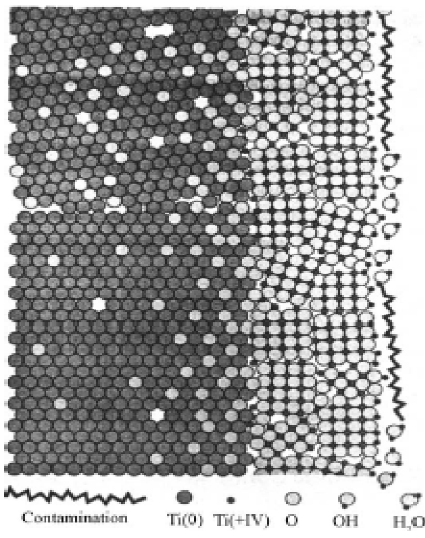

Figure 1.9: Schematic view of the oxide film on pure titanium. [Te2001]

The protective nature of TiO_2 produces continuous, pore free and adhesive films, and thereby exhibit a high degree of immunity to attack by most mineral acids and chlorides. To improve those properties different surface modification methods are introduced to the surface of titanium such as chemical etching, thermal treatment and electrochemical anodization. [Va2008]

Table 1.2 lists the properties of titanium and TiO_2 which clearly justifies the applications of the titanium metal/oxide combinations in advanced applications such as medicine, microelectronics, aerospace, etc'. In addition, their suitability into different mediums such as acidic/basic environments for which further alloying of titanium is shown to improve its corrosion resistance by shifting its corrosion potential is also implementable. [CERAM2002]

Table 1.2: Various properties of titanium and TiO_2

Properties	**TiO_2**	**Ti**
Density	4 g/cm^3	4.50 g/cm^3
Porosity	0%	---
Young's Modulus	230 GPa	116 GPa
Shear Modulus	90 GPa	43.0 GPa
Dielectric Constant (1MHz)	85	---
Thermal Conductivity (25°C)	11.7 WmK-1	21.9 WmK-1
Breakdown Potential	2 MV/m	80 V (in tap water)
Resistivity	1×10^{11}ohm.m	56×10^{-8}ohm.m

1.1.2.2 Corrosion characteristics of titanium and its oxide films:

Corrosion resistance of titanium is achieved by the formation of a protective surface film of stable oxide or chemically absorbed oxygen. However, anhydrous conditions in the absence of a source of oxygen may result in titanium corrosion due to the fact that the protective film may not be regenerated or could be damaged. Corrosion of titanium is uniform since there is little evidence of pitting corrosion or other serious forms of localized attack on titanium surface. Generally, it is not subject to stress corrosion, corrosion fatigue, or galvanic corrosion. Its corrosion resistance is equal or greater to 18-8 Stainless Steel. High temperature oxidation tends to enhance the formation of the chemically resistant, highly crystalline rutile, whereas, lower temperatures often generates the more amorphous anatase state, or a mixture of rutile and anatase.

Experiments with acid and saline solutions show titanium polarizes readily. The resultant effect is generally the reduction in current flow in galvanic and electrochemical corrosion cells. Corrosion currents on the surface of titanium and metallic couples are naturally limited. This relatively accounts for good resistance to many chemicals. In addition, the material may be used with some dissimilar metals with no harmful galvanic coupling effects on either metal. The primary forms of corrosion that have been observed on titanium and its alloys include general corrosion, crevice corrosion, anodic pitting, hydrogen damage, and stress-corrosion cracking. [To2001]

1.1.3 Electrochemical methods for surface passivation evaluation

In a testing system, an electrochemical (polarization) cell is setup as illustrated in Figure 1.10 that is consisting of an electrolyte solution, a reference electrode, a counter electrode, and the metal sample of interest connected to the working electrode. The electrodes are connected to an electronic instrument called a potentiostat. The working, reference, and counter electrodes are immersed in the electrolyte solution, generally a solution that most closely resembles the actual application environment of the material being tested. In this cell, an electrochemical potential (voltage) is generated between the different electrodes. These types of experiments measure and/or control the potential and current of the oxidation/reduction reactions. [HA2014] [Ro1990]

Two types of electrochemical surface evaluation tests are introduced in this work on titanium and other materials to investigate their corrosion and film growth

characteristics are introduced in the following namely the potentiostatic and potentiodynamic polarizations.

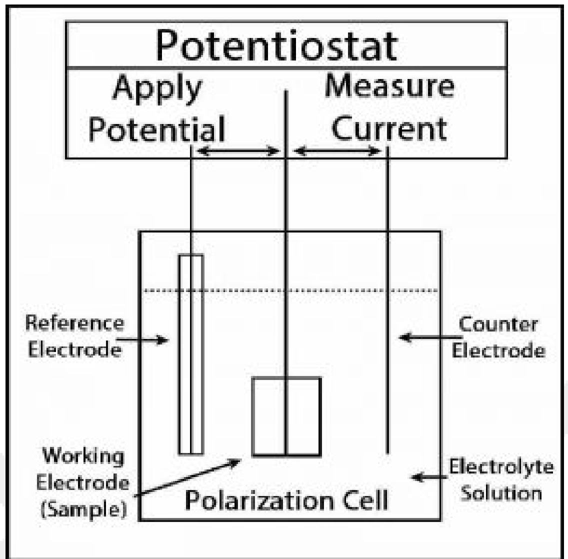

Figure 1.10: Setup of electrochemical measurement.

1.1.3.1 Potentiostatic (current vs. time) transient

The potentiostatic test allows controlled polarization on metal surfaces where constant potential is applied between the sample (working electrode) and the reference electrode for a predetermined time period in order to observe cathodic and anodic behaviors. The reference electrode is used to monitor and maintain potential at the working electrode surface. The potentiostat monitors ionic current passing through the electrolyte solution between the counter electrode and the working electrode, and electron current passing between the counter electrode and the working electrode. The resultant current measured on the sample's surface and plotted versus time. Depending on the surface characteristics and the weight of the applied potential in reference to critical (pitting) potential, the response can indicate film growth (passivation), pitting or

breakdown as illustrated in Figure 1.11. This method of evaluation can assist in determining the following properties in the material; [Co2017]:

- Open circuit or corrosion potential
- Instantaneous corrosion rate
- Passivation behavior
- Pitting potential and susceptibility
- Crevice corrosion susceptibility
- Sensitization of heat affected zones
- Galvanic corrosion behavior of dissimilar metal pairs

In the case of metals like titanium that experience oxide film formation in the presence of oxidizing media, film growth kinetics fit the model proposed by MacDonald [Mac1981];

$$I = At^{-n} \tag{1.2}$$

where A and n are constants dependent on the value of the applied potential and the type of electrolyte. The value of n represents the oxide growth rate and is given by the slope of the descending part of the relationship.

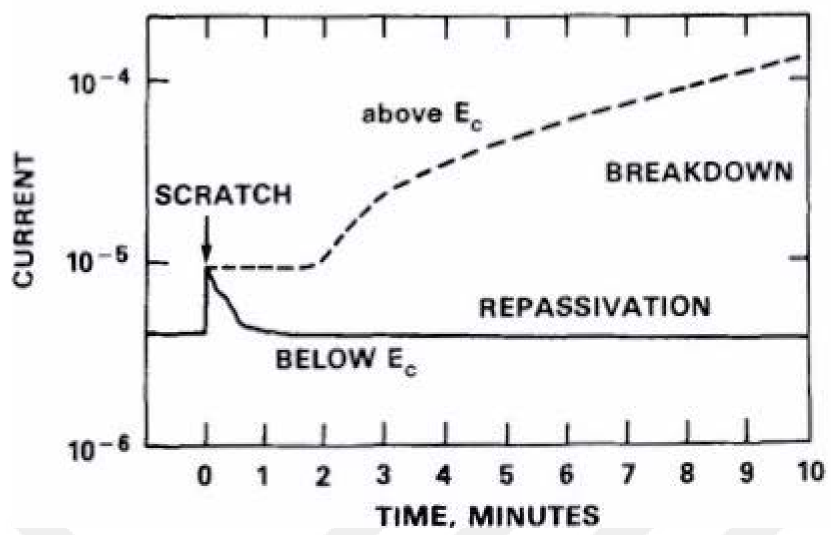

Figure 1.11: Potentiostatic current–time transient. [Ro1990]

1.1.3.2 Potentiodynamic polarization

Potentiodynamic scan is a qualitative test to evaluate the passivation propensities of a metal sample by producing its current-potential relationship under the controlled test conditions. This scan allows for the extrapolation of the kinetic and corrosion characteristics of a metal substrate in aqueous environments. Cathodic or anodic polarization can be performed via this test. In potentiodynamic anodic polarization the specimen's potential (working electrode) is scanned slowly from negative to positive direction acting as an anode such that it corrodes or forms an oxide film. Investigations such as passivation tendencies and effect of oxidizers or inhibitors on the tested sample is accomplished via this method. It is also a commonly used technique to simulate corrosion characteristics of metals during chemical mechanical planarization (CMP). [PrCORR-1]

In a single sweep, the applied potential is increased as a function of time while the current is constantly monitored. As shown in Figure 1.12, the electrical potential is plotted versus the logarithm of current (or current density). The theoretical current for the anodic and cathodic reactions is represented as straight lines. The curved line is the total current, which is the sum of the anodic and cathodic currents.

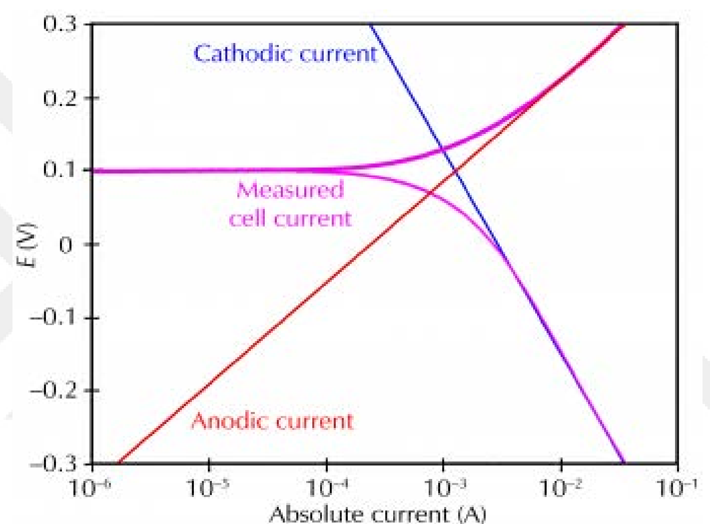

Figure 1.12: Corrosion process showing anodic and cathodic components of current. [Gamry2017]

When the sample's surface is placed in a corrosive medium, both oxidation and reduction reactions occur, where usually the sample oxidizes (corrodes) and medium solution is reduced. Both anodic and cathodic currents occur as illustrated in Figure 1.12 as straight lines intersecting at the point of equilibrium potential as both cathodic and anodic currents are present on the surface, where the rate of oxidation is equal to the rate of reduction. At this point, the potential and current values are designated as E_{CORR} and I_{CORR}, respectively.

The corrosion potential (E_{CORR}) is measured by the potentiostat as an energy difference between the working electrode and the reference electrode. At the cathodic part of the potentiodynamic curve (below E_{CORR}), the current decreases as the specimen's surface tends to passivate. In the contrary, the anodic part (below E_{CORR}) shows the current increasing as the passive film breaks down in that region and electrons flow from the surface. The corrosion current (I_{CORR}) can be estimated from the curve and is used to calculate the corrosion rate of the metal. In any real system, I_{CORR} and corrosion rate are a function of many system parameters, including type of metal, composition of the solution, temperature, movement of the solution, metal history etc'. [Ga2017]

Tafel plots:

A Tafel plot is achieved by extrapolating the linear portions of the logarithmic current versus potential plot back to their intersection at E_{CORR}. The corrosion current (current density) is obtained from this plot at the point of intersection followed by the corrosion rate, which is calculated from I_{CORR}. Tafel equations for the anodic and cathodic reactions in a corrosion system are combined to generate the Butler-Volmer equation that is implemented with the mixed potential theory resulting in the basic kinetic equation as given in Equation 1.3, [Zh2009]:

$$I = I_{corr}\left(e^{\frac{2.303\,(E-E_{corr}\,)}{\beta a}} - e^{\frac{2.303\,(E-E_{corr}\,)}{\beta c}}\right) \tag{1.3}$$

where, E is the potential applied to polarize the corrosion system,$I$is the measured current from the cell in amperes; and E_{corr} and I_{corr} are the corrosion

potential and corrosion current in amperes, respectively. βa and βc are the cathodic and anodic Tafel slope, respectively, and are given in volts/decade.

The next step is to calculate corrosion rate which implements Faraday's law and weight loss calculations to deduce to the following formula in Equation 1.4;

$$\text{Corrosion Rate (mpy)} = \frac{I_{corr}\, K.EW}{d.A} \tag{1.4}$$

Where EW is the equivalent weight of the specimen in grams/equivalent, K is a constant that defines the units for the corrosion rate, $d$is density of the specimen in g/cm^3, A and is the sample area in cm^2.

1.1.4 Impact of self-protective surface film for application of titanium in biomedicine

1.1.4.1 Biocompatibility of titanium

A material implanted in a human's body requires to be biocompatible, that is it does not educe an adverse reaction with the host for its designated application surrounded by human tissues and fluids. Biocompatibility of titanium is concerned with two main issues which are thrombosis, that involves blood coagulation and adhesion of blood platelets to biomaterial surface, and the fibrous tissue encapsulation of biomaterials that are implanted in soft tissues. [Vi2017] The relative inertness of titanium is due to its surface oxide film that inhibits corrosion significantly in a biological environment.

In the implantation of a blood contacting biomaterial, the first action that rapidly takes place is blood protein adsorption at the solid-liquid interface. Titanium is found to

readily adsorb proteins and depending on the exposure time, the composition of the adsorbed protein layer varies and proteins with stronger adsorption are favored. A resident protein layer is formed which impacts the interaction of platelets, activation of intrinsic coagulation, adhesion and aggregation of platelets and activation of the complement system. Several studies have reported the haemo-compatibility of titanium. [Ba2012]

For bone implants, osseo-integration must be achieved, particularly by creating a strong and long lasting connection between the implant surface and peri-implant bone, leading to a stable mechanical attachment of the implant at the location of the implantation. [Br1977] Titanium surfaces support cell growth and differentiation. It is integrated in bone in close apposition to the mineralized tissues under the proper pre-conditions. It is generally accepted that the osteo-progenitor cells migrate to the implant site and differentiate into osteoblasts that make the bone tissue. However, titanium and bone surface are generally separated by a thin soft tissue layer as a result of a weak foreign body reaction that prevents titanium from being in direct contact with the bone. Instead, the bond associated with osteo-integration is regarded to be mechanically interconnecting to the titanium surface asperities and pores in the bones. [Xi2001]. Moreover, for both orthopedic and dental implants, fibrous encapsulation is not desirable as it cannot withstand the same physical stresses as bone, thus leading to micro movements.

Surface modifications on metals are required to overcome biocompatibility issues and to decrease implant failure or rejection. Bone regeneration is a slow process and therefore improvements are researched in order to achieve faster osseo-integration, either by morphological modifications or by various coatings. Another common cause

of implant failure is bacterial infection and the possibility of a bacteria repellent surface modification is worth investigating. The current most common method of surface improvement is by modification of the implant's surface properties, either morphologically and/or by biochemical coatings. It follows that there is a great need for surface modification of implants in order to improve tissue adhesion, implant integration, decrease bacterial adhesion and decrease inflammatory response or to avoid the foreign body response. [Ku2014]

1.1.4.2 Surface modifications of titanium implants

This section follows the discussion of enhancing titanium's biocompatibility by presenting surface modification methods, including the mechanical, chemical and physical methods used for surface morphology modifications through increasing roughness, downscaling topography from the micro- to the nano-scale, tailoring the nanoscale morphology, or for achieving different coatings on the surface of the implant. Results of in vivo and in vitro tests provided that the micro structured surfaces deliver a better implant surface to bone contact and an increased mechanical retention after implantation.

Mechanical methods:

The primary goal of mechanical modification is to obtain specific surface topographies, to clean or roughen the surface, which could lead to enhanced adhesion in bonding, as the roughness of the structure would be more favorable for bio-mineralization due to the increased surface area. [Go2011] Titanium based biomedical devices such as orthopedic devices, surgical bone fixture and plates, fixation screws, prosthetic dental implants, orthodontic mini screws, etc., are generally milled from

blanks of titanium alloy. Common mechanical surface modification methods, such as machining, polishing, and blasting involve physical treatment by shaping or removal of the materials surface to modify its characteristics and features.

Machining is one of the mechanical processes where the surface features of the metal is modified by cutting them into a desired final shape and size by a controlled process of material removal. This method is utilized to shape titanium alloys. Issues with machining titanium alloys originate from high cutting temperatures, chemical reactions with tool, and relatively low modulus of elasticity [Ma1990].

Polishing of titanium and titanium alloys produces a high level of surface planarity which is typically in the range of micrometer to nanometer level. Polishing of titanium can be performed mechanically; by using polishing agents such as silicon carbide, diamond paste, alumina, as well as through electrolytic process (by applying a low voltage). Polishing offers specific benefits like creating shiny and mirror like finish, easy maintenance of hygienically clean surface due to reduced particles adhesion, providing metallic purity in addition to low cost. [Bl1998]

Blasting the surface of titanium with silicon carbide (SiC), alumina (Al_2O_3), biphasic calcium phosphate (BCP) and beta-tricalcium phosphate particles of appropriate size is one of the most used methods of achieving the desirable surface roughness. Surface roughness created by these methods provides an expectable attachment and growth of oral soft tissues (e.g. human gingiva and periodontal ligament fibroblasts) on the treated titanium surface [Co1994]. There are some concerns regarding the blasting of titanium surface by using SiC and Al_2O_3 because of higher odds of surface contamination and localized inflammatory reaction of the hard and soft

tissues due to localized dissolution and leaching of the alumina particles into the host hard and soft tissues. [Gb2003]

Physical methods:

Physical surface modification methods cover processes such as thermal spraying, physical vapor deposition (PVD), ion deposition and glow discharge plasma treatment, where chemical reactions are absent. The surface modified layer, film or coating obtained on the titanium substrate is largely a product of the thermal, kinetic, and electrical energies.

In thermal spraying methods, the coating thickness is in the range of micrometers to millimeters. It is obtained by thermally melting the coating materials into liquid droplets and spraying them onto the titanium surface at high speeds. According to the maximum tolerable temperature, thermal spraying may be separated into flame and plasma spraying, in which, plasma spraying can be utilized at very high temperatures. Other methods can be listed as arc spraying, laser spray and detonation gun spray. The characteristics and performance of plasma spray material coatings on titanium surface is dependent on several factors such as particle size and velocity, plasma gas and its flow, substrate angle, distance and cooling rate. [Gr1998] The quality of the coating is assessed by measuring its porosity, oxide content, macro and micro-hardness, bond strength and surface roughness. For titanium implants used in orthopedics, this method is favorable for bone substitutes since it produces a rougher surface as compared to other methods. Plasma spray of titanium coatings with porous structures has been commonly used in dental applications like prosthetic implants and bone plates. The porosity on the modified titanium alloy surface excites the growth of

hard tissue, which in order provides the mechanical retention and support to the prosthesis.

Hydroxy apatite coating on titanium has been applied through high velocity oxy-fuel torch (HVOF) and Detonation (DGUN) with satisfying results. HVOF technique has been shown to improve the mechanical properties of hydroxy apatite based coatings on titanium alloys [Kh2003]. The second technique produced denser amorphous coating of hydroxy apatite. The intrinsic features such as lower crystallinity and higher residual stress of the hydroxy apatite coating via DGUN results in improved rate of its dissolution in vitro and in vivo as compared to the plasma coating. [Gr2002]

Physical vapor deposition (PVD) consists of evaporating or sputtering the target materials in a vacuum that is then deposited on the surface of the substrate where a thin film is gown by condensation or by reaction with the surface of the material. This method is applied on titanium surface as to improve and enhance biocompatibility, bioactivity and triobological behavior of the implant. Physical vapor deposition includes evaporation, ion plating and sputtering.

In evaporation, there is collision transport of coating at pressure of 0.1-1 Pa, which gets condensed on the titanium substrate kept at the ground potential. Deposition rate of target material is typically in the range of 10,000-25,000 nm/min. It is successfully used for obtaining TiC and TiN coatings by evaporation of Ti in the presence of an acetylene and nitrogen plasma [Ja1993]. In ion plating, high energy particles bombarded on titanium surface influencing film formation. It is possible to achieve optimal tribological properties and chemical inertness of the modified surface. The deposition rate of the coating material is generally in the range of 10,000-25,000

nm/min. Out of all the previously mentioned PVD methods, sputtering is preferred for deposition of thin films on titanium due to its simplicity and flexibility. For biomedical applications, sputtering is mainly used to deposit thin films on titanium and its alloys so as to enhance their bioactivity, biocompatibility, wear and corrosion resistance. Deposition rate for target material is in the range of 25-1000 nm/ min with pressure in the range of 2-15 Pa. Recently, sputtering was also used for deposition of hydroxyapatite nano-coatings for biomedical applications [Me2013]. Ion implantation is performed by introducing ions when bombarding the surface layer of a solid substrate and depending on the shape of the sample, conventional beam-line ion implantation or plasma immersion ion implantation are used. Both methods have proved to improve the corrosion resistance of metals and alloys. Most commonly used elements for ion deposition on titanium alloys are nitrogen, carbon and phosphorous. [Sh2015]

Chemical methods:

These methods equip titanium with bioactive surface characteristics and improve bone conductivity, corrosion resistance and removal of contamination. The mostly applied chemical surface modification methods are chemical treatment of titanium surface with acid/alkali, chemical vapor deposition and sol-gel deposition.

Chemical treatment is applied by immersing titanium in alkali solution and applying heat treatment, to dissolve the surface oxide layer and form an amorphous layer on the surface, which contains alkali ions. Alkali and heat treatment or acid etching followed by alkali treatment of titanium alloy causes formation of bioactive, nanostructured titanate layer on the outer layer of the surface. Placing those treated

surface in contact with bodily fluids, the surface chemically reacts with the surrounding C^+ ions that leads eventually to the formation of calcium titanate, which is essential for the adhesion, spread and growth of the osteogenic cells. Studies show that this treatment allows direct growth of hard tissues on its surface without any intermediate fibrous layer formation when placed inside a biological system [Ho2009]. The rate of formation of apatite in titanium alkali with heat treatment is considerably rapid and the bond strength in between the implant bone interface is adequately high. Acid treatment of the titanium utilizes a combination of acids such as is nitric acid and hydrofluoric acid and is also routinely used for removal of surface contamination and for providing a clean and uniform surface. During these treatments transformation of the titanium surface to soluble titanium fluorides takes place which roughens the metal's surface.

Hydrogen peroxide treatment of titanium is an adverse technique for chemical dissolution and oxidation. Treatment of titanium with hydrogen peroxide and hydrochloric acid in the temperature ranges of 400-500°C leads to more stable titania gel structure, which Improves biocompatibility, bioactivity and bone conductivity due to the gel formed on the surface inducing the formation of apatite nucleation site when soaked in the bodily fluid [Wa2002].

In Chemical Vapor Deposition (CVD) procedure, which is widely used, chemical reactions occur between the chemicals in the gas vapor and the chemicals on the surface of the titanium. As a consequence, a non-volatile compound is deposited on the substrate of the metal. One of the most capable applications of this process in the field of biomedical sciences is diamond like carbon (DLC) coating of titanium alloys. Diamond like carbon coated metals and alloys have interesting biomedical features due to their better tribological features such as the improved wear resistance, corrosion

resistance and blood compatibility. Diamond like carbon coating is the only surface modification procedure of titanium and its alloys, which provide both increased hardness and low friction under dry as well as wet sliding conditions. This feature is important for orthodontic wires and various joint implants. [Ko2005]

In sol-gel deposition method, chemical reactions happen not at the interface between the sample surface and solution or gel, but rather in the solution, which contains solid particles dispersed in the liquid as a colloidal suspension. Largely, the sol-gel method is used in order to deposit thin (<10μm) ceramic coatings. The sol-gel process can be divided into five main steps; hydrolysis and poly-condensation, gelation, aging, drying and densification, and crystallization. Sol-gel method differs from the conventional thin film processes; as it ensures better control of the chemical composition and microstructure of the coating, preparation of homogeneous films and reduction of the densification temperature. Many coatings, such as titanium oxide (TiO2), calcium phosphate (CaP), TiO2–CaP composites and silica-based coatings have been prepared on titanium and its alloys for biomedical applications [Li2004].

1.1.5 Use of titanium and its films in microelectronics applications

1.1.5.1 Tungsten in interconnects and vias

Interconnects in microelectronics manufacturing have evolved as the back-end technology has progressed. The primary requirements placed on interconnects are low resistivity, good adhesion to underlying films, stability during processing and operation, and the ability to be deposited and etched easily and effectively. Aluminum and aluminum containing multilayers technology has been the dominant interconnects in silicon technology initially. However, Al has several drawbacks such as; (i) instability

during processing and operation due to electro-migration which degrades the overall device performance, (ii) low melting temperature; where it cannot withstand high processing temperatures and (iii) inadequate resistivity for ULSI types of applications since Al is vulnerable to void formation and tensile stresses upon cooling causing a great increase in the interconnects electrical resistance. Another material that has been used for local interconnects is tungsten. However, this material also showed degraded performance at high temperatures as it reacted with silicon and formed silicide. TiN is also commonly utilized as a local interconnect in SRAM cells, where small cell size is critical, and it acts as a diffusion barrier for most dopants.

In multilevel interconnects and contacts as shown in Figure 1.13, many methods have been established to improve the final planarity of the structures either for metals or dielectrics. One example to help achieve planar metal layers is by using a tungsten (W) contact or via fill, also called a W plug. A common method of depositing W plugs by CVD is using blanket W in a damascene process followed by an etch back. Using W plugs produces a smoother topography over the contact or via. [Pl2000]

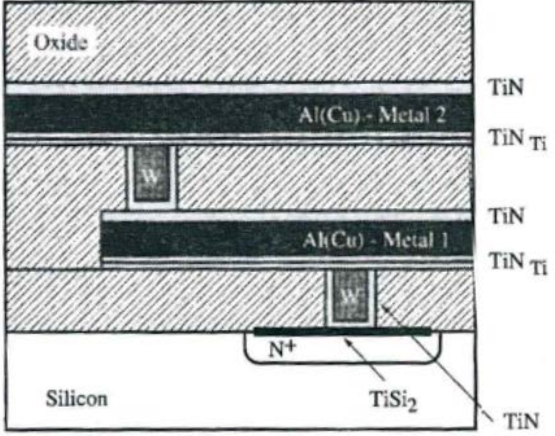

Figure 1.13: Metallization scheme used in IC technology, showing evolved multilayer structures .

1.1.5.2 Introduction of metal barrier (Ti/TiN)

In via and metal contacts (such as Al), a barrier or an adhesion layer such as TiN (commonly used with Al) is deposited and then followed by W plug. Ti can be deposited under TiN to help with the adhesion and contact and it provides a good electrical contact. Also, Ti layer is used as an oxygen gettering layer for contacts as it reacts with the residual oxygen to reduce its content in vacuum. TiN can also serve as an adhesion layer in the case of W contact between the metal and the dielectric as well as a barrier to prevent WF_6 from reacting with the underlying Ti during the W CVD process. A Ti/TiN layer provides good contact with the conductor (i.e. Al) and W and prevents any reaction in between them. These interlayers in interconnects help in electro-migration protection for two reasons. First, by using Ti or TiN, it reacts with Al to form $TiAl_3$, which is mechanically harder than Ti and reduces the effects of electro-migration. Second, Al deposited on Tiexhibits a better grain texture where the grains are located closer to each other. This also improves the electro-migration resistance. Ti/TiN stack shows superior barrier characteristics when compared to TiW; which is also used as a barrier material in metallization of VLSI based Al devices. According to one study, the interface reaction between TiW and Si layer is sensitive to the deposition temperature of the barrier metal, while W/Ti/TiN/Si was not. [Eu1995] It also provides a better electro-migration lifetime performance than TiN process that forms TiN-Ti compound from a multi-Ti-mono-N cluster. [Xu2012]

1.1.5.3 Tungsten and barrier (Ti/TiN) CMP:

Chemical mechanical polishing (CMP) process is being extensively used for the global planarization of multi-level interconnect structures. The wafer is held face down

against a spinning polishing pad and a slurry; containing chemicals and mechanically abrasive particles, is supplied between the pad and the wafer as demonstrated in Figure 1.14, [Ka1991]. For metals, this solution oxidizes the surface making it susceptible to mechanical abrasion by the slurry (e.g. silica or alumina). The resulting defect free surface is indispensable for the high density and high performance of the devices.

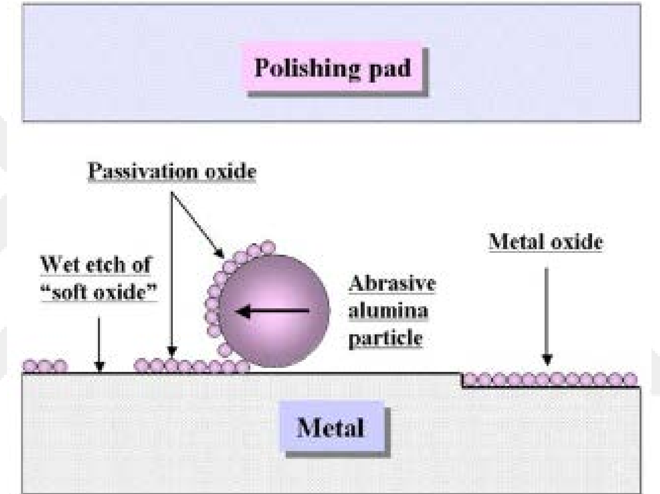

Figure 1.14: Schematic of metal CMP mechanisms [Se2005].

The CMP removal of tungsten and the barrier/adhesive layers, is required at high removal rates. Tungsten possesses high polishing rates due to the oxide (passivation) layer (known as WO_3) which plays an important role in W CMP. Accordingly, the CMP of the barrier (the case in this work Ti/TiN) is expected to produce the same behavior utilizing the oxide layers formed during the CMP application via slurry abrasives action and a strong relation between the metals CMP and the slurries oxidizer exists. [Se2005] Thus, an important issue in metal-CMP process is to minimize the

polishing selectivity between the metal interconnection material and the barrier layer material (Ti/TiN), and the dielectric layer.

Titanium with the outstanding engineering applications mentioned in this chapter concludes the importance of developing the properties of titanium by introducing innovative manufacturing processes and improving the capacity of its industrial applications. Applications of titanium in biomedicine and in microelectronics are the concern if this study. Biomedical based titanium implants as explained in this chapter provide suitable performance in contact with human tissues and blood due to such improvements in surface abilities. Also, titanium application in microelectronics as barrier materials for tungsten based vias and interconnects have been showing an efficient performance among other materials utilized. These topics are evaluated and results of surface experiments are presented to show the importance of surface treatment and the behavior of titanium in such conditions.

CHAPTER II

TITANIUM OXIDE NANO-FILM EVALUATION IN BIOMEDICAL APPLICATIONS

2.1 Introduction

In this chapter, passivation and corrosion behaviors of pure titanium plates are investigated by performing electrochemical analyses on their surfaces. When an implant is placed in-vivo, corrosion and dissolution are the two mechanisms for releasing additional ions into the human's body. It has been determined that the biocompatibility of titanium is not deduced only from corrosion products, but also from exchange and surface conducting currents, Tafel slopes and reaction products. Therefore, electrochemical methods are commonly included in testing metallic biomaterials for in vitro measurements [Ku1988]. Passivation ability of titanium is favorable due to the high values of exchange currents and limiting diffusion currents reflecting as low values for Tafel extrapolation data.

When chemical mechanical polishing (CMP) is performed on titanium implants to change the surface texture, oxide growth and corrosion rates are key values obtained from Tafel slopes and reduction plots. Titanium is tested in environment where a known amount of oxidizer at a selected concentration is introduced as the electrolytic medium for the electrochemical cell. The suitable amount of oxidizer in the CMP process is decided based on the formation of the titanium oxide layer that can be adequately removed by the mechanical action of the slurry particles. CMP is a surface modification method introduced to titanium based biological implants, where both surface roughness

and oxide film formation is controlled for the best performance of implants inside the human's body. The in-vivo performance is evaluated based on promoted cell attachment as well as attachments of biocompatible coatings and limited bacteria growth. [Oz2016] Therefore, application of CMP on titanium implant surfaces is studied in this chapter under the variation of slurry oxidizer concentration. This will help understand the best CMP performance based on minimum removal rates with the desired topography and surface roughness.

2.2 Experimental Approach

In this section bulk Ti square plates obtained from Good Fellow Company in UK were cut into 1.5 by 1.5 cm^2 dimensions and used in the experiments. The oxidizer solution used in these experiments is hydrogen peroxide (H_2O_2) and is obtained from *SIGMA ALDRICH* with a stock percentage of 35% (w/w). For CMP slurry abrasives, NexSil silica (SiO_2) was used at different solids loadings concentrations.

2.2.1 Electrochemical analyses on biomedical grade Titanium plates

2.2.1.1 Electrochemical measurements on pure Ti plates

Initially, potentiostatic transient and potentiodynamic polarization methods were investigated. The electrochemical cell setting used for both type of scans is shown in detail in Figure 2.1. Bulk titanium was connected to be the working electrode. Output signals were measured between the working and counter electrodes in the cell. The counter and reference electrodes used in these measurements were platinum and SCE (Saturated Calomel Electrode), respectively. The potentiostat used to conduct the scans was a Gamry Interface 1000 along with the software of Gamry framework. Subsequently, raw data were analyzed by using *Gamry Echem Analyst*.

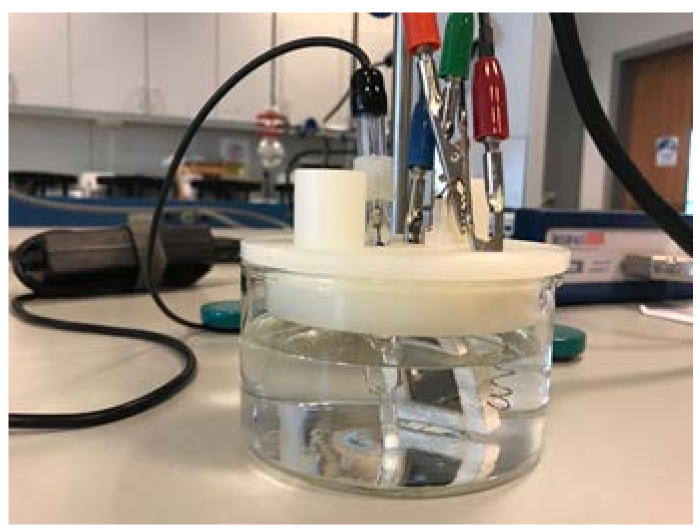

Figure 2.15: Electrochemical cell setting.

Prior to conducting the electrochemical experiments, Ti samples were cleaned by implementing a buff CMP at pH 5 to remove any contaminants and residual oxide on the surface. Both measurements were conducted on the titanium plate surfaces to study their film formation and corrosion characteristics by immersing the samples in H_2O_2 solutions at seven different concentrations selected (i.e. 0M, 0.001M, 0.01M, 0.1M, 0.2M, 0.3M and 0.5M). The total volume of the solutions was 150 ml in each case.

2.2.1.2 Potentiostatic scan of Ti as a function of oxidizer concentration

Potentiostatic (current versus time) transient experiments were set for a continuous duration of 1100 seconds. Input potential was set to a low value, which was close to zero Volts vs. E_{ref} (the real value shown during the test were ~ 90–100 µV, which was negligible and assumed to be zero). The average area of the plates was taken as 1.95 cm^2 and the density of titanium was also taken into account in the experimental settings. All the plates were immersed in deionized water in the beginning of the experiments before the measurements then were started. After a few seconds, different

concentrations of H_2O_2 diluted from a stock concentration of 35 wt% were added according to the desired molarity in the solution of the final volume of 150 ml. Solutions with 0M, 0.001M, 0.01M, 0.1M, 0.2M, 0.3M and 0.5Mconcentrations were tested individually. Finally, the samples were rinsed and dried with nitrogen to prepare the surfaces for post evaluations.

2.2.1.3 Potentiodynamic polarization of Ti as a function of oxidizer concentration

Potentiodynamic scans were performed on the Ti plates in H_2O_2 solutions with the seven different concentrations in 150 ml solutions which were already prepared prior to the scan. Before starting the polarization scans, open circuit delay voltages were measured for 10 seconds. Potentiodynamic scan output signal (current I_m) was collected at a range from -5 V to 8 V input potential with a scan rate of 50 mV/s and a step of 1 mV for each point. Consequently, a total scan period was around 30 minutes. The resultant curve was plotted as potential (Volts) versus log current (Amperes). Tafel data were calculated for each scan, which were used to calculate the corrosion rate, I_{corr} and E_{corr} by the *Gamry Echem Analyst* software.

2.2.1.4 Surface characterization on TiO_2 films

Following the potentiostatic measurements surface characterization methods were applied on titanium surface to study the topography and wettability of the TiO_2 thin films formed as a result of the dipping process which changed the surface current density as demonstrated in the curves (included in chapter one Fig.1.11), previously.

2.2.1.5 Contact angle and wettability measurements

Wettability of surfaces is known to be affected by the surface chemistry as well as nano/micro topography. Sessile drop method was used to conduct the contact angle measurements post potentiostatic scans on the titanium plate surfaces by using deionized water as the condensed liquid phase in air. The size of the drop was ~160 µm and the KVS *AttentionTheta* Goniometer was used for the measurements.

2.2.1.6 Surface topography measurements

Atomic force microscopy by *Nanomagnetics* Instruments was utilized to quantify the surface roughness. The surface topography of the bulk titanium plates was scanned in the contact mode. The scan area was set to 10x10 µm with a scan speed of 6 µm/second. Three measurements were taken for each sample to have an average room mean square (rms) roughness value. The topographic images and their 3D and cross sectional views were analyzed to validate roughness values.

2.2.2 Application of Chemical Mechanical Polishing on Ti plates

2.2.2.1 CMP application on Ti surface by controlling slurry oxidizer concentration

Bulk titanium plates were treated by CMP at the selected concentrations of the electrochemical measurements. CMP treatment is capable of tuning the surface topography smoother or rougher through controlled cyclic chemical and mechanical actions. The surface oxide formation is affected by the concentration of the slurry oxidizer, which is the hydrogen peroxide (H_2O_2) in this study. Five different concentrations of H_2O_2 (0 M, 0.001 M, 0.01 M, 0.1 M and 0.3 M) were experimented to analyze the chemical action and TiO_2 formation. The mechanical abrasion was enabled in the CMP process by utilizing the silica nanoparticles in the slurry at a fixed slurry solids loading of 3%wt. The polishing was performed for 2 minutes, at a down force of

30 N and a rotation speed of 150 rpm. The polishing pad used for titanium CMP was IC1000/Suba IV stacked pad. After polishing, titanium plates were cleaned with acetone and DI water in an ultrasonic bath for 5 minutes and dried with nitrogen gas. Post evaluation of the surface via contact angle (wettability) and roughness data were performed by using the same settings as mentioned in the above.

2.2.2.2 Material removal rate calculations

To determine the material removal rate during CMP, weight measurements were conducted for titanium plates pre and post polishing. Measurements were conducted using a high precision balance (PrecisaGravimetrics) with an accuracy of ±0. 01 mg. The difference in weight was applied in finding the removal rate for each oxidizer concentration during the application of CMP. The removal rate calculations depend on several material properties of titanium such as density along with the weight change, surface area and the duration of CMP.

2.2.2.3 Surface characterization of chemical mechanical polished treated Tiplates

Surface characterization of CMP treated titanium samples were conducted through measuring surface roughness and surface contact angle. Before analyzing the wettability of the samples surfaces through contact angle measurements, titanium plates were cleaned with ethanol in an ultra-sonic bath for 10 minutes, then with DI water for another 5 minutes and dried with nitrogen gas. Whereas the surface roughness measurements were done by AFM scanning and the average RMS values were obtained from a total of three scan positions for each sample and each treatment.

2.2.2.4 Effect of slurry solids loading on titanium CMP and material removal rate

In this section, chemical mechanical polishing is studied within the mechanical abrasion capabilities of the slurry as the slurry solids loading concentration contributes on the surface roughness and material removal rates by changing the pressure by particle. The nanoparticle silica concentration in the slurry was tested at solids loadings of 3%, 5% and 10%wt. At each of the selected solids loading percentage, the previously tested hydrogen peroxide concentrations were examined. Accordingly, removal rates and surface quality responses were evaluated.

2.3 Results and Discussions

2.3.1 Corrosion studies on titanium and TiO_2 film

2.3.1.1 Electrochemical analyses on pure Ti

2.3.1.2 Potentiostatic scan of Ti in presence of H_2O_2 solutions

To understand the passivation behavior of the Ti plates under the influence of oxidizing chemical (in this case hydrogen peroxide), titanium samples were initially evaluated through potentiostatic scans as a function of oxidizer concentration. As shown in Figure 2.2, for each solution concentration a different response was observed depending on the surface chemical activity and the oxide formation. It can be seen that as the added H_2O_2 molarity increases as compared to 0.01 M of the initial concentration the surface conductivity decreases which is measured through the passed current (I_m). In that, the slope of the curve increases with the oxidizer concentration indicating that more oxide is potentially grown inhibiting surface conductivity and decreasing the current levels. A steady state current value is observed after the initial passivation on the surface that is observed through the decrease of the current. At this stable region, it is believed that the oxide film has grown continuously to completely passivate ion transfer

(in the case of a “pore free and adherent” surface oxide film) and limit current conductivity on the surface.

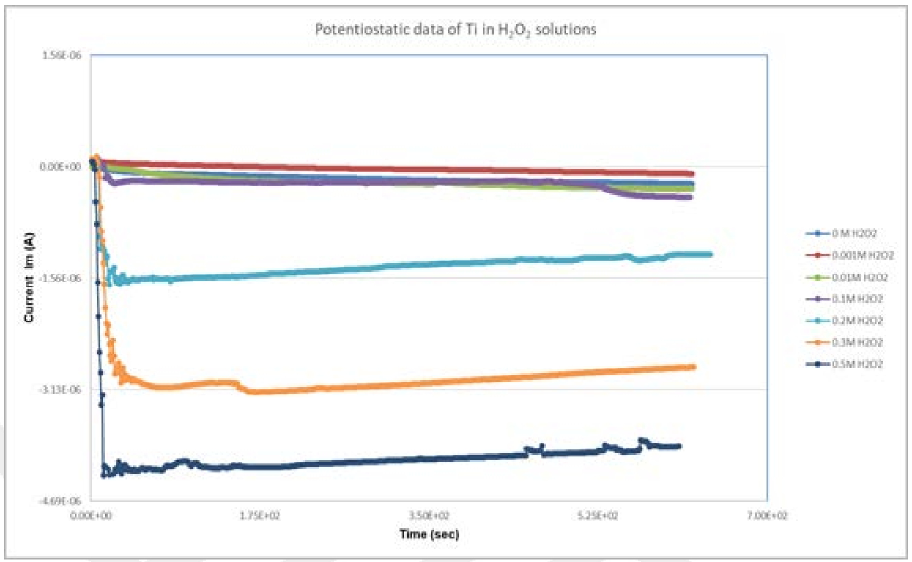

Figure 2.16: Potentiostatic (current vs time) curves of titanium in different H_2O_2 molar concentrations mediums.

Also, at 0 M concentration the current behavior noticeably follows the curve of 0.01M oxidizer addition, whereas at 0.001 M of oxidizer concentration less passivation is observed. This could be attributed to the fact that this is a very low concentration of oxidizer and could be acting as a surface cleaning agent rather than the passivation and hence allowing more current to pass. However, the results at these very small concentrations are statistically the same within the reproducible standard deviation. Yet, at the higher H_2O_2 concentrations, a significant degree of passivation is observed on the titanium surface with statistically significant difference in the results as observed in Figure 2.2.

2.3.1.3 Oxide growth rates calculation

To interpret the curves shown in Figure 2.2 in relation to the oxide growth and surface passivity, the passivation slopes were calculated as given in Table 2.1 for each curve at each oxidizer concentration.

Table 2.3: Calculated slopes of titanium curves in H_2O_2 solutions.

Sample Concentration	Slope (A/s)
0 M	3.82E-10
0.001 M	3.04E-10
0.01 M	1.70E-09
0.1 M	1.37E-08
0.2 M	1.13E-07
0.3 M	1.69E-07
0.5 M	4.52E-07

The initial passivation slopes of titanium curves confirmed the passivation observation discussed earlier as the higher oxide growth rates are attained with higher solution molarity of the oxidizer [2003]. The steeper the slope is, the more intense and faster surface chemical reactions are believed to take place during the addition of oxidizer. This behavior provides excellent corrosion resistance characteristics on the titanium surface. Additionally, the growth rate is an indicator of how well the amorphous oxide layer is forming on the titanium surface to enhance cell attachment in case of its application in body implants.

2.3.1.4 Potentiodynamic polarization of Ti in presence of H_2O_2

Corrosion rate analyses are driven from the potentiodynamic sweeps that are collected on the bulk titanium's surface in the predetermined concentrations of H_2O_2.

Figure 2.3, demonstrates the potential versus current relationship at each concentration where the cathodic and anodic responses of the curves are observed to change along with the passivation current points. The anodic and cathodic responses of each curve correspond to the current conductivity through negative to positive potential sweeps.

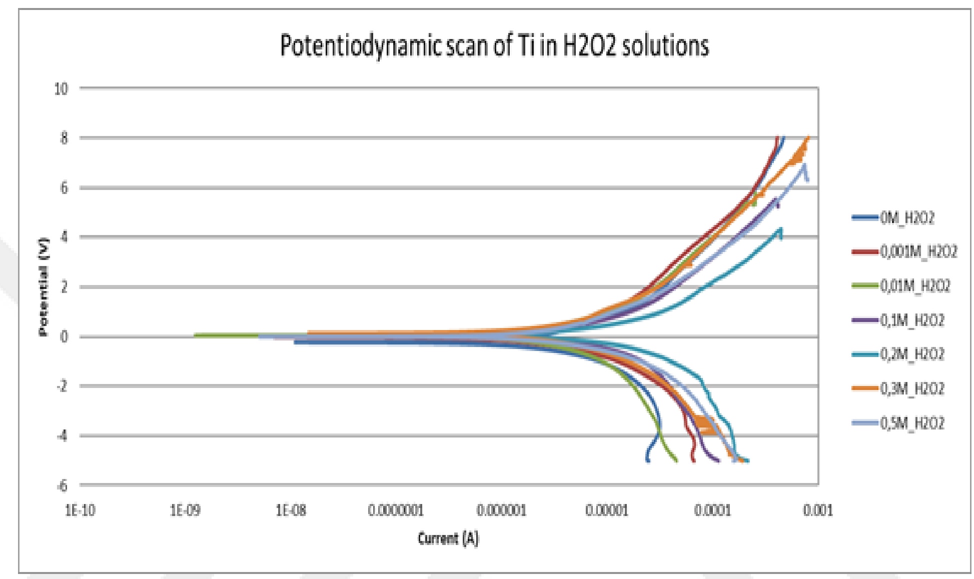

Figure 2.17: Potentiodynamic curves of bulk titanium at seven H_2O_2 concentrations.

In between the recorded sweeps is the region where passivation current corresponds to the lowest point along the x-axis. The anodic behavior of titanium shows a continuous increase in the surface current conductivity as the positive potential increases for all the tested concentrations.

2.3.1.5 Tafel extrapolation and corrosion data calculations

To understand the significance of the potentiodynamic curves in determining the corrosion behavior of titanium within the selected oxidizer concentrations, Tafel extrapolations of each curve are given in Table 2.2. Corrosion current values vary with the hydrogen peroxide concentration affecting the corrosion rates, where the highest

rate is attained at 0.2 M at a value of 10.27 mpy (milli inch per year) followed by 0.1 M at 7.16 mpy. The rest of the concentrations are close in the attained rates. The higher corrosion rates may indicate higher removal rates and faster dissolution if the grown TiO_2 film is not protective in nature.

Table2.4: Tafel extrapolation data of titanium potentiodynamic curves.

Tafel Variables	0 M H_2O_2	0.001 M H_2O_2	0.01 M H_2O_2	0.1 M H_2O_2	0.2 M H_2O_2	0.3 M H_2O_2	0.5 M H_2O_2
Beta A (V/decade)	4.934	4.396	3.858	4.036	3.377	3.935	3.440
Beta C (V/decade)	6.762	4.344	7.291	6.323	4.819	3.911	3.657
I_{corr} (µA)	13.00	9.200	9.580	17.90	25.60	9.870	10.40
E_{corr} (mV)	-236.0	-22.90	46.50	87.30	67.60	122.0	2.050
Corrosion Rate (mpy)	5.203	3.687	3.839	7.159	10.27	3.954	4.185

2.3.1.6 Surface characterization of the electrochemically treated TiO_2 films

The titanium samples treated with the different concentrations of the oxidizer in the electrochemical evaluations were also tested for their surface nature by wettability and surface topography responses.

Following the electrochemical evaluations, post potentiostatic analyses were performed on the titanium samples where the wettability responses of the treated surfaces are shown through contact angle data in Figure 2.4. The contact angle values show a tendency to increase with the increasing oxide concentration, except for the last highest concentration of 0.5 M oxidizer addition. As the concentration of H_2O_2 for each

scan increases, the oxide layer is expected to grow thicker as observed from the potentiostatic curves. The growth in the oxide thickness also affects the surface roughness as can be seen in Figure 2.5. Figure 2.6 (roughness figure) similarly shows the surface roughness data as a function of H_2O_2 concentration. It can be seen that there is a good correlation of wettability to the surface roughness of the samples. Simply, the air pockets introduced by the increased roughness of the surface tend to increase the hydrophobicity of the surface. The contact angle value of the highest concentration (0.5 M) with a lower surface roughness and corresponding lower contact angle data indicate a change in the surface oxide layer formation which is smoother, or simply a second layer of oxide starts to form on the preliminary oxide layer.

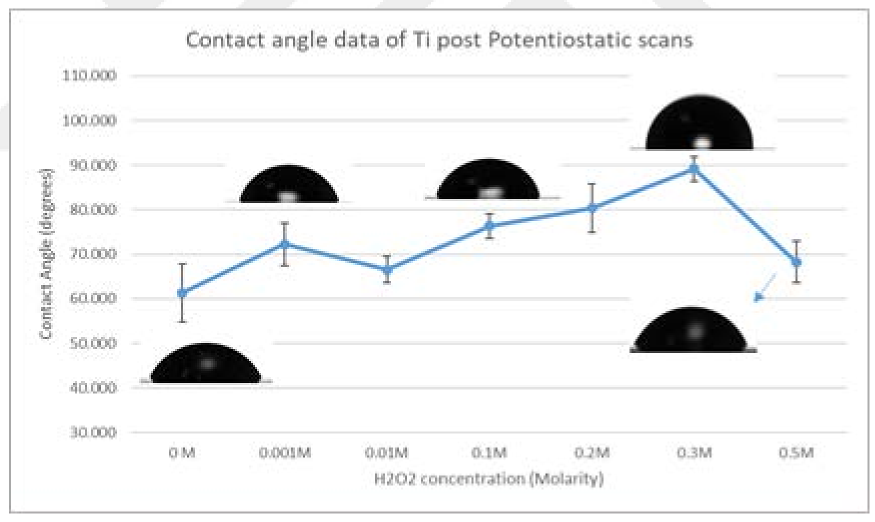

Figure 2.18: Contact angle data of titanium post potentiostatic scans at different H_2O_2 solutions concentrations.

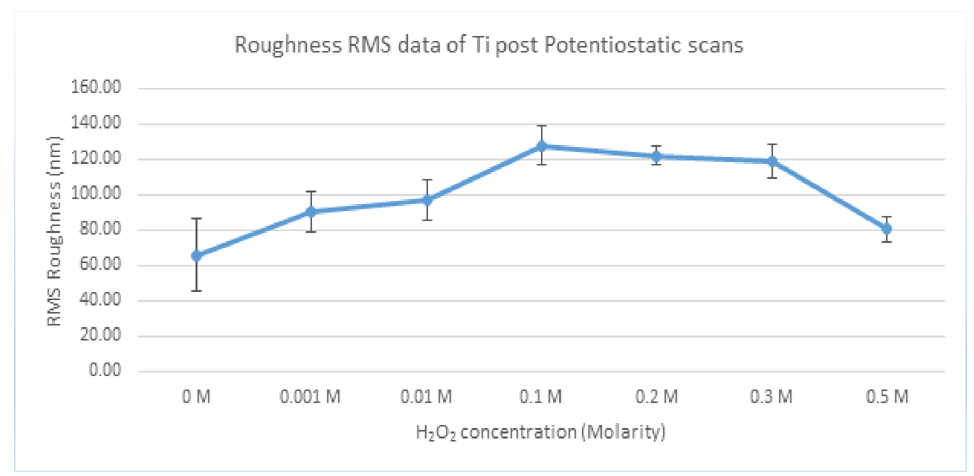

Figure 2.19: RMS roughness series of Ti post potentiostatic measurements.

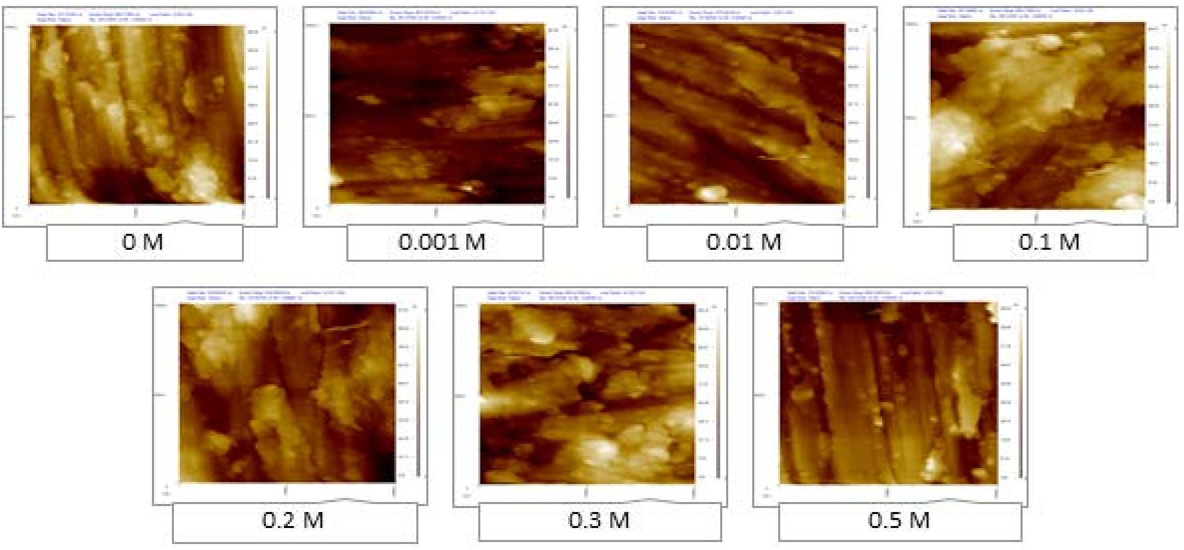

Figure 2.20: AFM images of titanium surface at potentiostatic tested molar concentrations.

2.3.2 Application of Chemical Mechanical Polishing on biomedical Ti surface

2.3.2.1 Material removal rates of CMP application

To observe the effect of oxide formation on the CMP performance of titanium, samples were treated by CMP and the material removal rates were calculated for the selected concentrations as shown in Figure 2.7. The material removal rates tend to be lower at the higher concentrations of oxidizer in the polishing slurry. This can be attributed to the formation of better quality oxide on the surface and insufficient mechanical action provided by the fixed number of slurry abrasive particles at the given slurry solids loading. There is a slight increase in the MRR value at the higher concentration of 0.3 M, which also suggest that the oxide quality tends to change at the higher concentrations of the oxidizer.

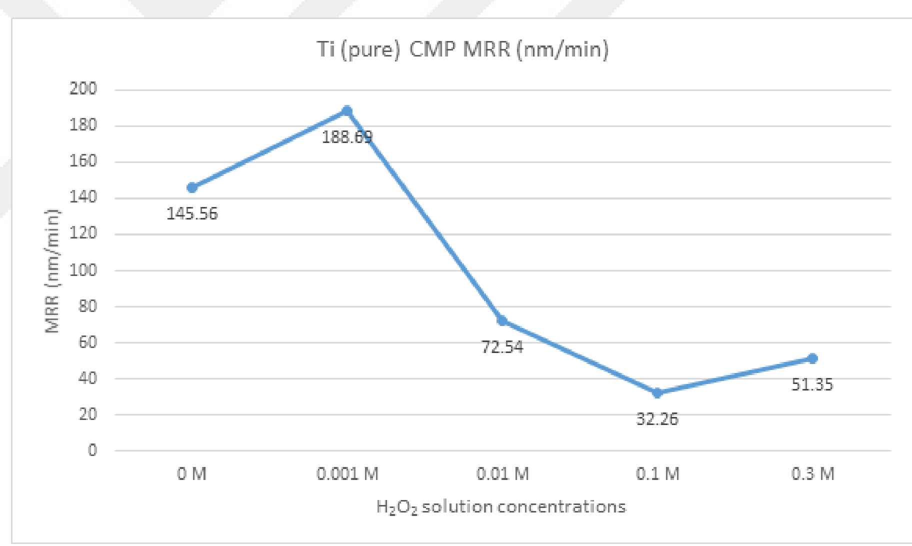

Figure 2.21: Removal rates of Ti CMP at 5 different concentrations.

2.3.2.2 Post CMP surface quality characterization as a function of slurry oxidizer concentration

The surface quality of the CMP treated samples were evaluated through contact angle and surface roughness measurements. Figures 2.8 and 2. 9 show the measured contact angle and surface roughness values as a function of H_2O_2 concentration in the

slurry during the polishing experiments. It can be seen that in the absence of the oxidizer the surface is more hydrophobic which can be attributed to the lack of oxide on the titanium surface. The hydrophilicity increases when the oxidizer is added to the slurry ascan be seen by the lowered contact angle values. This can be simply explained by the oxide form of metals tend to be more water liking as compared to the metallic form.

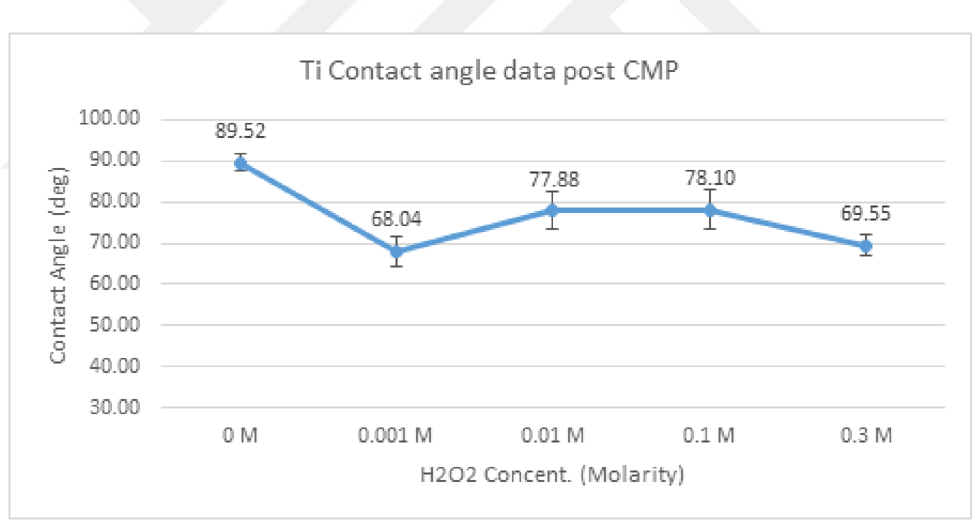

Figure 2.22: Ti bulk contact angle data post CMP at 5 H_2O_2 concentrations.

Surface roughness evaluations in Figures 2.9 and 2.10 also show an improved surface planarity and surface smoothness as compared to the pretreated surface RMS value of an average of 91.038 nm of the original titanium plates. As it can be seen from the AFM images as well, there is not much of a divergence in roughness values up to

0.1 M oxidizer concentration. A lower RMS is attained at 0.3 M, which might be indicative of the change in oxide film formation.

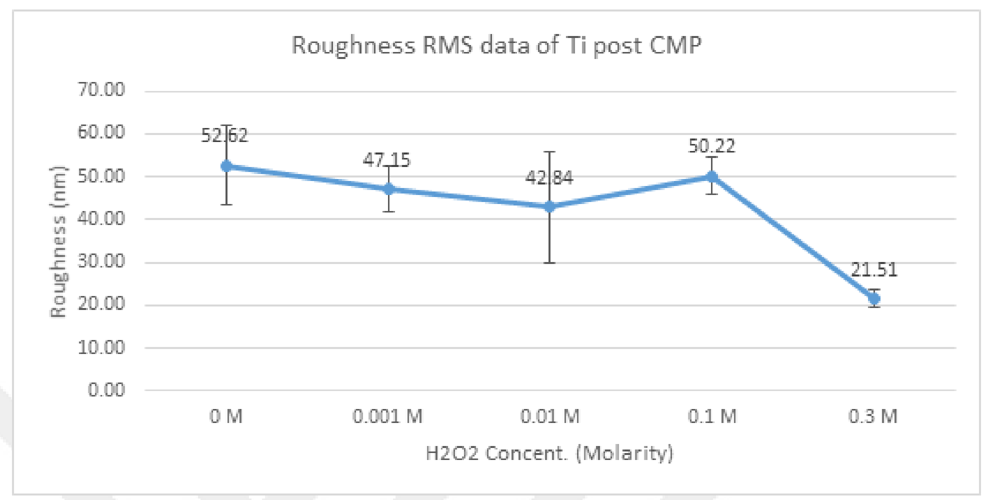

Figure 2.23: Post CMP roughness RMS data of Ti with different slurry oxidizer concentrations.

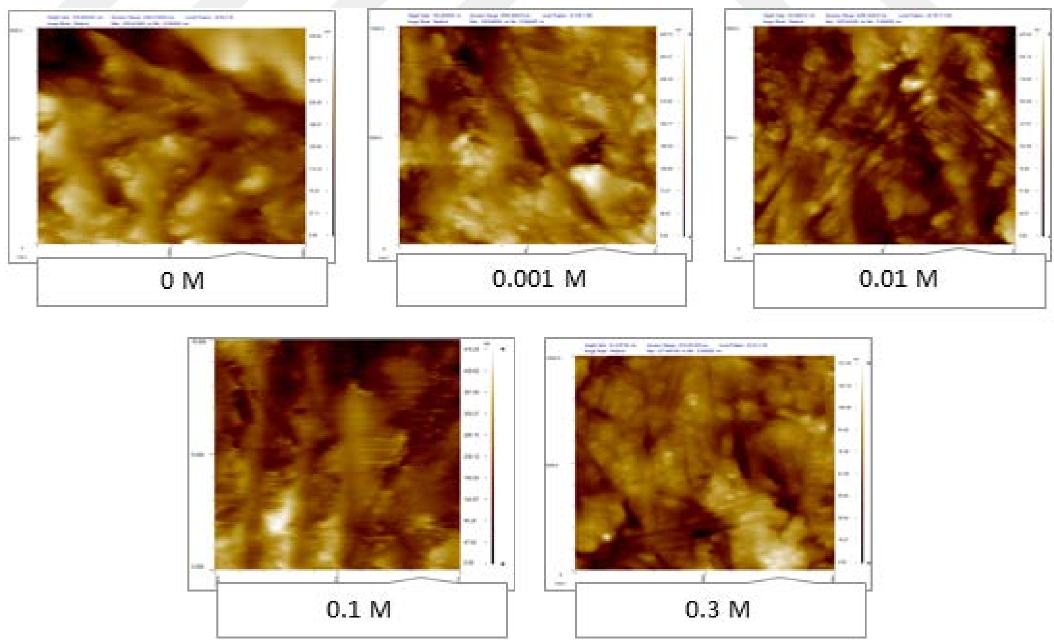

Figure 2.24: AFM images of titanium surface under CMP at different concentrations.

2.3.3 Effect of slurry solids loading on bulk titanium plate CMP performance

In order to analyze the effect of the chemical and mechanical interactions on the titanium CMP, experiments were conducted as a function of slurry solids loading at the 0, 0.001, 0.01 and 0.1 M oxidizer concentrations. The CMP test results for the material removal rates are illustrated in Figure 2.11 which were contacted at 3wt%, 5wt% and 10wt% slurry solids concentrations. It is clearly seen that when a thick and dense surface oxide is formed on the titanium plates, the MRR values tend to decrease at the low slurry solids loadings such as at 3 and 5wt% solids loading slurries. However, at 10wt% solids concentration, the MRR values continue to increase with the increasing oxidizer concentration due to the fact that there are enough slurry particles to act as mechanical abraders during polishing that can keep up with the continuous formation of the oxide on the titanium plate.

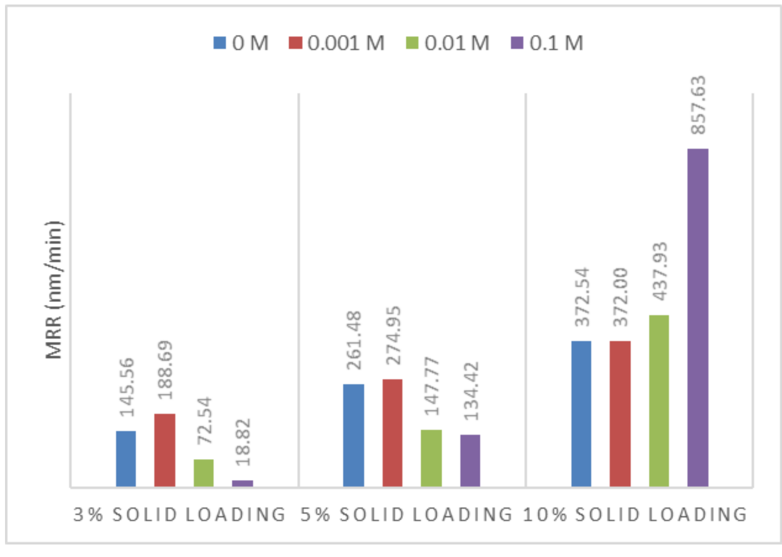

Figure 2.25: Removal Rates of bulk Ti at different solids loading percentages.

2.4 Summary and Conclusions

In this chapter electrochemical analyses in combination with CMP experiments were performed on bulk titanium plates in order to study the effect of the presence of hydrogen peroxide on the formation and growth of natural titanium oxide films which effect the surface nature. Results via potentiostatic measurements showed that the presence of an oxidizer increases the rate of oxide growth and as the oxidizer concentration increase the surface current density levels tend to decrease. This is owed to the self-passivation ability, continuous and pore free structure of the TiO_2 film. Post surface evaluation of titanium surface at the selected H_2O_2 concentrations showed correlation between the contact angle and the surface roughness measurement results. The forming oxide layer generally increases the surface roughness through increased surface topography. The increase in the roughness values can be attributed to the nature of the thick oxide layer forming in the presence of the oxidizer. Yet, at relatively higher concentrations, the surface tends to smoothen due to a second layer of oxide forming on the preliminary bulk oxide.

CHAPTER III

MICROELECTRONICS APPLICATIONS OF TITANIUM/TITANIUM NITRIDE FILMS AS A BARRIER FOR TUNGSTEN BASED INTERCONNECTS IN CMP APPLICATIONS

3.1 Introduction

In this chapter, tungsten deposited wafers were investigated for corrosion behavior along with titanium and titanium nitride deposited wafers in micro-electronics as via and interconnect metal and barrier materials, respectively. Tungsten application as plugs for multilevel interconnects lacks adhesion strength with SiO_2 layer, which is compensated by adding Ti and TiN layers as adhesive and diffusion limiting barrier layers. The passivation layer forming during W and Ti CMP plays an important role in this process to enable 1:1:1 selectivity of material removal of W/Ti/TiN layers. The presence of H_2O_2 as an oxidizer in the slurry, affects the polishing rates and polishing selectivity as its concentration changes during the CMP applications.

Before conducting CMP experiments, the passivity and corrosion characteristics of the W and barrier films were examined since W CMP occurs as a result of continuous actions of WO_3 oxide layer formation and removal and when the Ti/TiN barrier is reached, Ti produces TiO_2 which is mechanically removed by the slurry abrasive particles such as silica. It is observed that the higher the oxidizer concentration, the faster is the passivation rate and that the corrosion rates increase up-to a point where the behavior of the oxide film changes. Electrochemical analyses of surface film formation provide important information to set the optimal slurry

formulation during the CMP process by controlling the corrosion rates of each metal. Dissolution currents and removal rates of tungsten and titanium are to be looked at as to have a relationship as the oxidizer concentrations in the slurry are changed.

3.2 Experimental Approach

3.2.1 Corrosion evaluation of tungsten, titanium and TiN through electrochemical measurements

Tungsten, titanium and TiN wafers obtained from Texas Instruments Inc. were cut into square shaped coupons of 1 by 1 cm in size. All wafers were cleaned prior to the electrochemical tests, where Ti and TiN coupons were immersed into pH 9 solution and put in an ultrasonic bath for 5 minutes to open up the metal's surface. The tungsten surface, on the other hand was buffed with the same slurry used for the CMP operations to open up the surface oxide layer. The hydrogen peroxide was used as the oxidizer at concentrations of 0.1 M, 0.2 M, 0.3 M and 0.5 M.

3.2.1.1 Potentiodynamic polarization responses of W, Ti and TiN in H_2O_2 mediums

All potentiodynamic scans were performed in an electrochemical cell with the same electrode setup configuration. Titanium, tungsten and TiN, were the working electrodes and the rest of the electrodes in the cell were set as described earlier. The potentiodynamic sweeps were set between -5 V and 6 V for a scanning rate of 50 mV/second. Those parameters; which were inputs to the potentiostat software, were fixed for all the materials selected (equivalent weight and density were material dependent parameters). The wafer coupons as the working electrodes were immersed in

hydrogen peroxide mediums and concentration was varied according to the corrosion rate measurements as studied earlier and the results were compared.

3.2.1.2 Potentiostatic transient response of W, Ti and TiN in H_2O_2medium

The electrochemical cell was setup as mentioned in the previous sections. Ti, TiN and W coupons were tested in H_2O_2 solutions with its molarity variation effect observed by the resulting current versus time plots. The input step potential was set to 0.001 Volts and the test period was set to 18 minutes. The output curves were recorded and from those curves passivation slopes were calculated. Accordingly, the passivation behavior and surface conductivity were evaluated for each sample. Post scan evaluations were performed through wettability and surface roughness AFM measurements to observe the changes on the surface oxide quality formed at the various H_2O_2 concentrations.

3.2.2 CMP application on W and Ti/TiN barrier films and surface characterization

3.2.2.1 CMP study as a function of slurry oxidizer concentration

The effect of chemical mechanical polishing on metal's surface and the changes in its topography was investigated as a function of H_2O_2 concentration in the polishing slurry. Pre cleaned titanium, TiN and tungsten surfaces were subjected to CMP for an optimal of 30 seconds duration to ensure that the deposited film is not totally polished. The down force of the polishing head was set to 30 N with a polishing rotational velocity of 150 rpm. After CMP application, samples were cleaned in ultra-sonic bath in beakers containing acetone and deionized water for 5 minutes each. Following the

ultrasonic-cation, samples were dried with nitrogen gas and weighed to calculate their removal rates by subtracting the sample weight prior CMP utilizing the density value in the literature by taking the sample area into account.

3.2.2.2 Post CMP performance evaluations

Because the resulting effect of CMP on the materials surface can differ according to their surface oxide density and nanotopography, a post treatment surface qualification is necessary. Different surface roughness measurements can be observed by different oxidizer levels for different metals and semi-metals. Along with the weight measurements, samples were also characterized by generating surface AFM scans to measure the surface roughness and contact angle data. As for AFM measurements, three topographic images were taken for each sample and the average root mean square (rms) roughness value was reported. Following roughness measurements, contact angle data were obtained for all three material surfaces. At each oxider concentration an average of 4 contact-angle values were recorded for each sample.

3.3 Results and Discussions

3.3.1 Corrosion evaluation of tungsten through electrochemical measurements

3.3.1.1 Potentiodynamic polarization responses of W in H_2O_2 mediums

Tungsten CMP requires the exposure of the wafer to slurry oxidizer to promote formation of WO_3 as an oxide layer as observed through potentiodynamic curves. As it is shown in Figure 3.1, in the presence of hydrogen peroxide at the specified concentrations, all curves show a similar cathodic response.

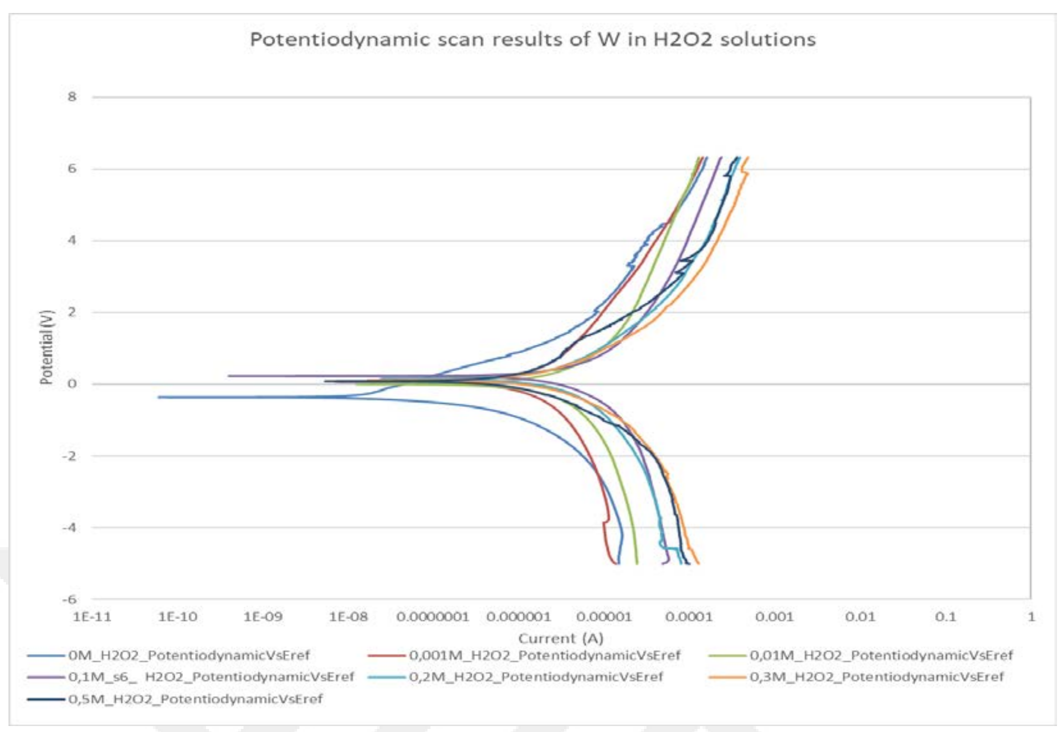

Figure 3.26: Potentiodynamic polarization curves of tungsten in hydrogen peroxide mediums.

The conductivity on the surface decreases with the applied potential reaches the zero potential current then start progressing into the anodic polarization portion of the curve.

3.3.1.2 Tafel data extrapolation

Looking at the Tafel data in Table 3.1 of the above polarization curves, low corrosion rates are attained at 0.5 M concentration of H_2O_2, whereas, a high rate of 9.7 mpy was found at 0.1 M oxidizer addition. At 1 M, an extremely high corrosion rate was calculated. This also causes the surface layer of tungsten to corrode as shown in the accompanying Figure 3.2. As a result, a very high material removal was observed and the deposited W films got completely removed. At 0.2 M and 0.3 M

concentrations, a similar rate was observed residing between the rest of the concentrations.

Table 3.5: Tafel data and calculated corrosion rates of tungsten at five concentrations.

Tafel Variables	0.1 M H2O2	0.2 M H2O2	0.3 M H2O2	0.5 M H2O2	1 M H2O2
Beta A (V/decade)	6.188	3.806	3.278	2.922	6,072
Beta C (V/decade)	13.57	6.925	4.351	3.288	37,72
Icorr (µA)	25.90	12.10	9.930	3.950	192,0e-6
Ecorr (mV)	227.0	148.0	113.0	82.30	-14,50
Corrosion Rate (mpy)	9.794	4.562	3.758	1.497	145.5

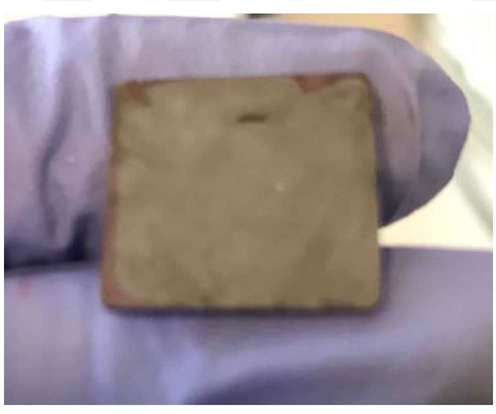

Figure 3.27: Corroded W surface post potentiodynamic treatment at 1 M.

3.3.1.3 Potentiostatic transient response of W in H_2O_2 mediums

Figure 3.3 shows the current vs time transient of tungsten immersed in hydrogen peroxide mediums. As time progresses each curve is settling at lower current levels and

depending on the added H_2O_2 amount, the slope was affected and the steady state passivation level was recorded at lower current levels as the concentrations was increased other than 1 M oxidizer addition.

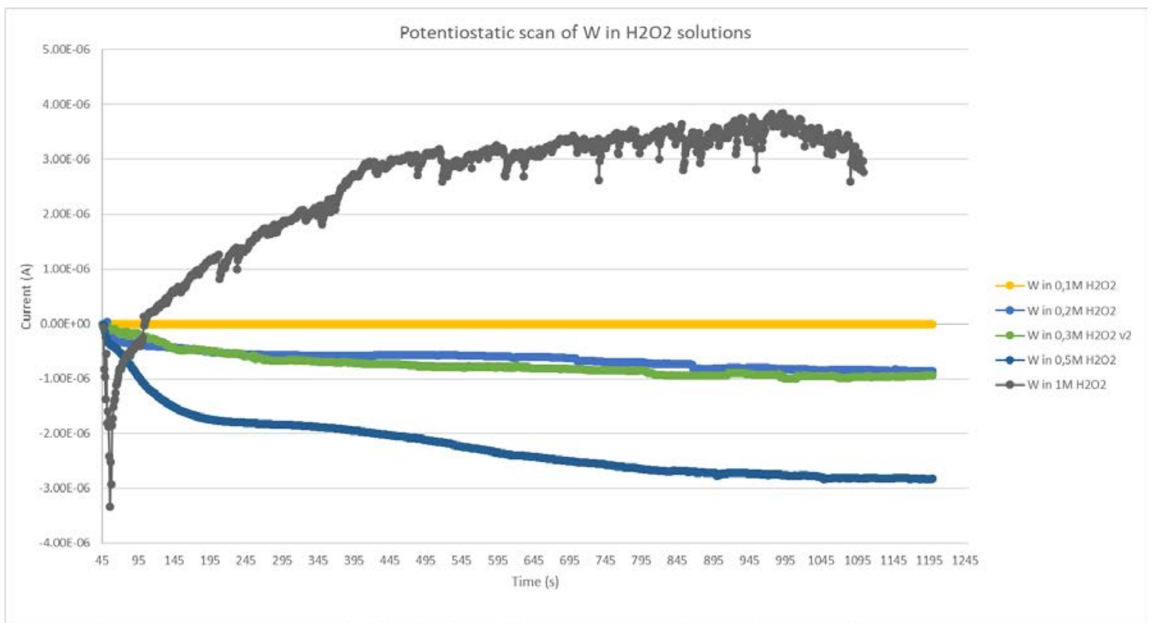

Figure 3.28: Potentiostatic responses of tungsten at different H_2O_2 concentrations.

In agreement with the Table 3.1 results, when the corrosion rates decrease, current levels measured as a function of time also show lower values indicating more passivation is achieved. 1M H_2O_2 addition on the other hand, results in an abnormal behavior as recorded on both measurements, where increasing surface conductivity is observed indicative of no passivation taking place at this extremely high concentration.

3.3.1.4 Rate of passivationapproximation

The slopes of passivation calculated as the amount of current decrease at a given time were utilized to predict the rate of passivation on the W surfaces. The increase in

the calculated values indicate a faster oxide formation as more oxidizer is available close to the metal's surface. The calculated rates were similar at 0.2 and 0.3 M oxidizer concentrations, which also relates to the similar corrosion rates. At 1 M of H_2O_2 addition, an initial fall was observed that resulted in a high A/s rate as shown in Table 3.2 but the current rises immediately due to no passivation on the surface.

Table 3.6: Calculated slopes of W curves in H_2O_2 solutions.

Oxide concentration	Slope (W) A/s
0.1 M	2.416-14
0.2 M	4.175-10
0.3 M	5.87E-10
0.5 M	2.059E-09
1 M	2.85E-07

3.3.1.5 Surface oxide evaluation

3.3.1.6 Surface nanotopography measurements

Figures 3.4 and 3.5 summarize the roughness data evaluations on the tungsten surface indicating a uniform layer formation at the concentrations of 0.1, 0.2 and 0.3 M with low roughness values. At 0.5 M and 1 M oxidizer addition, on the other hand, where less passivation was observed particularly at 1 M concentration, a more porous surface nature is observed.

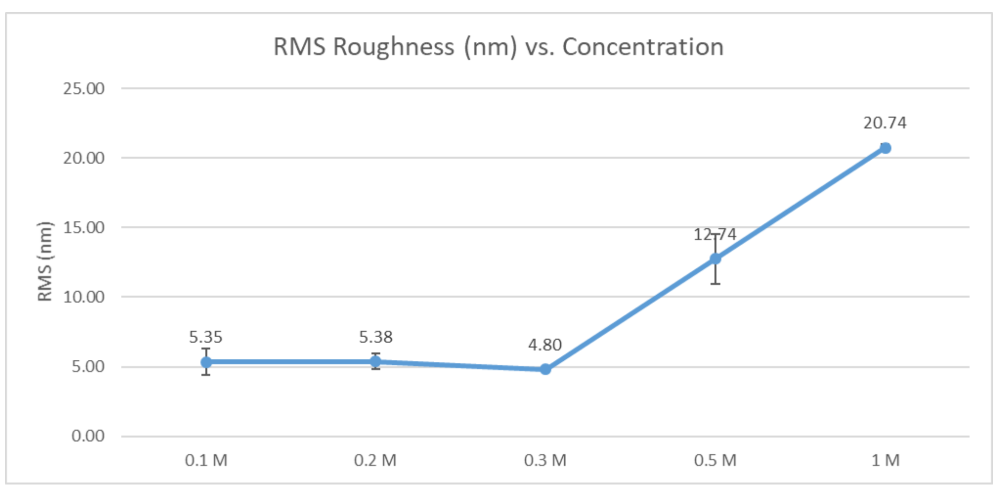

Figure 3.29: Roughness RMS value of W surface post potentiostatic transients in H_2O_2 mediums.

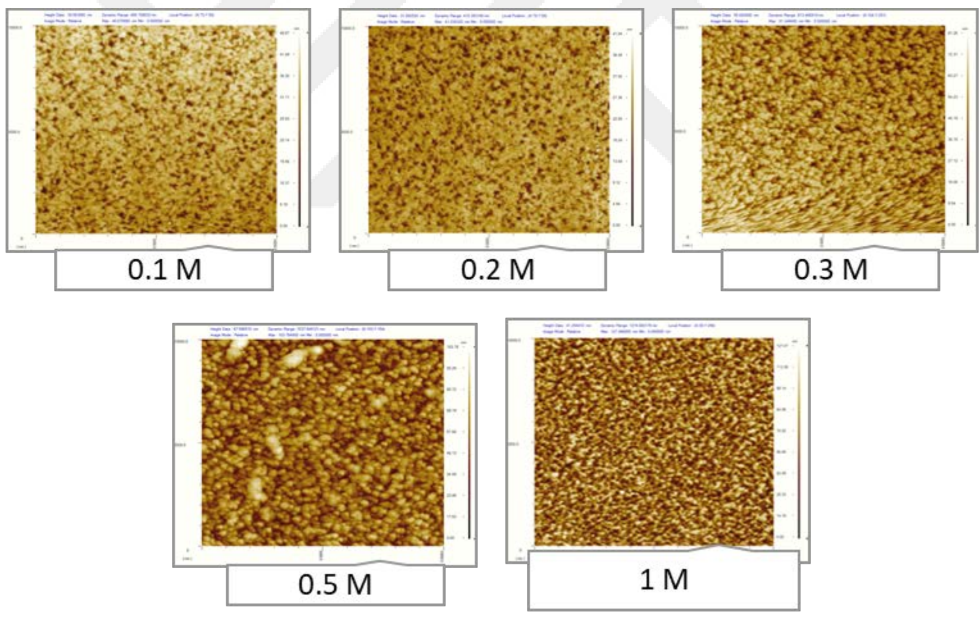

Figure 3.30: AFM images of tungsten post potentiostatic scan.

3.3.1.7 Contact angle measurements

The contact angle values - Figure 3.6 - evaluated as a measure of the surface wettability and indicator of the surface energy were between 50 and 80 degrees, except at 1M concentration were the angle exceeded this range to an approximate 90 degrees.

This result indicates a change in the surface wettability towards an increased hydrophobicity. This finding is consistent with the fact that more metal is exposed at the W surface and a rougher surface finish results in an increased contact angle which is believed to be due to the fact that the air pockets are trapped on the surface of the wafer.

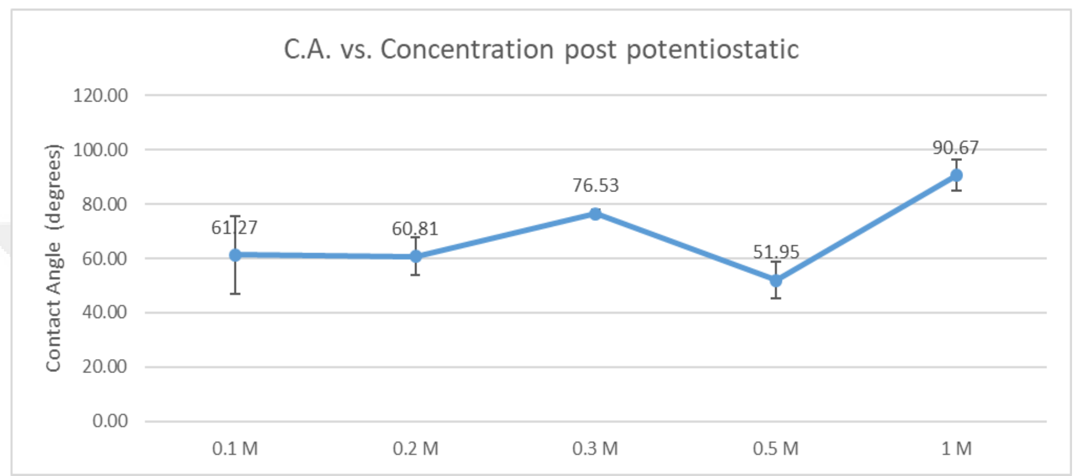

Figure 3.31: Contact angle data of W surface post potentiostatic transients in H_2O_2 mediums.

3.3.2 Ti/TiN electrochemical corrosion evaluations as a barrier for tungsten

3.3.2.1 Potentiodynamic polarization responses of Ti/TiN in H_2O_2 mediums

Potentiodynamic curves for Ti and TiN in hydrogen peroxide mediums are shown in Figure 3.7 and Figure 3.8, respectively. For both materials, anodic and cathodic sections of the curves show similar behavior where both tend to show the passivation currents at zero potential levels. For titanium the lowest zero potential conductivity is observed to be at 0.2 M of H_2O_2 addition. There is a small variation within the titanium curves at the selected concentrations. Yet the TiN curves show more variability which is further discussed in the following sections.

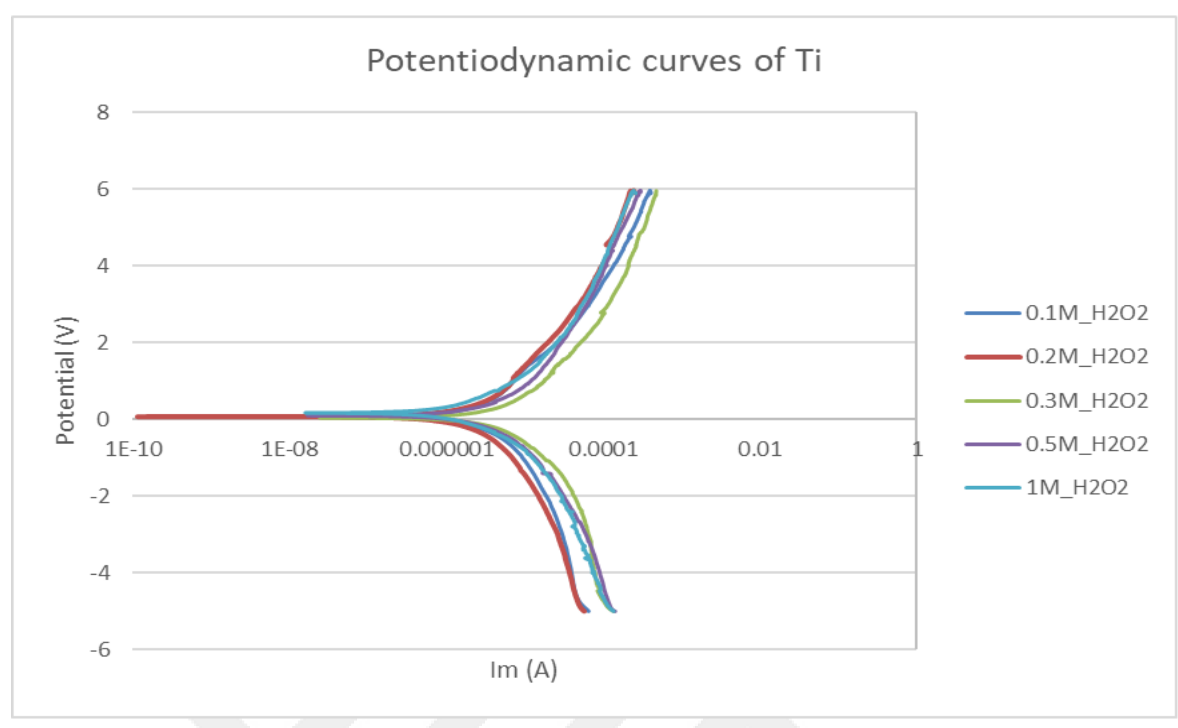

Figure 3.32: Potentiodynamic curve of deposited Ti in five H_2O_2 concentrations.

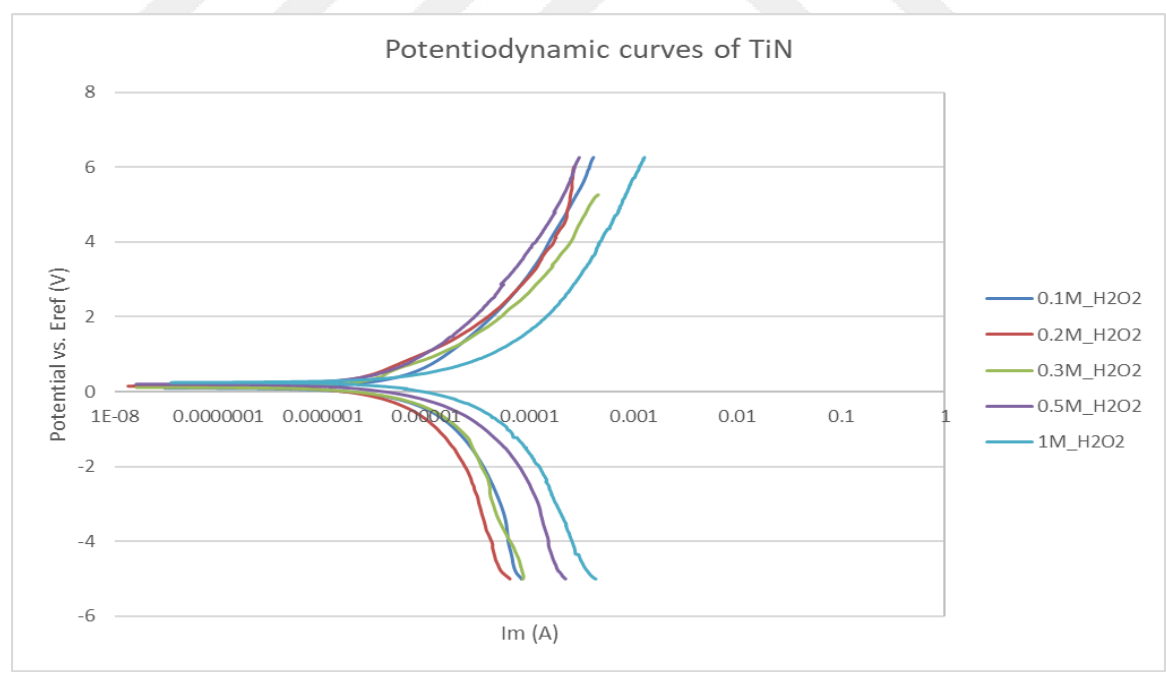

Figure 3.33: Potentiodynamic curve of deposited TiN in five H_2O_2 concentrations.

3.3.2.2 *Tafel data extrapolation*

Table 3.3 shows titanium Tafel extrapolation data. The corrosion potentials showed a maximum value at 1 M concentration whereas the corrosion current densities were the highest at 0.3 M concentration of H_2O_2 medium. At 0.2 M oxidizer addition, the calculated corrosion current and I_{corr} value were the lowest confirming the observation in potential current relationship at this particular concentration (Figure 3.7).

TiN Tafel data shown in Table 3.4 show much higher corrosion values as compared to titanium. The highest corrosion rate was reached at 1 M and measured as 42.38 mpy. The lowest corrosion was measured as 12.23 mpy at 0.5 M. Such high current densities and corrosion rates of TiN can indicate a less stable oxidation and passive and continuous surface film formation as compared to Ti. That's why titanium is the main protective layer and TiN works better as a the dielectric-metal adhesion layer in the W/Ti/TiN deposition.

Table 3.7: Tafel data of deposited titanium potentiodynamic scans.

Tafel Variables	0.1 M	0.2 M	0.3 M	0.5 M	1 M
Beta A (V/decade)	3.334	3.726	4.059	4.120	3.754
Beta C (V/decade)	5.525	5.604	6.349	4.612	4.143
I_{corr} (A/cm²)	3.840e-6	3.500e-6	9.850e-6	5.810e-6	3.850e-6
E_{corr} (mV)	63.20	71.30	38.70	96.50	168.0
Corrosion Rate (mpy)	3.019	2.752	7.734	4.562	3.023

Table 3.8: Tafel data of deposited TiN potentiodynamic scans.

Tafel Variables	0.1 M	0.2 M	0.3 M	0.5 M	1 M
Beta A (V/decade)	4.946	3.588	3.302	4.620	4.116
Beta C (V/decade)	9.495	7.454	6.163	4.139	6.081
I_{corr} (A/cm²)	12.70e-6	12.30e-6	14.60e-6	7.780e-6	26.60e-6
E_{corr} (mV)	96.90	149.0	114.0	200.0	246.0
Corrosion Rate (mpy)	20.25	18.17	21.55	12.23	42.38

3.3.2.3 Potentiostatic transient response of Ti/TiN in H_2O_2 mediums

Figure 3.9 demonstrates titanium current steady state behavior as a function of the oxidizer concentration. Within the 0.1 M to 0.5 M concentrations lower current values are attained as a function of increasing oxidizer amount. The recorded values are parallel to the oxide growth and surface dissolution throughout the scan period. As the final conductivity level indicates the passivation of titanium surface or the formation of a semi-continuous but pore free layer. The similar behavior is observed with TiN surface potentiostatic measurements as shown in Figure 3.10. The curves continue to passivate as more oxidizer is added into the solution and hence a lower conductivity is achieved. Both material passivation curves for Ti and TiN at 0.2 M oxidizer show less reduction as compared to the lower concentration of 0.1 M addition suggesting that the latter concentration is more stable. In addition, TiN shows lower surface conductivity than Ti at this particular surface composition as it is generally expected to passivate less than the metals; Ti and W, as in the previous results (Figures 3.9 and 3.3).

Comparing all the films from the passivation point of view, Ti shows lower passivation currents as compared to W, which aligns with the fact that the oxide film of Ti that is known to be titanium dioxide is more stable than the tungsten oxide. Titania, TiO_2 with an approximated thickness of 5nm (Liu et al., 2004) typically has a better surface coverage than the (WO_3) film formed on the W surface (Seo et al., 2017).

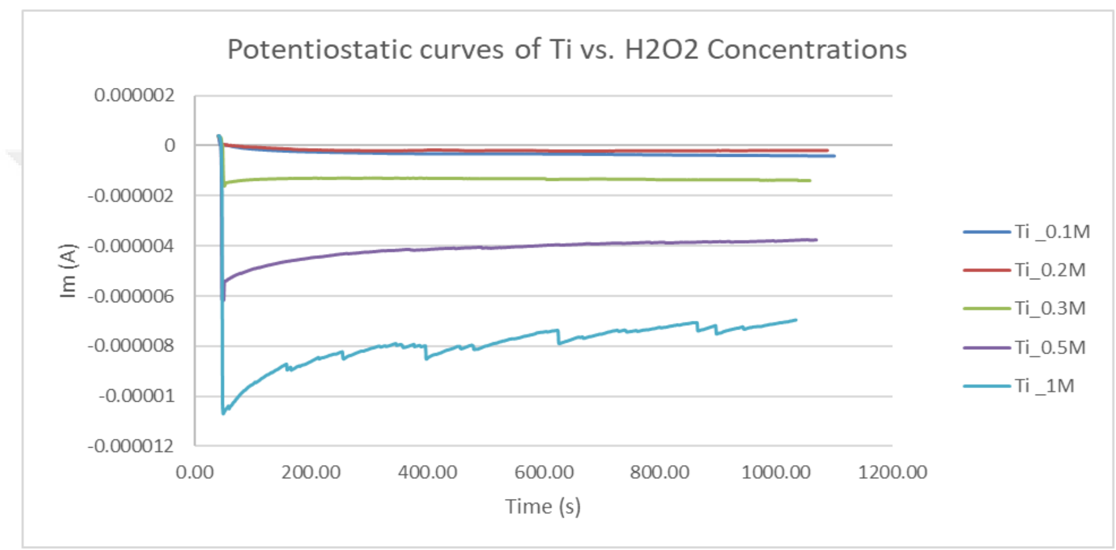

Figure 3.34: Potentiostatic (current-time) sweep of titanium in hydrogen peroxide solutions.

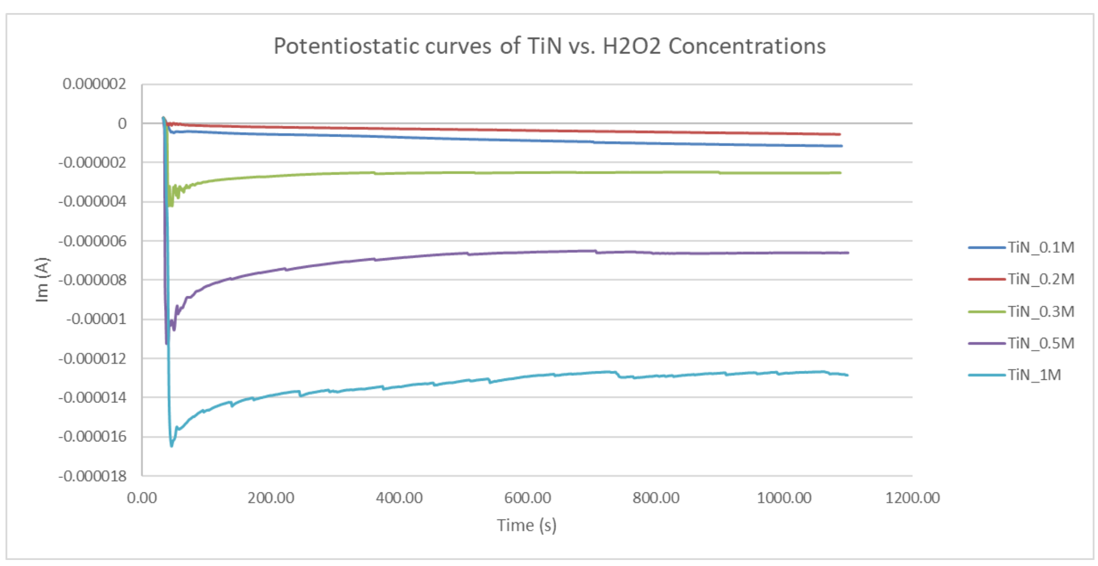

Figure 3.35: Potentiostatic (current-time) sweep of TiN in hydrogen peroxide solutions.

Table 3.9: Calculated slopes of Ti and TiN curves in H_2O_2 solutions.

Hydrogen Peroxide Concentrations	Titanium Slope (A/s) abs	TiN Slope (A/s) abs
0.1 M	7.25E-09	5.88E-08
0.2 M	8.98E-09	2.36E-08
0.3 M	6.33E-08	5.13E-07
0.5 M	3.17E-07	8.96E-07
1 M	1.45E-06	1.69E-06

3.3.2.4 Oxide formation rate predictions

Similar to the W experiments, slopes of the resulting curves of titanium and TiN were also calculated and presented in Table 3.5. Growth rates were related to the passivation slopes reported in A/s. As mentioned before the exponents in the MacDonald's model represents the oxide growth rate, which in this case is increasing as more oxidizer is added to the total solution for Ti and TiN. Between the growth rates measured at 0.1 M and 0.5 M for titanium the increase is in the calculated slope is three times, whereas the TiN showed an increase of four times.

3.3.2.5 Surface oxide evaluation

3.3.2.6 Surface roughness measurements

Figures 3.11 and 3.13 show post potentiostatic measurement roughness data of Ti and TiN wafer coupons, respectively. Titanium shows similar RMS roughness values for concentrations within 0.1 M to 0.3 M yet a relative increase at higher concentrations of 0.5 M and 1 M of hydrogen peroxide addition. This increase can be indicative of thicker oxide layer formation on the surface as can be seen topographically in Figure

3.12. On the other hand, TiN RMS roughness data illustrated in Figure 3.13 show lower RMS values as compared to the titanium with minor variations among the studied concentrations with AFM micrographs given in Figure 3.13.

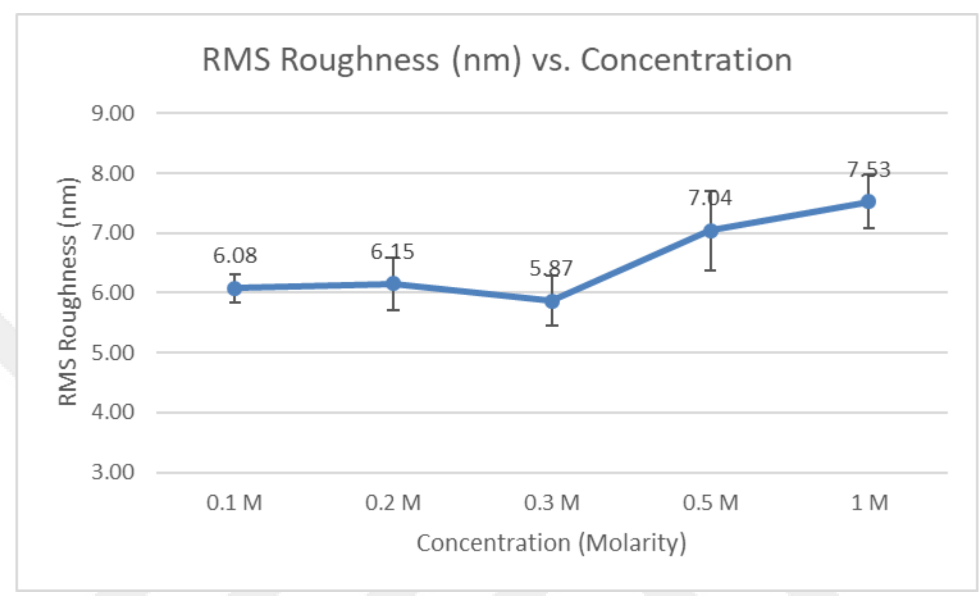

Figure 3.36: RMS roughness of deposited titanium post potentiostatic.

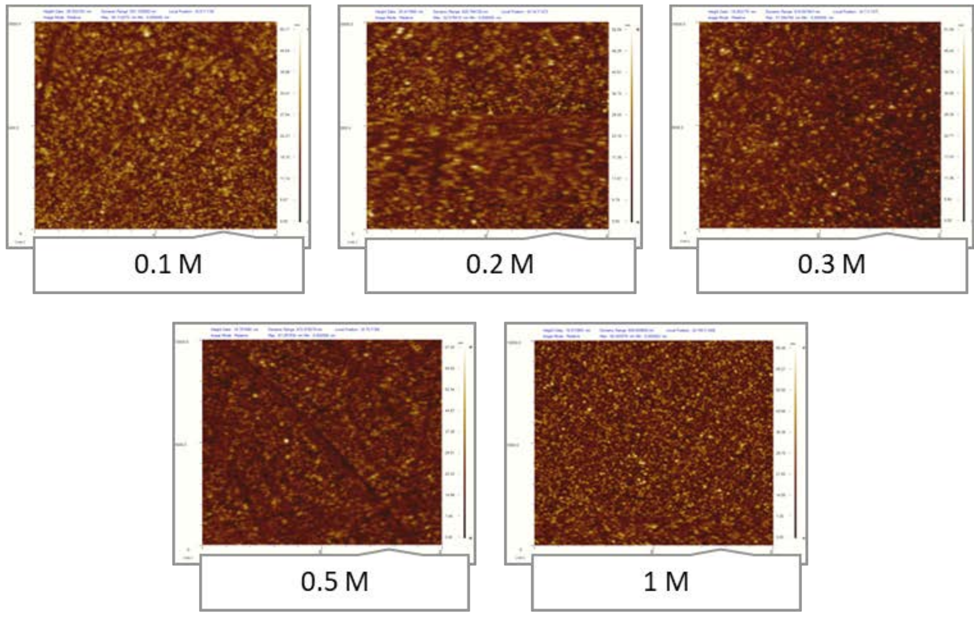

Figure 3.37: AFM topographic images of titanium post potentiostatic.

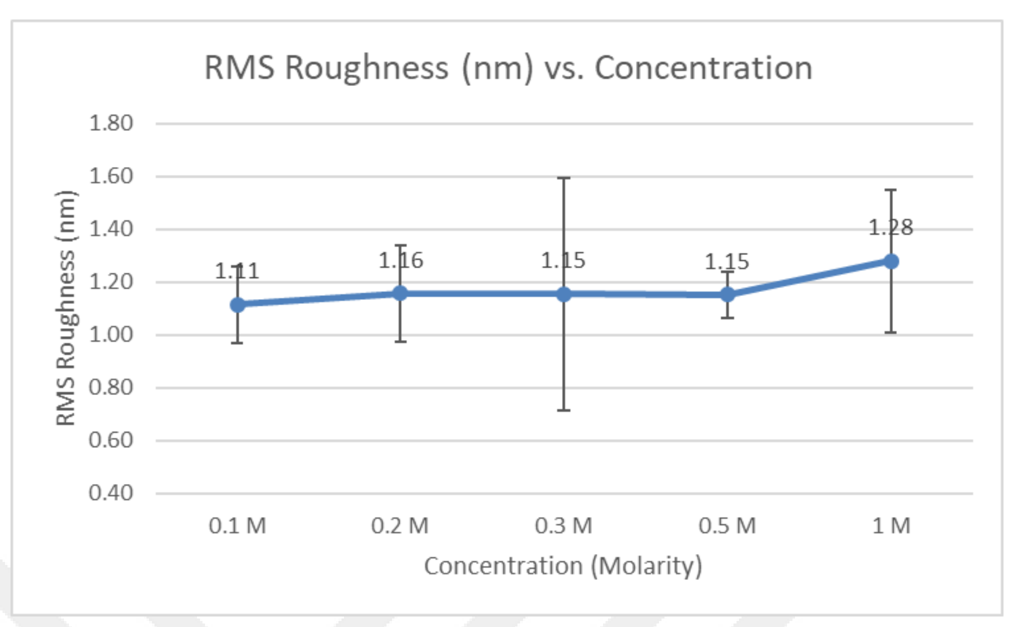

Figure 3.38: RMS roughness of deposited TiN post potentiostatic.

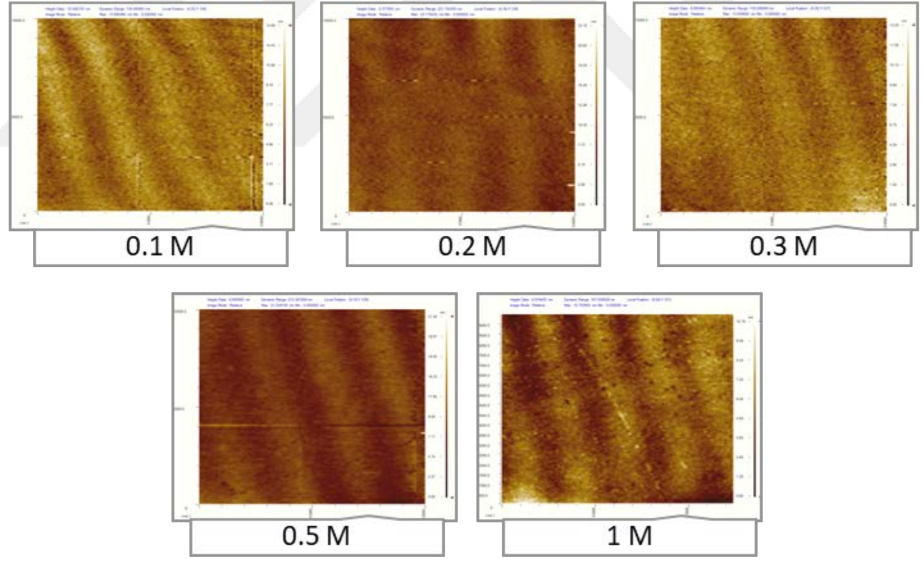

Figure 3.39: AFM topographic images of TiN post potentiostatic.

3.3.2.7 Contact angle measurements

Both Ti and Ti N films were observed to give high contact angles as can be seen in Figures 3.15 and 3.16. Although the measured contact angles of the TiN surfaces were slightly higher, the main change in the wettability responses were not statistically

significant in between the two films and within the measurements of the same film at different oxidizer concentrations.

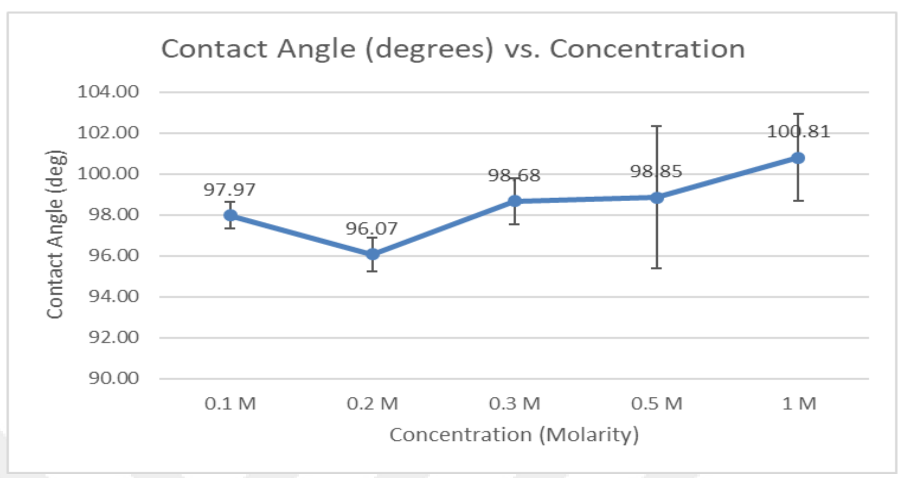

Figure 3.40: Contact angle data of deposited titanium post potentiostatic.

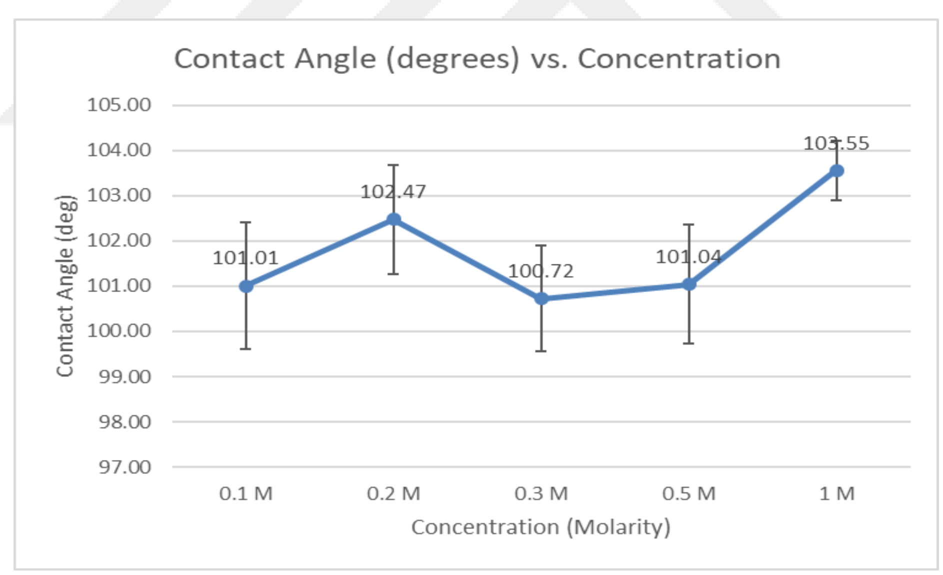

Figure 3.41: Contact angle data of deposited TiN post potentiostatic.

3.3.3 CMP application and performance evaluations on W and Ti/TiN barrier films as a function of slurry oxidizer concentration

3.3.3.1 Material removal rate evaluations

Table 3.6 summarizes the material removal rates of Ti, TiN and W wafer coupons calculated based on the weight loss and film thickness calculations at the five different oxidizer concentrations. Within the titanium CMP evaluations, removal rates showed an increase as the molarity of the H_2O_2 increased in the formulated slurries. Hence, it can be concluded that the formation of the passivated TiO_2 film improves the polishing rates by forming a thicker surface oxide. TiN wafers follow the similar trend except for the relative decrease at 0.5 M concentration. Tungsten, however, shows an irregular removal rate behavior along the selected concentration which was found to be resulted from the the nature of the oxide layer formed as WO_3. At 0.2 M oxidizer addition, on the other hand, all three materials share close MRR values indicating suitable slurry settings are provided to enable 1:1:1 MRR selectivity.

Table 3.10: Calculated removal rates of Ti, TiN and W under the effect of varying slurry oxidizer concentrations.

H_2O_2 Concentrations	Ti MRR (nm/min)	TiN MRR (nm/min)	W MRR (nm/min)
0.1 M	41.82	83.48	184.09
0.2 M	74.94	79.16	76.40
0.3 M	86.53	188.40	396.05
0.5 M	275.54	88.27	140.22
1 M	204.68	221.88	73.27

3.3.3.2 Characterization of post CMP surface quality

3.3.3.3 Roughness measurements and topographic data

Titanium Surface Topography Analyses with Atomic Force Microscopy:

Figure 3.17 illustrated the RMS surface roughness as a function of hydrogen peroxide concentration added into the CMP slurry during the polishing experiments. It can be seen that post CMP surface roughness measurements were well reproducible based on the standard deviations of the data points. Based on the 2-D AFM micrographs in Figure 3.18, post CMP titanium had controlled surface roughness and better smoothed finish. Particularly at the lower concentrations up to 0.3M, the surface roughness values were the same statistically and an increase is observed at 0.5 M concentration which follows the higher removal rates at this concentration as presented in Table 3.6, the promoted surface chemical activity resulted in higher removal rates.

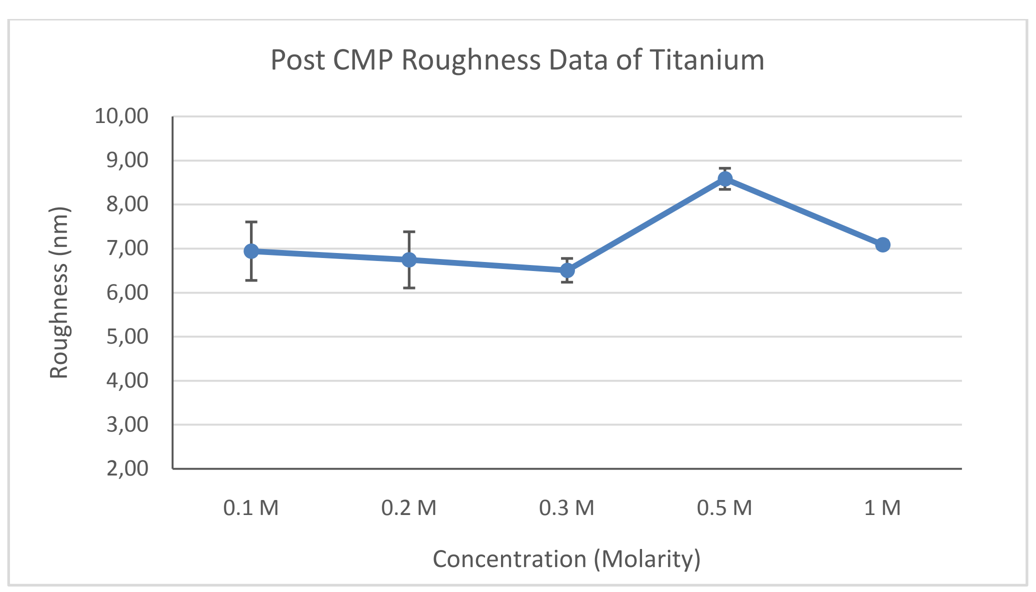

Figure 3.42: Titanium (deposited) RMS roughness data post CMP at five concentrations.

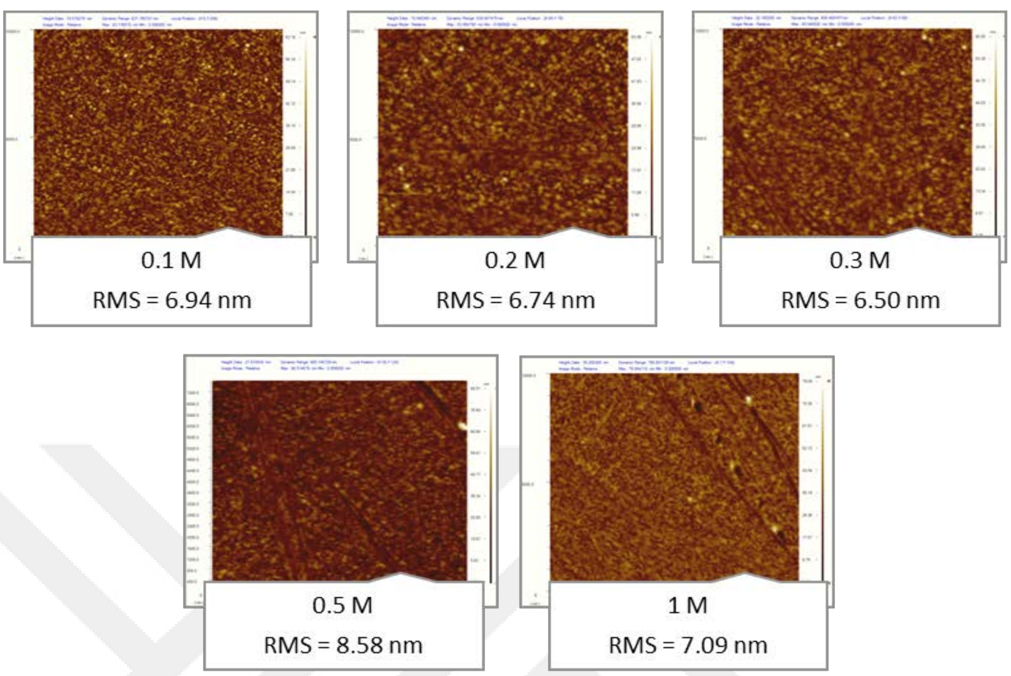

Figure 3.43: Titanium (deposited) AFM images post CMP at five concentrations.

Titanium Nitride Surface Topography Analyses with Atomic Force Microscopy:

Surface topography evaluations of TiN were also observed to get affected by the CMP treatments. Consequently, the roughness data given in Figure 3.19 and topographical images shown in Figure 3.20 indicate a slight increase with the increasing of H_2O_2 concentration as a predicted consequence of a higher oxide formation rate and a stable mechanical abrasion. At 0.5 M, the observed high standard deviation in surface roughness could relate to the change in the oxidation mechanisms on the material surface. Consequently, the removal rates are also lower and the surface is rougher. Overall, the average roughness values of TiN surfaces are relatively lower as compared to Ti.

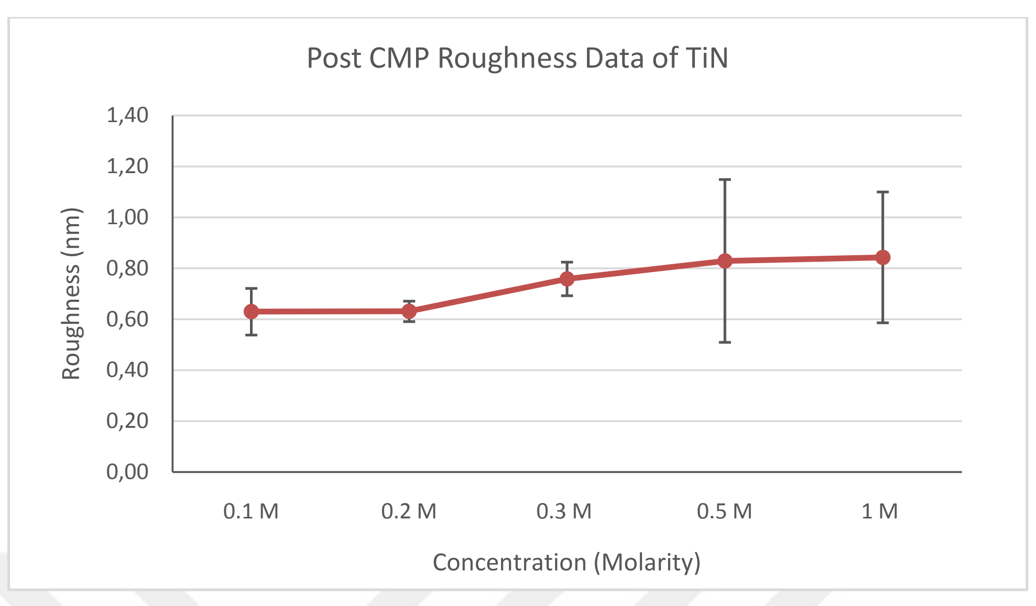

Figure 3.44: TiN (deposited) RMS roughness data post CMP at five concentrations.

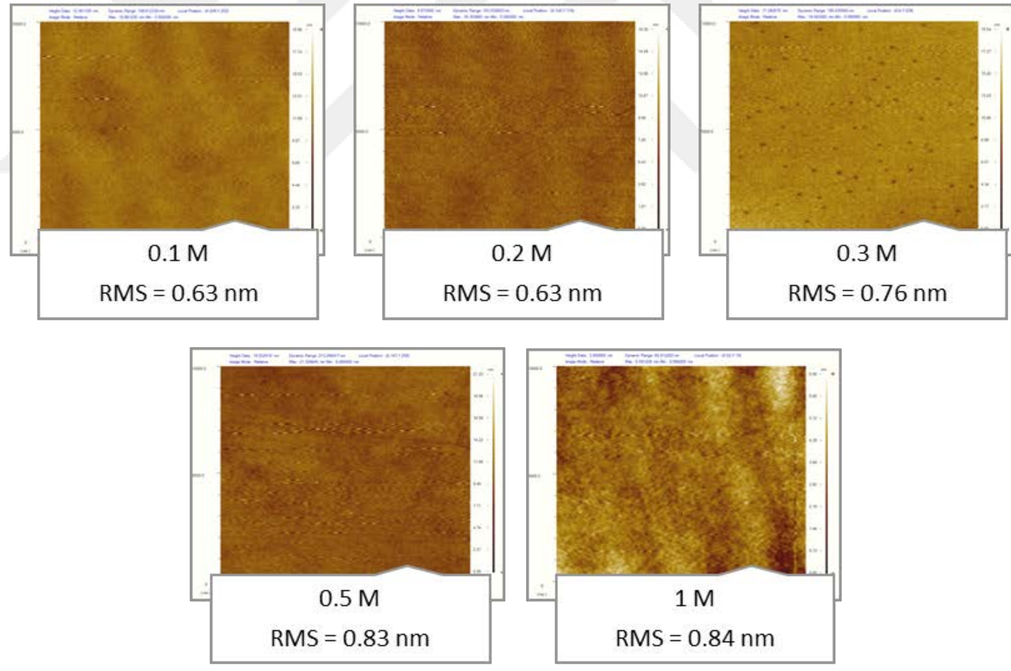

Figure 3.45: TiN (deposited) AFM images post CMP at five concentrations.

Tungsten Surface Topography Analyses with Atomic Force Microscopy:

Figure 3.21 show an increase in roughness of W surface as a function of increasing oxidizer concentration particularly at the two highest concentrations of 0.5 M

and 1 M. The AFM images in Figure 3.22 show the WO_3 film is uneven in structure due to nucleation and growth mechanism governed by Oswald Ripening at these concentrations. The measured RMS roughness values are closer to the measurements on titanium rather than TiN due to the metallic nature.

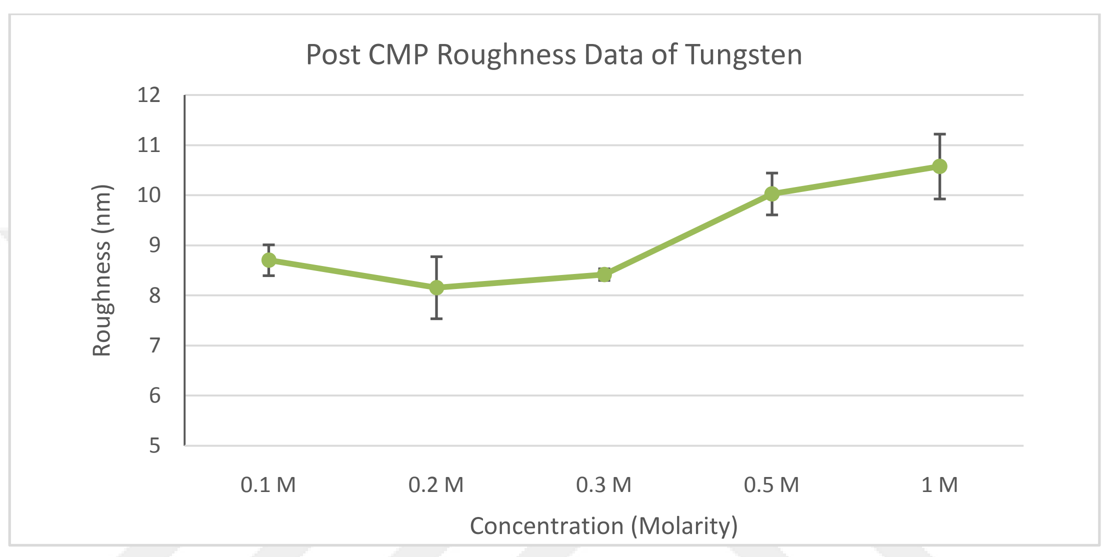

Figure 3.46: Tungsten (deposited) RMS roughness data post CMP at five concentrations.

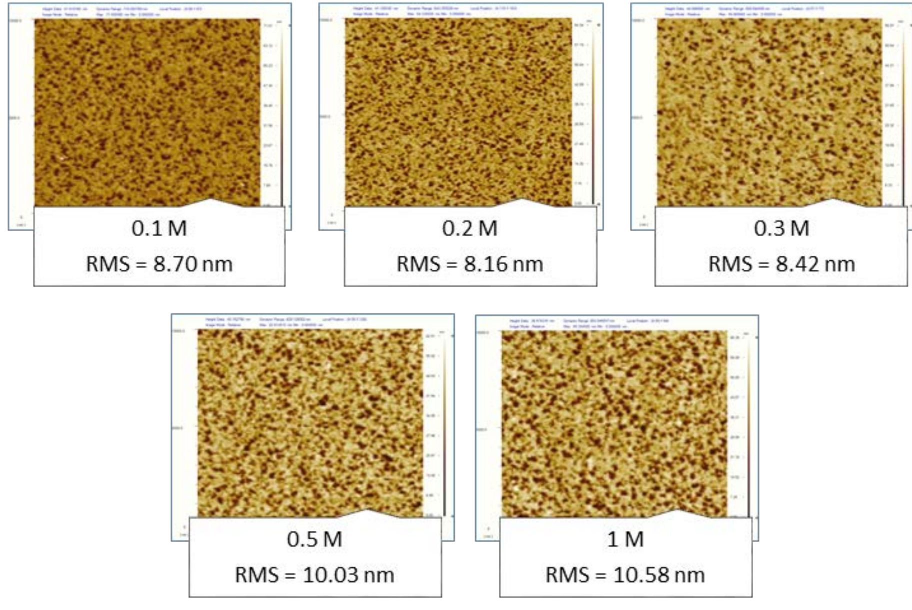

Figure 3.47: Tungsten (deposited) AFM images post CMP at five concentrations.

3.3.3.4 Contact angle and wettability measurements

The contact angle measurements taken on the Ti surfaces post CMP treatments are shown in Figure 3.23. It can be seen that noticed that there is a slight descend in hydrophobicity initially up to 0.3M concentration which further accelerates at 0.5 M and 1 M oxidizer addition. The surface topography was also observed to change at these concentrations affecting the wettability measurements. TiN, however, showed a gradual decrease in wettability (increase in contact angle), as illustrated in Figure 3.24. In the case of W, more hydrophilic nature is recorded with stable contact angle measurement series except for the 1 M concentration where a decrease is observed as given in Figure 3.25.

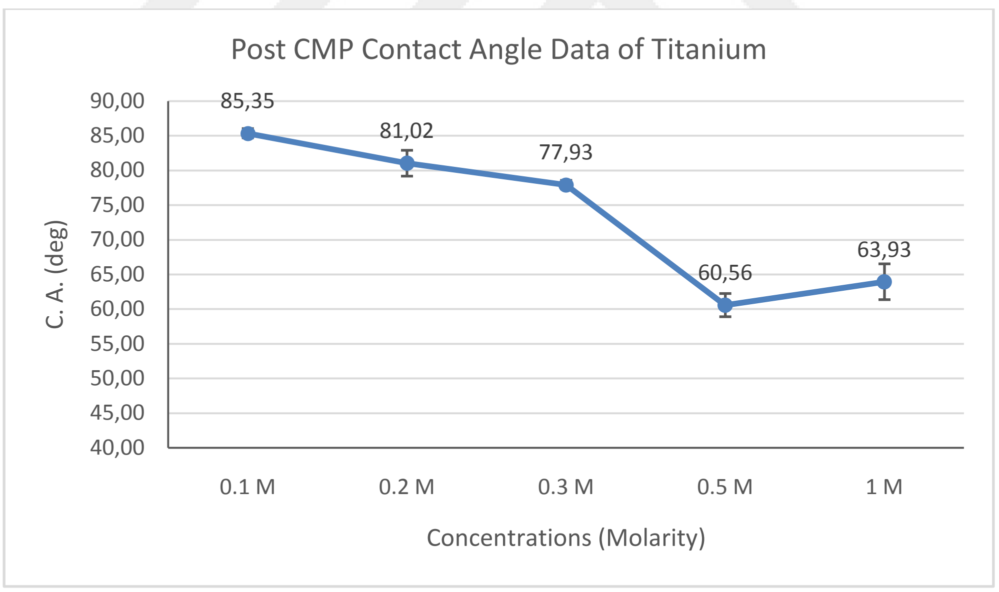

Figure 3.48: Titanium (deposited) contact angle data post CMP at five concentrations.

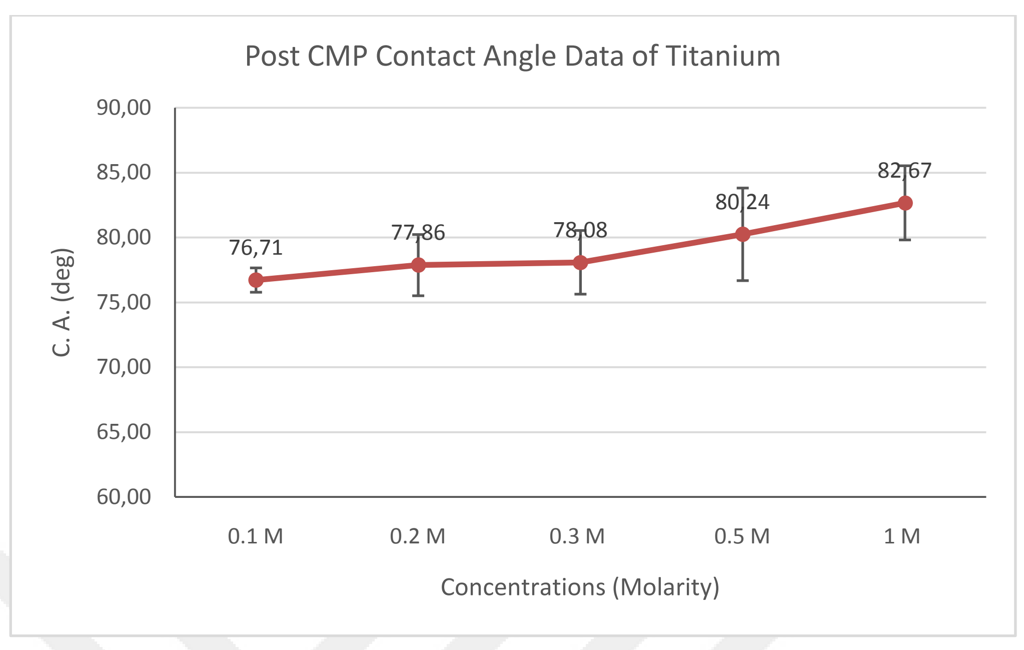

Figure 3.49: TiN (deposited) contact angle data post CMP at five concentrations.

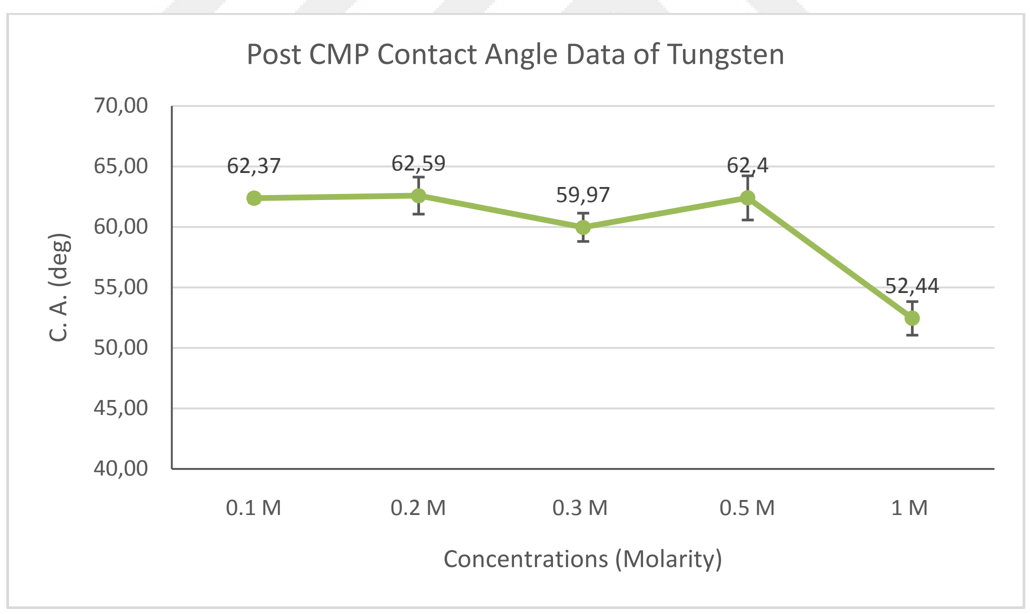

Figure 3.50: Tungsten (deposited) contact angle data post CMP at five concentrations.

3.4 Summary and Conclusions

This chapter focused on the application of titanium and TiN films in tungsten CMP ass barrier material as it applies to ULSI technology. A conformal planarization

through CMP application requires a thermally and chemically stable barrier layer which is expected to produce a compatible polishing rates as the interconnects or plugs during planarization. To understand the best slurry configurations for a compatible removal rate and surface finish during planarization electrochemical analyses of metal and barrier films were explored through potentiodynamic and potentiostatic methods.

The presence of oxidizer in the CMP slurries has an important role to promote chemical activity during the processing. The formation of oxide layers and the removal of the oxidized layer through particle abrasion involves controlling polishing synergy between the chemical and the mechanical actions.

In summary the CVD tungsten was electrochemically studied as its surface was exposed to oxidizer at different concentrations, which induced the oxide layer formation as WO_3. Potentiostatic scans showed the effect of H_2O_2 concentration on surface passivation where a decrease in corrosion rates were observed and current levels decreased throughout the passivation activity. The increasing slope of passivation curves (rates) indicated faster oxide formation as more oxidizer was available close to the metal's surface. Similar passivation rates were noticed at 0.2 and 0.3 M oxidizer additions which also reflected as similar corrosion rates. At 1 M concentration, on the other hand, immediately after addition of H_2O_2 current rose with no passivation achieved. Surface characteristics indicated low roughness and a uniform oxide layer forming at the concentrations of 0.1, 0.2 and 0.3 M and higher roughness was observed at the higher molar concentrations. Corrosion rates at 0.2 M and 0.3 M concentrations were close and observed to reside in between the 0.1 and 1 M concentrations, where higher rates were attained.

In addition, potentiostatic and potentiodynamic curves were produced for titanium and TiN in hydrogen peroxide mediums. TiN Tafel data showed much higher corrosion rate values as compared to titanium indicating that the latter is the protective layer and TiN works better as a dielectric-metal adhesion interface. Conductivity levels in potentiostatic sweeps indicated passivation of titanium surface or the formation of a semi pore free layer. The same general scheme was observed with TiN surface potentiostatic measurements. However, TiN showed lower surface conductivity than Ti as the nature and composition of the surface were different for this non-metallic layer. Surface roughness data for concentrations showed an increase at 0.5 M and 1 M of hydrogen peroxide concentrations relative to the lower concentrations due to the thicker oxide layer formation on the surfaces. In general, TiN RMS roughness was lower relative to to titanium.

The effect of chemical mechanical polishing on metal's surface and the changes in surface topography was investigated as a function of H_2O_2 concentration in the slurry environment. Titanium removal rates showed an increase accompanying the increase in the oxidizer concentration, as formation of TiO_2 film improves polishing rates at the fixed slurry solids concentration. TiN follows the same analogy except at 0.5 M a slower rate is observed. Tungsten removal rates were sought to be affected by the nature of the oxide layer formed as WO_3. At 0.2 M all the materials shared close MRR values indicating suitable slurry settings as discussed more in detail in the next chapter. Likewise, looking at the roughness data of the treated Ti and W surfaces, both showed similar values while TiN showed much smoother surface finish. Furthermore, TiN gradually decreased in wettability in agreement with the roughness measurements, whereas tungsten produced lower values than Ti and TiN. It shows a stable contact

angle series except at 1 M where a decrease has occurred due to continuous corrosion of the film. Consequently, it is observed that materials surface topography responses change as a function of the oxidizer concentration, which in turn affects the surface wettability, total surface energy and by that leading to variable control of polishing rates and the surface quality responses.

CHAPTER IV

OPTIMIZATION OF TIO_2 NANO-FILM FORMATION AND PERFORMANCE IN TUNGSTEN BARRIER CMP APPLICATIONS

4.1 Introduction

This chapter focuses on optimization of barrier CMP application for tungsten films where a Ti/TiN film stack is used to achieve proper adhesion on silicon while limiting the metal diffusion into the transistors. Slurry contributes chemically and mechanically to the polishing process and controlling these inputs produces controlled surface quality and polishing rates for W/Ti/TiN layers can be achieved Titanium surface layer targeted to be achieved for removal during the CMP produce is an oxide film, which forms as the fresh Ti layer is exposed in a cyclic manner to slurry chemicals and solid abrasives. The passivation properties of the tungsten, titanium and the titanium nitride films were studied in detail in the previous chapter. In order to achieve a compatible removal rate selectivity and minimum roughness during barrier CMP to enable multi-layer metallization the CMP performance evaluations are presented in this chapter.

In order to quantify the necessities for improved CMP outputs, the methods investigated in the previous chapters were utilized to explore desired selectivity between W/Ti through Ti/TiN barrier layers. Electrochemical methods were evaluated to understand oxide film growth mechanisms and corrosion outputs for the studied layers.

Material removal rates on the blanket W, Ti and TiN films are used as the key to calculate the desired selectivity values for barrier CMP. Chemical activity during the

CMP process is controlled by the addition of hydrogen peroxide into the slurry at different concentrations and the formation of the chemically modified metal-oxide layer is studied through electrochemical passivation and surface topography and wettability responses. Mechanical activity provided by the slurry abrasives is analyzed based on solids loading percentages of the nano-scale silica particles in the slurry pumped within the wafer surface/pad interface. Post CMP surface evaluations were performed to assist in understanding the quality of the interface between W/Ti/TiN layers.

4.2 Experimental Approach

4.2.1 CMP Experiments on titanium/titanium nitride and tungsten Chemical Vapor Deposited (CVD) films

In order to achieve an optimized material removal rate selectivity of CMP on deposited W/Ti/TiN stack, blanket films of each layer were polished and analyzed for material removal rates as a function of the process chemical and mechanical variables. Electrochemical methods were used to evaluate the metal oxide film growth rates as the wafers were reacted with the H_2O_2, which is validated as an important input to the process performance. It was observed that the CMP applications indeed followed the electrochemical observations outlining the passivation rates in alignment with the removal rate selectivity. The optimized slurry oxidizer and abrasive solids loading ratios eventually led to an improved performance of the selected layers.

4.2.1.1 Passivated oxide film formation evaluations through electrochemical studies.

Potentiostatic and potentiodynamic electrochemical evaluation methods tested on Ti/TiN and W metal surfaces under the influence of certain concentrations of the selected oxidizer. Through potentiostatic measurements oxide film growth and passivation was observed for each material and the data from these experimental curves were presented. Similarly, potentiodynamic polarizations under selected concentrations of the hydrogen peroxide mediums were conducted. The resultant corrosion rates for the materials in study were compared and analyzed in this chapter. The findings were used to optimize surface oxidation performances of W/Ti and TiN wafer coupons.

4.2.1.2 Material removal rate evaluations on Ti/TiN and W during CMP under oxidizer variations.

Titanium and TiN material removal rates were evaluated at the concentrations of 0.1 M, 0.2M, 0.3M, 0.5M and 1M of hydrogen peroxide. The same procedure was applied to tungsten, where at each of these concentrations slurry solids loading percentage of 3%wt was used. The process of polishing was applied at 30 N down force with a rotational speed of 150 rpm. The weight measurement and calculations were done as detailed in the previous chapter. In this chapter, a comparative study is presented to find the optimal concentration of slurry oxidizer (i.e. H_2O_2).

4.2.1.3 Slurry solids loadings optimization for CMP of Ti/TiN/W stack films.

Each material has gone through CMP at fixed oxidizer concentration of 0.2 M that was optimally found to have desired removal rates. At this oxidizer concentration, for each material the slurry solids loading was varied at four different concentrations of 3%, 5%, 10% and 15%, respectively. The slurry abrasive used in this experiment was silica. The polishing process was set to 30 seconds with a down force of 30 rpm and a

co-rotational speed of 150 rpm. Weight measurements were conducted before and after polishing to finally enumerate the removal rates for W, Ti and TiN at aforementioned silica percentages. Surface topography was evaluated by using AFM measurements at contact mode where images were obtained at a quality of 10 by 10 micrometers.

4.3 Results and Discussions

4.3.1 CMP selectivity evaluations based on electrochemical measurements on Ti/TiN/W films

4.3.1.1 Potentiostatic oxidation rate evaluations of Ti and TiN and W Films

The series of potentiostatic passivation slopes (the surface oxide growth rates, as described earlier) are shown in Figure 4.1 for tungsten, titanium and titanium nitride surfaces. For each material, there was a noticeable increase in the rate of current reduction on surface as the oxide formation took place as explained in the previous chapter. Comparing the rates at 0.1 M and 0.2 M H_2O_2 addition, relatively similar rates of oxide growth was observed indicating a similar response to the presence of H_2O_2 at these concentrations. Hence, it is expected that the formed oxide films are similar in form and thickness at these concentrations.

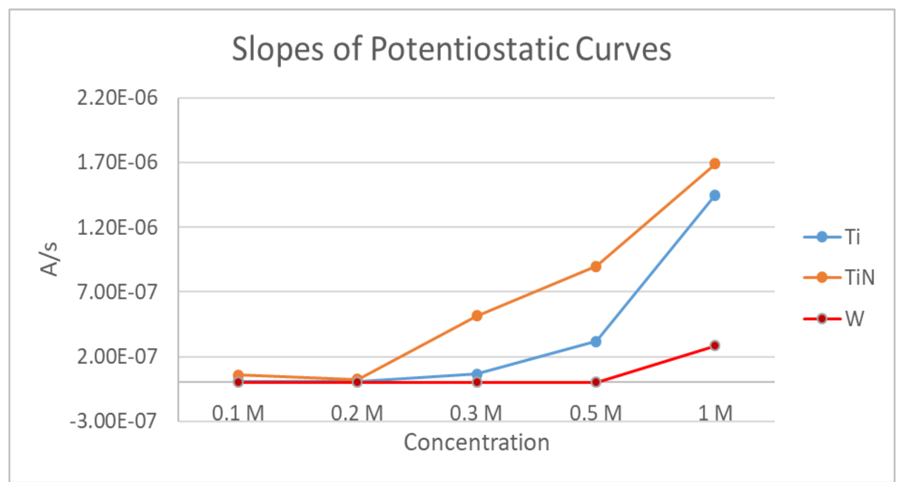

Figure 4.51: Potentiostatic passivation slopes in A/s for Ti/TiN and W in H2O2 mediums.

4.3.1.2 Post potentiostatic scan roughness and contact angle data:

Figure 4.2, illustrates the surface RMS roughness values of the tested materials. It is known that post CMP titanium and tungsten would form TiO_2 and WO_3 films on their surfaces,respectively. Consequently, these metallic films show similar roughness values for the first three H_2O_2 concentrations. A spike in RMS roughness is observed for tungsten at the higher concentrations indicating a change in the surface oxide morphology affecting the measured surface topography. TiN shows a lower surface roughness as compared to both titanium and tungsten due to its non-metallic nature.

Contact angle data for W/Ti/TiN are also illustrated post treatment in Figure 4.3. In this case, Ti and TiN follow close and relatively steady wettability throughout the increasing oxidizer concentrations. Whereas, tungsten shows a fluctuating wettability response and has contact angle values lower than both Ti and TiN. The similar nature of the Ti and TiN films tend to control the surface energy and wettability more dominantly throughout oxidation in this case. In the case of tungsten, however, a

permanent corrosion takes place at the relatively high concentrations changing both the surface topography and the wettability.

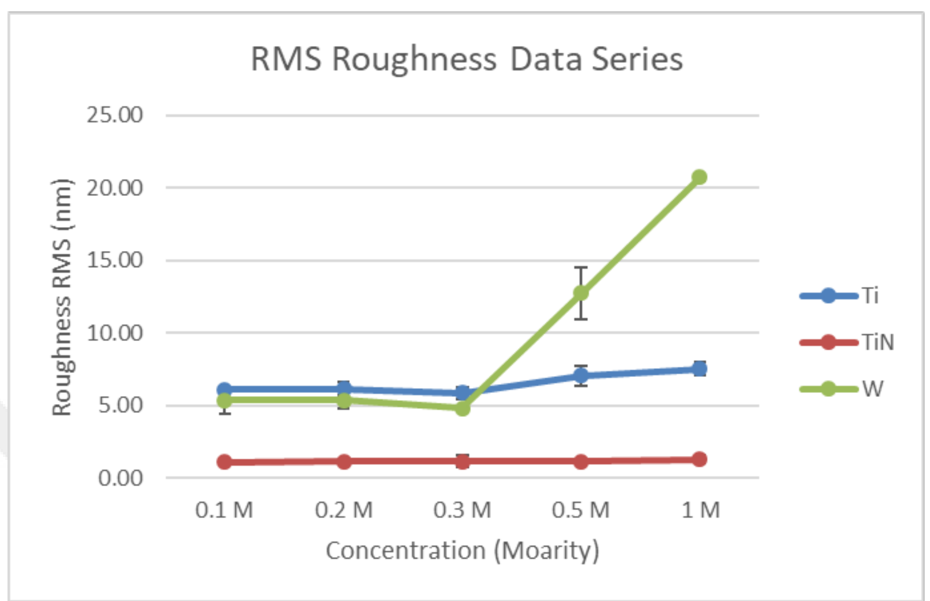

Figure 4.52: RMS roughness series of deposited Ti, TiN and W post potentiostatic scan at different H_2O_2 concentrated mediums.

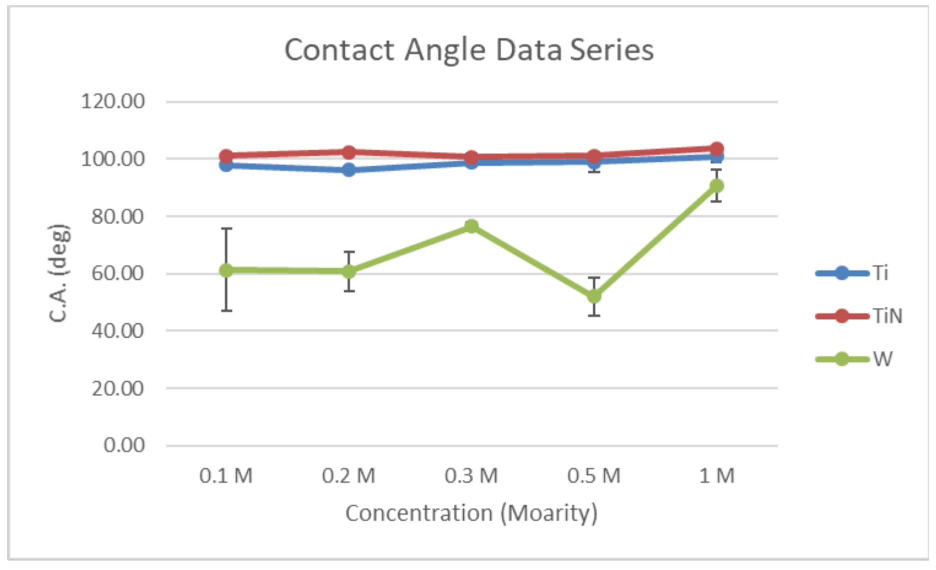

Figure 4.53: Contact angle series of deposited Ti, TiN and W post potentiostatic scan at different H_2O_2 concentrated mediums.

4.3.1.3 Potentiodynamic responses and corrosion rates of Ti, TiN with W films

Calculated corrosion rates from potentiodynamic curves are reproduced in Figure 4.4 for titanium, TiN and tungsten. Each material demonstrates a stable corrosion rate along the given concentrations except at the highest value of 1 M. This is indicating that at the very high concentration of the oxidizer the chemistry of oxidation highly dominates making the process highly unpredictable. Titanium and TiN show similar corrosion rates as compared to W. Therefore, both can be considered as suitable barrier layers where TiN is placed at the interface with the dielectric substrate. In summary, corrosion rates and oxide growth rates show a good selectivity at the low concentrations of 0.2 M and 0.3 M of hydrogen peroxide addition.

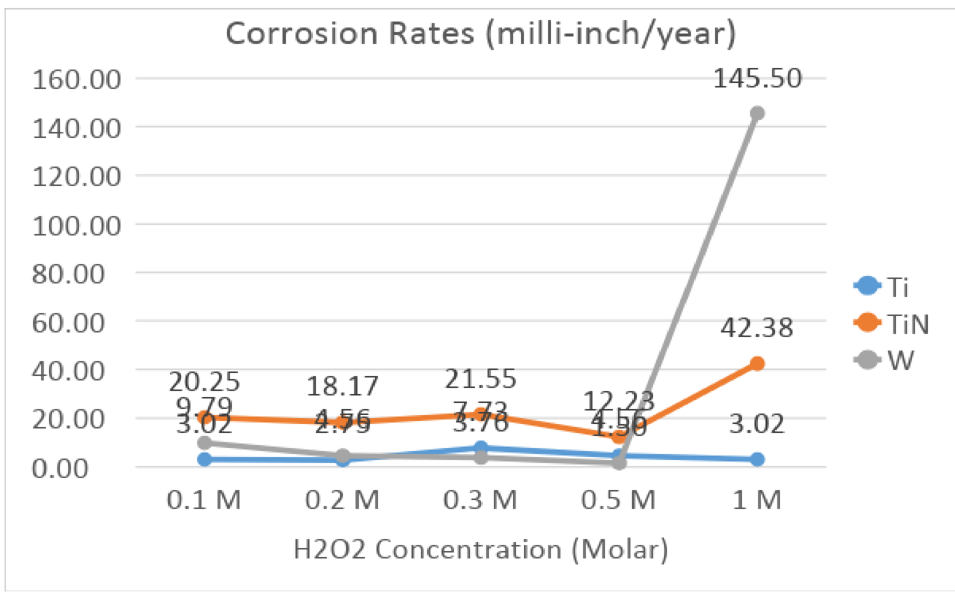

Figure 4.54: Corrosion rates series of Ti, TiN and W extrapolated from Tafel data of potentiodynamic in oxidizing mediums.

4.3.2 Material removal rate selectivity calculations of Ti/TiN/W films

Material removal rates calculated for Ti/TiN and W films as a function of slurry oxidizer concentration are presented in Figure 4.5. As the molarity of the oxidizer increases, the removal rates for the selected materials vary. Yet, similar rates are observed at 0.2 M H2O2 concentration indicating an optimal point for W/Ti/TiN with an average MRR value of 77 nm/min. This finding is also in agreement with the previous electrochemical measurements.

Looking at produced surface roughness data in Figure 4.6, titanium and tungsten metal surfaces are similar in topography and rougher than the TiN surface. TiN roughness values show a little or no change along the concentrations used in the experiments, while tungsten and titanium showed slight increase in roughness at the higher concentrations.

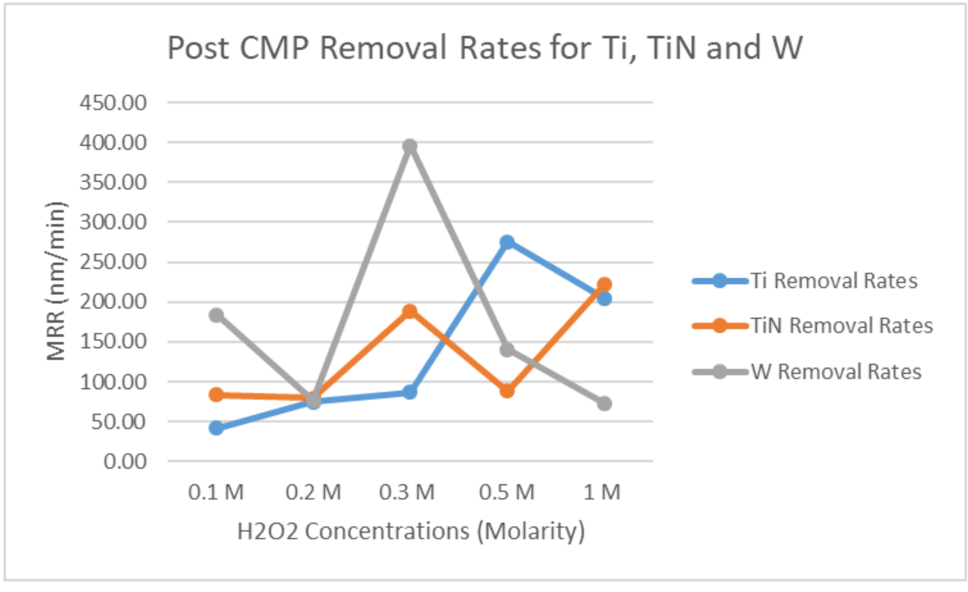

Figure 4.55: Post CMP calculated removal rates for Ti/TiN and W in H_2O_2 mediums.

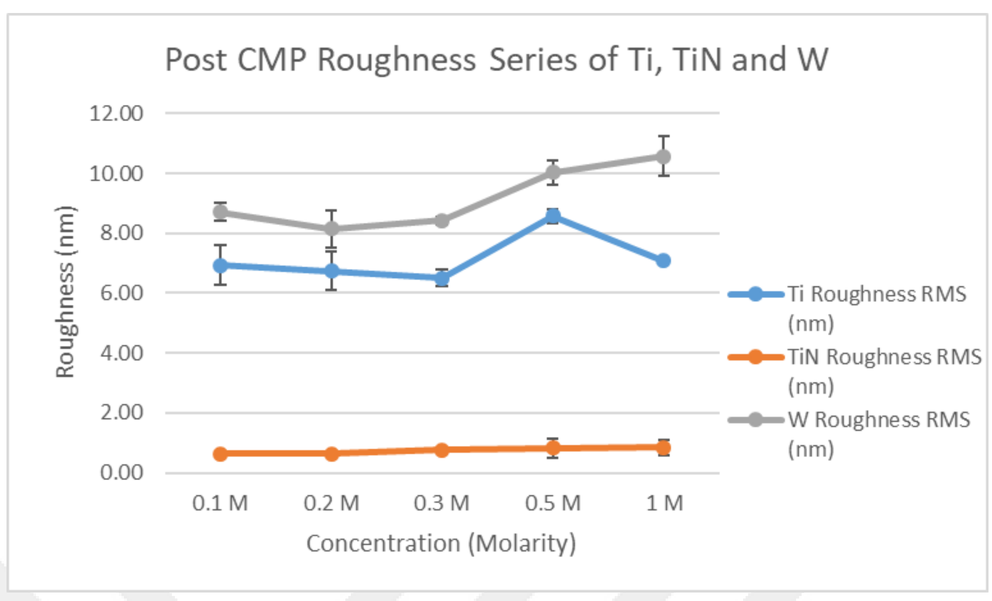

Figure 4.56: Overlaid RMS roughness series for Ti,TiN and W post CMP application

4.3.3 CMP slurry solids loadings effect against fixed oxidizer concentration.

4.3.3.1 Assessing material removal rates post CMP of W, Ti and TiN

Another important input to the chemical mechanical polishing process is the control of slurry abrasive concentration which provides the mechanical action in between the polishing pad and the wafer sample. Hence, the slurry solids loading was varied to calculate the Ti/TiN and W removal rates at the chosen optimal oxidizer concentration of 0.2 M. Figure 4.7 illustrates the optimal MRR to achieve 1:1:1 selectivity for Ti/TiN/W films is at 0.2 M and 3wt% slurry solids loading. Tungsten shows stable removal rates across the selected slurry solids loading percentages as the chemical surface oxide formation regulates and controls the material removal for the very hard tungsten material. Titanium experiences a sudden increase in the removal rates at 5% solids loading, which descends along the higher silica solids loading concentrations.

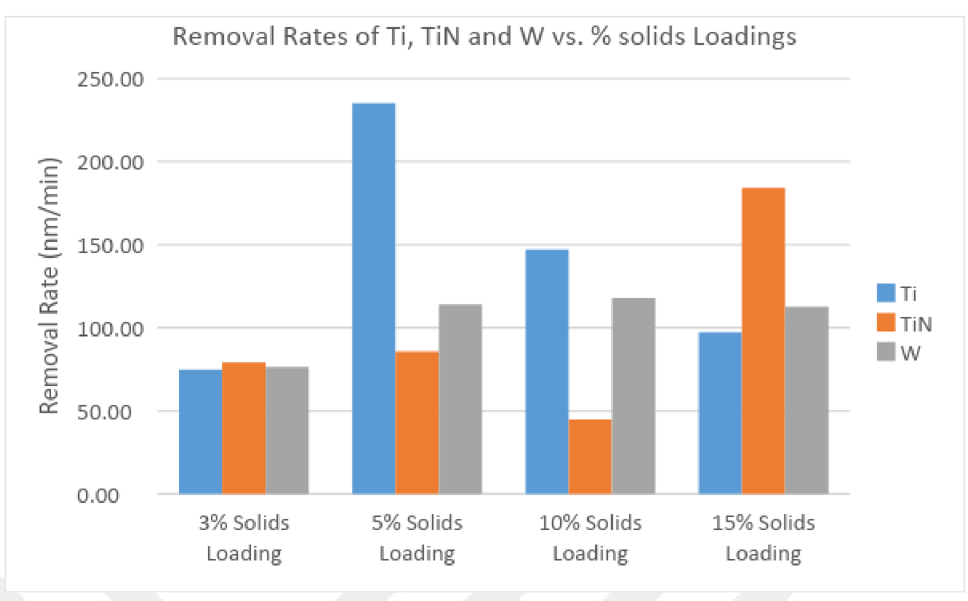

Figure 4.57: Removal rates as a function of silica solids loadings on CMP of Ti, TiN and W at a fixed oxidizer concentration.

The lower removal rates indicate that the slurry abrasives are occupying larger surface area and there is lower pressure per particle reducing the MRR. TiN film, however, demonstrates a somewhat of decreasing rate trend with a sharp increase attained at 15% solids loading.

4.3.3.2 Surface characterization post CMP application on Ti, TiN and W via roughness measurements

RMS roughness data under solids loading experiments are shown in Figure 4.8, where tungsten surface shows the highest roughness values following the titanium wafers. The decrease in the surface roughness of Ti films at the highest concentration is indicative of the formation of the protective TiO_2 film at the surface. On the other hand, TiN shows the lowest roughness output and the RMS values show a slight increase as shown in Figure 4.9 and more surface topography is observed.

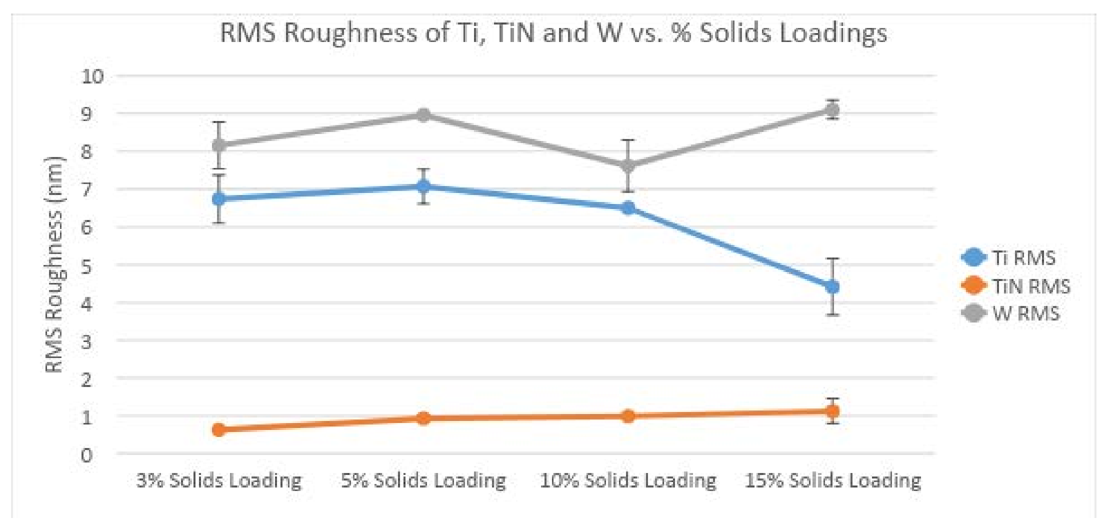

Figure 4.58: RMS roughness data as a function of silica solids loadings on CMP of Ti, TiN and W at a fixed oxidizer concentration.

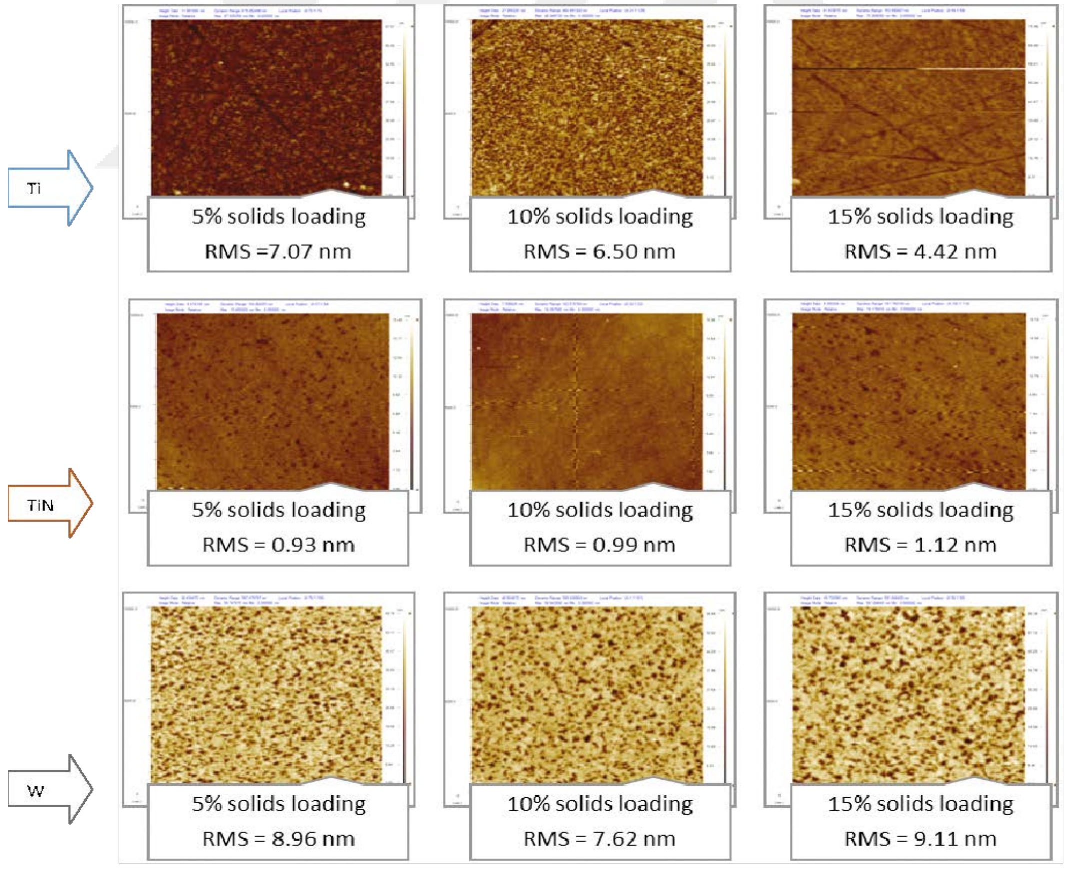

Figure 4.59: AFM surface images of Ti, TiN and W post CMP in different silica solids loadings percentages.

4.4 Summary and Conclusions

Optimization of the W CMP barrier process is presented in this chapter. The role of oxidizer to produce compatible oxide layers especially for tungsten and titanium surface was evaluated through electrochemical tests to understand oxide growth rates in relation to the concentration of hydrogen peroxide is present in the medium.

The slopes of the potentiostatic oxidation/passivation curves for Ti/TiN and W were analyzed and the found to be similar at 0.2 M and 0.3 M of oxidizer addition pointing out similar responses to H_2O_2 mediums. At these values it is expected that the formation of passive oxide films on the surfaces follow a similar film thickness. As TiO_2 and WO_3, are surface oxidation products for titanium and tungsten, respectively, both materials show similar roughness output at the low H2O2 concentrations up to 0.3M, whereas TiN demonstrates a lower surface roughness as compared to Ti and W. Yet, both Ti and TiN showed similar surface contact angle values, which could be explained by the fact that the wettability response is more controlled through the chemical nature of the surface. Furthermore, corrosion rates produced from potentiodynamic tests also showed similar values for titanium and tungsten at the lower concentrations indicating a good selectivity at the added hydrogen peroxide concentration.

Initially the chemical component of the CMP process was optimized at the fixed slurry abrasive concentration. A good removal rate selectivity was achieved at 0.2 Molar concentration and ~76 nm/min in average MRR values were obtained. Treated surfaces were also examined for post CMP topography and defectivity. Titanium and

tungsten metals surfaces showed similar RMS roughness values, owing to their metallic naturethan the ones recorded for TiN.

Finally, the mechanical component of the CMP process was varied by changing the slurry abrasive concentration at the optimal oxidizer addition of 0.2 M. Titanium films showed high removal rates attained at 5% solids concentration where TiN achieved similar result at 15% solids loading. On the other hand, tungsten exhibited stable rates among the increasing particles loading. This concludes that the tungsten CMP is more chemically limited by the formation of the tungsten oxide film whereas the TiN film is removed more mechanically by increasing the abrasive concentration. Roughness data affirmed a better surface output at the higher slurry solids loadings since metals such as titanium exhibited micro scratches on the surfaces at the lower concentrations as shown by the topographical images in Figure 4.9.

CHAPTER V

CONCLUSIONS AND SUGGESTIONS FOR FUTURE WORK

5.1 General conclusion

The applications of titanium and its naturally forming TiO_2 film have been explored in this thesis as it applies to fields of advanced engineering. Owing to the impressive mechanical and chemical properties of titanium possess, versatile applications utilize this metal and its oxide film as introduced in detail in the first chapter. One of the main properties of interest here is titanium's high corrosion resistance that is advent due to the passive oxide layer forming on its surface once an oxidizing medium is available.

One application that benefits from such quality is in biomedicine. As titanium is used as implant material its oxide layer is known to enhance the bio-compatibility in the surrounding body environment. Surface modifications allow titanium to gain durability and a longer life time where tissues and body cells react as an interface. Chemical mechanical polishing (CMP) technique is one of the recent surface modification method introduced by our group to induce desired topography on the titanium-based dental implants. CMP method provides a selective approach to gain desired surface topography and a controlled surface roughness while promoting the formation of a surface protective layer. As the main principle of this process involves the creation and spontaneous removal of the metal oxide surface layer, the chemical and mechanical components of the process were investigated. Mainly, the slurry variables

were characterized as a function of the oxidizer and abrasive nano particle concentration.

Initially, effect of oxidizer concentration on bulk titanium's coupons was evaluated electrochemically by conducting potentiostatic and potentiodynamic tests in order to observe the quality of oxide forming under the different hydrogen peroxide concentrations. The effect of H_2O_2 concentration on the oxide formation and material dissolution rates was observed to be more passivation and reduced current density measurement on the titanium surface. Correspondingly the evaluation of titanium surface at the selected H_2O_2 concentrations showed a good correlation between the contact angle and the surface roughness measurements in that the forming oxide layer increases the surface roughness. The increase in the roughness values can be attributed to the nature of the thick oxide layer forming in the presence of higher oxidizer in the solution. The calculated corrosion rates also indicated higher rates and faster dissolution based on the growth of TiO_2 on the surface of titanium.

The above outcomes were further utilized to comprehend the role of oxidizer in the chemical mechanical polishing of biomedical implants. CMP was applied on bulk titanium surface with controlled slurry inputs. At relatively low concentrations of slurry oxidizer low removal rates were observed as compared to the higher oxidizer concentrations. This observation could be attributed to the limited chemical action leading to metal oxide formation in that the mechanical action can only remove the chemically modified layer. Hence, increasing the oxidizer concentration helps transforming more surface titanium to titanium oxide and hence more effective mechanical abrasion increasing the removal rates. Both post CMP contact angle and AFM based surface roughness measurements also confirmed an improvement in surface

topography and surface homogeneity with higher slurry oxidizer content as better surface smoothness and wettability control was achieved.

Following the studies on the role of slurry oxidizer in CMP, the role of slurry solids loadings was also studied on the bulk titanium surfaces to verify the effect of mechanical action during polishing. The silica particles spread between the interface of the surface oxide layer and the polishing pad at the set rotational speed providing the mechanical action for enabling material removal. By varying the slurry solids loading percentages the removal rates synergistically increased with the oxidizer concentration for both 3% and 5% solids loadings due to the increasing total surface area of the abrasives present at the polishing interface.

In Chapter 3, a CMP study of titanium and its oxide as a barrier layer for tungsten based plugs was presented. CVD tungsten was investigated as a plug material that functions with Ti/TiN barrier layer deposited before the W is deposited on the dielectric substrate. CMP tests were applied on both W and Ti metals along with the TiN as a semi-metal. Focusing onto the functions of inputs to the CMP process, the role of oxidizer was assessed again as the chemical slurry variable. The slurry oxidizer enables an important role in increasing the removal rate since the passivation layer (WO_3) has a lower hardness as compared to W. Underneath the W layer, TiO_2 layer forms when the barrier Ti layer is exposed to the slurry oxidizer. In between, TiN layer helps titanium adhere to W effectively so that there is a good adhesion between the layers in contact.

Electrochemical methods were also used to analyze the effect of oxidizer concentration on W/Ti/TiN interface within a range of selected molar concentrations. Potentiostatic transients and potentiodynamic sweeps of CVD tungsten, titanium and

TiN were measured experimentally and the performances were evaluated via surface passivation, wettability and topography responses Potentiostatic scans showed the that as the H_2O_2 concentration increased, the passivation slopes also increased indicating a faster oxide formation. The oxidation rates of W and Ti were noticed to be close at 0.2 and 0.3 M oxidizer concentrations, which also related to the similar corrosion rates measured. However, at 1 M H_2O_2 addition, the current rose immediately showing no passivation and extremely high corrosion. TiN Tafel plots showed higher corrosion rates as compared to the titanium indicating that TiN works better as a dielectric-metal adhesion layer supporting its used at the W/Ti/TiN interface. Conductivity levels in potentiostatic sweeps indicated passivation of titanium surface supported by the surface roughness measurements. TiN showed lower surface conductivity as compared to Ti as the nature and composition of the TiN is intended to limit such conductivity.

The effect of chemical mechanical polishing on W/Ti/TiN surface and the changes in their topographies were examined as a function of H_2O_2 concentrations in slurry solution after the electrochemical measurements. Titanium removal rates showed an increase accompanying the increase in oxidizer concentration since the formation of TiO_2 layer improves polishing rates at a given slurry solids loading. As the W, Ti and TiN are affected similarly by the mechanical effect of the slurry abrasives, their compatible removal is more controlled by the oxidation rates and it was observed that at 0.2 M H_2O_2 addition all the materials shared close MRR values indicating a good material selectivity. In addition, RMS roughness data of the treated Ti and W surfaces were also similar while the TiN showed much smoother surface topography. Materials surface topography responses as function of the oxidizer concentration affects the surface wettability, total surface energy and hence impact the CMP performance.

Chapter 4 evaluates the results of W/Ti/TiN according to their electrochemical and CMP responses as to control the polishing selectivity between the metal interconnection and the barrier layer materials. The slopes of the potentiostatic curves for Ti/TiN and W were analyzed giving similar values at the 0.2 M of oxidizer for all these three materials. Resultant material surfaces showed that both titanium and tungsten had similar roughness outputs whereas TiN demonstrated a lower surface roughness. Also, surface contact angles representing wettability for both Ti and TiN were close which could be explained by the fact that both have titanium in their structure. Agreeing with potentiostatic results, the corrosion rates were also similar for titanium and tungsten at the same molarity indicating very good material removal rate selectivity. This was further confirmed when CMP was applied and the best selectivity was attained at 0.2 Molar H_2O_2 concentration with Ti and W surfaces also showing similar RMS values slightly higher than for TiN.

In addition, slurry solids loading tests were conducted at the selected hydrogen peroxide concentrations to calculate the CMP removal rates for each material. Titanium showed high removal rate at 5% solids concentration, whereas TiN achieved similar rates at 15% slurry solids loading. On the other hand, tungsten exhibited stable rates among the increasing particle concentrations. Roughness data affirmed a better surface output at the higher solids loadings due to the increased surface area of the abrasives decreasing the pressure per particle as shown by the topographical images.

In conclusion, TiO_2 has proven to produce desired surface properties in its applications in titanium biomedical implants as well as in titanium based barrier layer in microelectronics CMP applications. This layer provided good control level in the surface treatments of titanium as being an important aspect in chemical mechanical polishing and surface material planarization. The bulk titanium used in biomedicine

showed a good response to CMP experiments that dealt with controlled slurry oxidizer and solid abrasive content regulating the surface topography. Through experiments titanium also provided desired removal rate selectivity with tungsten as a metallic interconnect in combination with TiN barrier layer.

5.2 Suggestions for future work

As the nature of titanium bulk and its oxide were evaluated through electrochemical measurements in hydrogen peroxide mediums. These measurements can be extended to understand such behavior of CMP titanium in body simulated fluids. Such solutions can be involved in electrochemical analysis as an electrolyte medium. The performance of polished titanium for biomedical application under different polishing conditions can be tested in Simulated Body Fluids (SBF). Such experiments allow more approximation and sample life time performance to real body fluids and tissues.

Further electrochemical measurements can be used to explore the characteristics of titanium surface, as further to understand the strength of oxide layer forming during the presence of an oxidizing medium and the resistance of this layer during electrochemical activity. Tests such as cyclic voltammetry can evaluate the durability of oxide films against corrosion initiated environments. Additionally, in microelectronics both the behavior and characteristics of both titanium and its semi metal layer can be compared upon evaluating pitting and film strength affecting their performance as a barrier layer.

Titanium as barrier can be studied with other type of interconnects or plugs such as copper based technology. As the new IC and contacts technologies are relying in copper and the presence of a barrier between the vias and silicon such Ti/TiN/Ti, such

evaluation methods performed in this study can be included with copper technology as the Cu-Ti contact presents good stability ensures a reliable and low resistance electrical contact especially at the vias. [Ca2004] Furthermore, this study has established the fundamental experimental techniques and evaluations to evaluate various barrier materials in the microelectronics applications. In this sense, it highlights potential evaluations of Ru, Co, Mn films and their nitrides as barrier combinations for Cu based interconnects.

BIBLIOGRAPHY

AZoM, Titanium Applications, Timet, March 4 ,2002.

J.D. Bobyn, R.M. Pilliar, H.U. Cameron, G.C. Weatherly, Clin. Orthop. 150 (1980) 263.

Boyer, R. and Briggs, R. (2005). The Use of β Titanium Alloys in the Aerospace Industry. Journal of Materials Engineering and Performance*, 14(6), pp.681-685.*

Bakir M. Haemocompatibility of titanium and its alloys. J. Biomater. Appl. 2012; 27: 3–15.

Branemark P, Hansson B, Adell R, Breine U, Lindstrom J, Hallen O, Ohman A. Osseointegrated implants in the treatment of edentulous jaw. Scand. J. Plast. Reconstr. Surg. Suppl. 1977; 16: 1–132.

A. Bloyce, P.H. Morton and T. Bell, Surface engineering of titanium and its alloys. In Surface Engineering of Nonferrous Metals, (Eds) C.M. Cotell, J.A. Sprague and F.A. Smidt Jr., ASM Handbook, 835-851, 1998.

D.L. Cochran, J. Simpson, H.P. Weber and B. Buser, Attachment and growth of periodontal cells on smooth and rough titanium, Int J Maxillofac Imp, 3, 289-297 (1994).

CERAM Research Ltd, Titanium Applications, Timet, AZoM, March 4 ,2002.

Corrosionpedia. (2017). What is Potentiostatic? - Definition from Corrosionpedia. [online]Availableat:https://www.corrosionpedia.com/definition/915/potentiostatic [Accessed 12 Dec. 2017].

Castoldi, L., Visalli, G., Morin, S., Ferrari, P., Alberici, S., Ottaviani, G., Corni, F., Tonini, R., Nobili, C. and Bersani, M. (2004). Copper–titanium thin film interaction. Microelectronic Engineering, 76(1-4), pp.153-159.

Derbyshire, K. (2017). Managing Parasitics for Transistor Performance. [online] SemconductorEngineering. Available at: https://semiengineering.com/managing-parasitics-for-transistor-performance/.

Eungsoo Kim, Sangchul Shim, Changbum Jeong and Soonkwon Lim (n.d.). A study of the interface phenomena of TiW/Si and TiN/Ti/Si. Proceedings of 4th International Conference on Solid-State and IC Technology, 1995.

P. Fromherz, Neuroelectronic interfacing: semiconductor chips with ion channels, nerve cells, and brain, Ed. R. Waser, Wiley-VCH, Berlin, 781ff (2003)

Gusev E P, Cartier E, Buchanan D A, Gribelyuk M, Copel M, Okorn-Schmidt H, D'Emic C. Ultrathin high-K metal oxides on silicon: processing,

characterization and integration issues. Micro-electronic Engineering, 2001, 59(1–4): 341–349

Gamry.com. (2017). Electrochemical Corrosion Measurements-Galvanic Corrosion. [online] Available at: https://www.gamry.com/application-notes/corrosion-coatings/basics-of-electrochemical-corrosion-measurements/ [Accessed 13 Dec. 2017].

Gongadze E, KabasoD, Bauer S, Slivnik T, Schmuki P, van Rienen U, Iglič A. Adhesion of osteoblasts to a nanorough titanium implant surface. Int. J. Nanomed. 2011; 6: 1801–1816.

U. Gbureck, A. Masten, J. Probst and R. Thull, Tibiochemical structuring and coating of implant metal surfaces with titanium oxide and hydroxyapatite layers, Mat Sci Eng. C, 23, 461-465 (2003).

K.A. Gross, B. Ben-Nissan, W.R. Walsh and E. Swarts, In Proceedings of the 15th International Thermal Spray Conference, 1133 (1998).

K.A. Gross and C.C. Berndt, Biomedical Application of Apatites, Rev Mineral Geochem, 48, 631-672 (2002).

W.F. Ho, H. Lai Ch, Hsu H-Ch and Wu S-Ch, Surface modification of low-modulus Ti-7.5Mo Allom treated with aqueous NaOH, Surf Coat Tech, 203, 3142-3150 (2009).

Handbook of Analytical Methods for Materials, Electrochemical Corrosion Testing, 2014 by Materials Evaluation and Engineering, Inc.

J.A. Jansen, J.G.C. Wolke, S. Swann, J.P.CM. Van Der Waerden and K. De Groof, Application of magnetron sputtering for producing ceramic coatings on implant materials, Clin Oral Imp Res, 4, 8-34 (1993).

Keister, F. (1965). Thin-Film Titanium Dioxide Capacitors for Microelectronic Applications. IEEE Transactions on Component Parts, 12(1), pp.16-20.

Kulkarni, M., Mazare, A., Schmuki, P. and Iglič, A. (2014). Biomaterial surface modification of titanium and titanium alloys for medical applications. In: Nanomedicine. *One Central Press (OCP).*

K.A. Khor, H. Li and P. Cheang, Characterization of the bone-like apatite precipitated on high velocity oxy-fuel (HVOF) sprayed calcium phosphate deposits, Biomaterials,24, 769-775 (2003).

S. Kobyashi, Y. Ohgoe, K. Ozeki, K. Sato, T. Sumiya, K.K.Hirakari and H. Aoki, Diamond like carbon coating on orthodontic wires, Diamond and Related Mat, 14, 1094-1097 (2005).

Kuhn, A., Neufeld, P. and Rae, T. (n.d.). Synthetic Environments for the Testing of Metallic Biomaterials. The Use of Synthetic Environments for Corrosion Testing, 1988, pp.79-79-19.

LIU, X., CHU, P. and DING, C. (2004). Surface modification of titanium, titanium alloys, and related materials for biomedical applications. Materials Science and Engineering: R: Reports, 47(3-4), pp.49-121.

Liu, Z., Zhong, X., Walton, J. and Thompson, G. (2015). Anodic Film Growth of Titanium Oxide Using the 3-Electrode Electrochemical Technique: Effects of Oxygen Evolution and Morphological Characterizations. Journal of The Electrochemical Society, 163(3), pp.E75-E82.

M. Peters, Titanium World 1995,2,15.

Masuda Y, Jinbo Y, Yonzawa T, Koumoto K. Templeted site selective deposition of Titanium dioxide and self-assembled monolayer. Chemistry of Materials, 2002, 14(3): 1236–1241

C.Y. Chao, L.F. Lin, D.D. Macdonald, J. Electrochem. Soc. 128 (1981) 1187–1194.

A.R. Machado and K.J. Walban, Machining of titanium and its alloys—a review, J Eng. Manuf, 204, 53-60 (1990).

Mediaswanti K, Wen C, Ivanova E, Berndt C, Wang J. Titanium Alloys – Advances in Properties Control (eds. Sieniawski J, Ziaja W), Intech, 2013; Available from: http://www.intechopen.com/books/titanium-alloys-advances-in-propertiescontrol/sputtered-hydroxyapatite-nanocoatings-on-novel-titanium-alloys-for-biomedicalapplications.

Ozdemir, Z., Ozdemir, A. and Basim, G. (2016). Application of chemical mechanical polishing process on titanium based implants. Materials Science and Engineering: C, 68, pp.383-396.

P. Paranjpe, A. (1998). SEMICONDUCTOR CHIP INTERCONNECT BARRIER MATERIAL AND FABRICATION method. US 6,294,836 B1.

Peters, M., Kumpfert, J., Ward, C. and Leyens, C. (2003). Titanium Alloys for Aerospace Applications. Advanced Engineering Materials*, 5(6), pp.419-427.*

Basics of Corrosion Measurements (Application Note CORR-1). Princeton Applied Research, Oak Ridge, TN 37830.

Plummer, J., Deal, M. and Griffin, P. (2000). Silicon VLSI technology. Upper Saddle River, NJ: Prentice Hall.

Rathee, D., Arya, S. and Kumar, M. (2011). Analysis of TiO2 for microelectronic applications: effect of deposition methods on their electrical properties. Frontiers of Optoelectronics in China, 4[4), pp.349-358.

T.C. Rintoul, K.C. Bulter, D.C. Thomas, J.W. Carriker, T.R. Maher, R.J. Kiraly, A. Massiello, S.C. Himely, J.F. Chen, K. Fukamachi, ASAIO J. 39 (3) (1993) 168.

Robert Baboian, Corrosion Testing and Evaluation: Silver Anniversary Volume, Issue 1000, 1990.

U. Rieck, in Advanced Aerospace Materials (Eds: M. Peters, W. A. Kaysser), DGLR, Bad Godesberg 2001, pp. 213±219.

Seybolt, A. U., Oxidation of metals, Advances in Physics, vol12, Jan 1963, pp l-43.

Jitendra Sharan, Shantanu V. Lale, Veena Koul, Monu Mishra and O. P. Kharbanda, An Overview of Surface Modifications of Titanium and its Alloys for Biomedical Applications, Trends Biomater. Artif. Organs, 29(2), 176-187 (2015).

Seo, Y. and Lee, W. (2005). Effects of oxidant additives for exact selectivity control of W- and Ti-CMP process. Microelectronic Engineering, 77(2), pp.132-138.

D. Taylor, T. and R. Laney, W. (2018). Types of dental implants include endosseous implants, subperiosteal implants, and transosteal implants. [online] Dentalimplants.uchc.edu. Available at: http://dentalimplants.uchc.edu/about/types.html [Accessed 2 Apr. 2018].

Corrosion of Titanium and Titanium Alloys, Total Materia , Sep-2001.

M. Textor, C. Sittig, V. Frauchiger, S. Tosatti, D.M. Brunette, in: D.M. Brunette, P. Tengvall, M. Textor, P. Thomsen (Eds.), Titanium in Medicine, Springer, Berlin, 2001, pp. 171–230.

Variola, F., Yi, J., Richert, L., Wuest, J., Rosei, F. and Nanci, A. (2008). Tailoring the surface properties of Ti6Al4V by controlled chemical oxidation. Biomaterials, 29(10), pp.1285-1298.

de Viteri, V. and Fuentes, E. (2017). Titanium and Titanium Alloys as Biomaterials. *Tribology - Fundamentals and Advancements.*

X.X. Wang, S. Hayakawa, K. Suru and A. Osaka, Bioactive titania gel layers formed by chemical treatment of I substrate with H2O2/ HCl solution, Biomaterials, 23, 1353-1357 (2002).

F. Wallrapp, P. Fromherz, J. Appl. Phys. 99, 114103 (2006).

Xiao S-J, Kenausis G, Textor M. Titanium in Medicine: Material Science, Surface Science, Engineering, Biological Responses and Medical Applications (eds. eds. Brunette D M, Tengvall P, Textor M, Thompson P), Springer-Verlag, Berlin and Heidelberg 2001; 417–455.

Xu, W., Liao, S., Jiang, L., Yang, J. and Yu, C. (2012). Major influence of Ti/TiN and TTN metal barrier layer deposition on electro-migration resistivity. 2012 IEEE

11th International Conference on Solid-State and Integrated Circuit Technology.

Zhang, X., Jiang, Z., Yao, Z., Song, Y. and Wu, Z. (2009). Effects of scan rate on the potentiodynamic polarization curve obtained to determine the Tafel slopes and corrosion current density. Corrosion Science, 51(3), pp.581-587.